Innovative polycarbonates for lithium conducting polymer electrolytes

Leire Meabe Iturbe

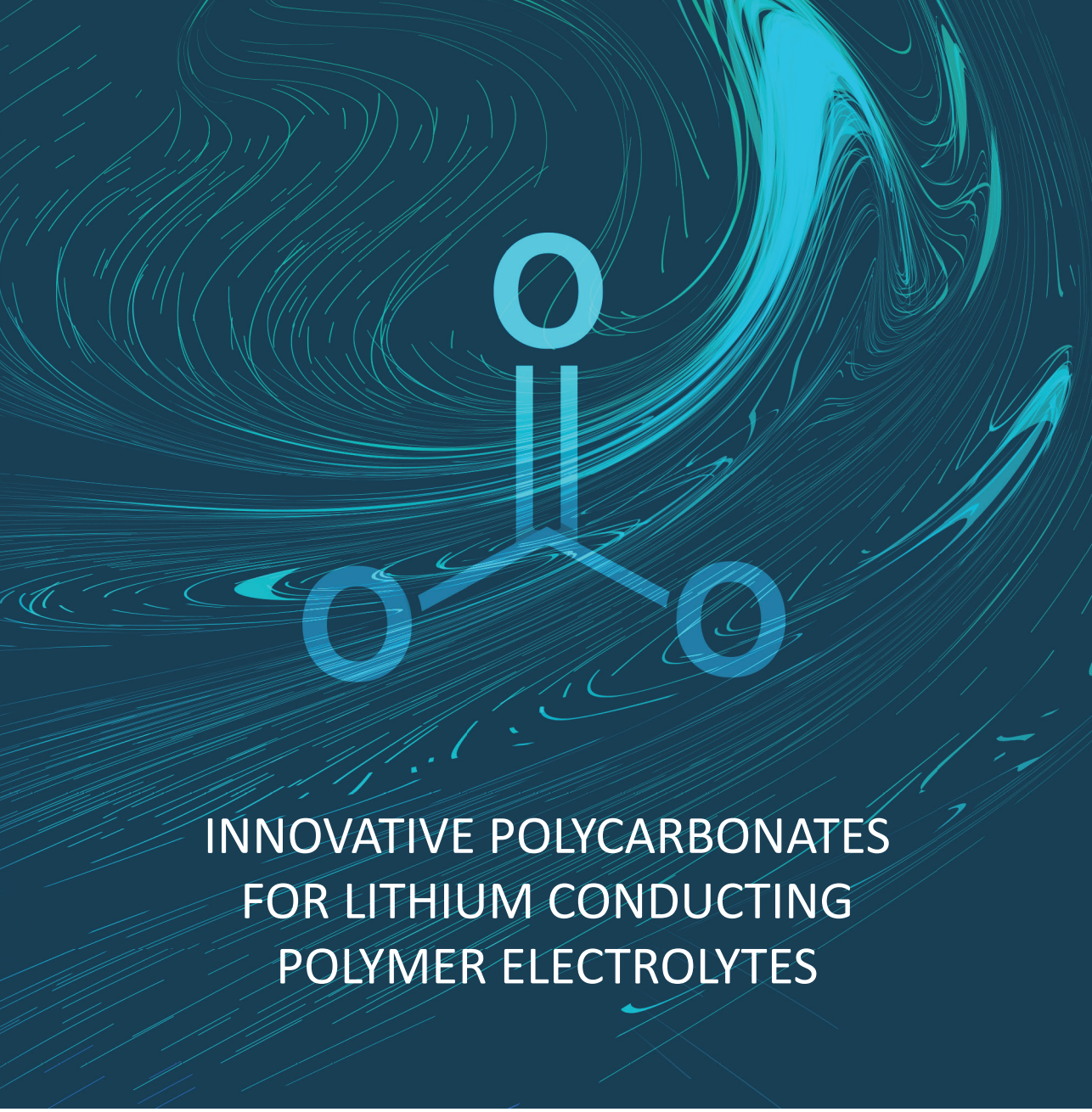

INNOVATIVE POLYCARBONATES FOR LITHIUM CONDUCTING POLYMER ELECTROLYTES

LEIRE MEABE ITURBE | PhD Thesis 2019

eman ta zabal zazu
Universidad del País Vasco
Euskal Herriko Unibertsitatea

IVERSITÉ DE PAU ET DES PAYS DE L'ADOUR

INNOVATIVE POLYCARBONATES FOR LITHIUM CONDUCTING POLYMER ELECTROLYTES

LEIRE MEABE ITURBE

Thesis advisor:

Prof. David Mecerreyes

Dr. Laurent Rubatat

Bihotz-bihotzez,

Aita, Ama, Jone, Nerea eta Xabiri

ACKNOWLEDGEMENTS

It has been a long journey full of energy and experiences, where I had the opportunity to work in different countries and meet wonderful people from all over the world. After 4 years, it is time to look back and begin to thank all the people who have been with me all this time.

First, I would like to thank the financial support that I got during the PhD, iPes (European Research Council, grant agreement number 306250), the Spanish Ministry of Education for the pre-doctoral fellowship (FPU14/05251), the grant obtained from the University of the Basque Country to trainee researchers to complete a jointly supervised doctoral thesis, and the travelling grants: BIODEST (H2020-MSCA-RISE-2017-778092), IONBIKE (H2020-MSCA-RISE-2018-823989) and FPU movilidad (EST18/00275).

I would like to start expressing my sincere gratitude to my supervisors, Prof. David Mecerreyes and Dr. Laurent Rubatat, for giving me the opportunity to join their groups with such a good environment, where it is easy to work and learn every day. Thanks David and Laurent, for the continuous support throughout my doctorate and for having the doors always open to progress as a scientist and as a person. Keep working hard & together, but always HAPPY!

I would also like to thank all the professors at POLYMAT, José M. Asua, Jose R. Leiza, María Paulis, Radmila Tomovska, Mariaje Barandiaran, Jose Carlos de la Cal, Alejandro J. Müller, Jaqueline Forcada, Thomas Schäfer, Ronen Zangi, Aurelio Mateo-Alonso, and Juan Luis Delgado for their discussions and advices during several seminars.

Special mention to Dr. Haritz Sardon, Dr. Jaime Martin, Dr. Kazuki Fukushima and Prof. Maria Forsyth. Eskerrik asko Haritz, etengabeko ideiazaparrada eta laguntzarengatik; Jaime, a ti también muchas gracias, por la ayuda y las recomendaciones, ありがとうございました Fukushima-sensei, for giving me the opportunity to work in your lab, and learnt from your culture. Ευχαριστώ Maria, we had a wonderful time in your group, where I had the opportunity to learn a lot and to enjoy summer time in Australia.

This PhD could not work without the infinite administrative work, Inés, Idoia, Izaskun, Mónica, Onintza and Liudmila, thank you for your daily support.

All the collaborators at CIC energiGUNE, Prof. Michel Armand and Dr. Chunmei Li, for your contribution on the thesis, being always helpful with your discussion and new ideas.

Although my PhD started in 2015, I first worked at POLYMAT as a summer student, during the summer of 2013, where I had the opportunity to learn with Paula Carretero. One year later, I did my Master project, where I started working at Innovative polymerization group. Eskerrik asko Maitane, zure laguntza guztiagatik, egunero-egunero zure goxotasunakin laguntzeko prest egotearren.

One year after, I started the PhD, where I had my pleasure to meet wonderful people! Asier, Guiomar, Manoj, Isabel, Daniele, Iñaki, Anto, Jorge, Luca, Coralie, Andere, Alex, Marta, Soline, Marine, Rafa, Daniela, Sara, Fermin, Álvaro, Antonio, Nerea Lago, Ali, Liliana, Ana Margarida, Ana Sanchez, Elena, Ester, Amaury, Naroa, Irma, Jeremy, Nicolas... Thank you guys for your support, kindness and friendship! I couldn't have a better group for the PhD! The best team to work and to be happy! I wish you all the best! I hope to keep in touch!

Also, I would like to also mention the people from the 3rd floor, who helped me during this journey. Thank you everyone!

Laura y Eddy, muchas gracias por acogerme en vuestra casa cuando iba a Pau. Muchas gracias por la compañía y la ayuda. ¡Os deseo lo mejor! A los compañeros de oficina: Mikel, Guilia, Iván, Borja, Javi, Maddalen! Muchas gracias por los ratos que hemos pasado juntos. ¡Mucha suerte! Agradecer también a los compañeros que de CIC energiGUNE. Muchas gracias por vuestra ayuda. ¡De aquí en adelante, nos veremos más!

Friends that I met in Japan and in Australia. Yuya, Keita, Yunko, Nozomi, Mai, Shunta thank you for your patient and your help every day in Yonezawa. A los bolivianos-japoneses (Valerie, Dereck, Debo, Rodri, Favio, Marcos) y a Adrián, muchas gracias por vuestra amistad, gracias por enseñarme Japón, la cultura y por todo el tiempo que pasamos juntos. People from all around the world that I meet in Australia: Nico, Danah, Tim, Karolina, Sneha, Tiago, Paolin, Paulin, Fernando, Laura, Matt, Tushan, Sam, Kalani, thank you all for your kindness. Great time that we had in Australia! I wish you all the best!

Nerea eta Esther, zela eskertu zuein eguneroko laguntasuna, beti irribarre bateaz eguna alaitziagatik. Eguneroko kafetxuak, berbaldixak, eguna samurraua izetia itxen dauielako. Mila esker benetan!

Eta zer esanik ez kotxeko bidaiak eramangarrixauak in ditxuzuenoi, egunero Donostiarako joan etorrixetan lagun izen zarienoi, Elene, Iñaki, Idoia eta Lander, mila esker.

AZK Taldeai be eskerrik asko! Zuein laguntza eta pasientzia danagatik! Diseinuan emundako laguntzagatik!

Kuadrilakuei be! Ainhoa, Idoia, Lur, Lore, Lorea, Oihana eta Maite. Eskerrik asko zuein animo, pasientzia, laguntza ta juerga danengatik! Kostata, baina azkenian, polimeruak zer dien ikasi dozue! jajaja

Eskerrik asko familixa ta inguruko danei, emandako laguntza ta animo danengatik, baina batezbe zuei: Ama, Aita, Jone, Nerea eta Xabi. Nola eskertu zuein laguntza, nire keja eta egun txarrei beti alde ona ateratziarren. Edozein lekutara noiela nire atzetik etortziarren! Mila esker! Hau ezingo zan in zuein barik, tesi hau zueina be badalako!

Table of contents

CHAPTER 1. Introduction

CHAPTER 2. Synthesis and characterization of aliphatic polycarbonates as solid polymer electrolytes

CHAPTER 3. Synthesis and characterization of poly(ethylene oxide carbonate) materials as solid polymer electrolytes

CHAPTER 4. Synthesis and characterization of Single-ion poly(ethylene oxide carbonate) polymer electrolyte

CHAPTER 1.

Introduction

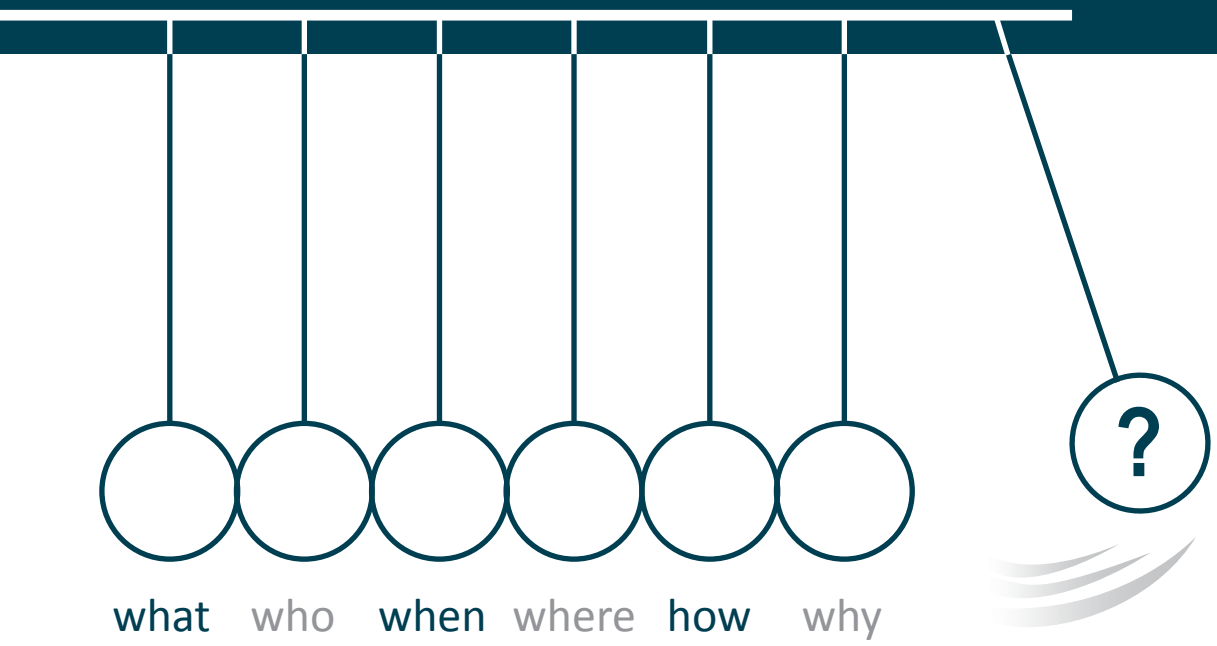

CHAPTER 1.

Introduction

1.1 Global Energy Scenario and Energy Sources

The highly qualified life, demanded by the society of the 21st century, requires constant scientific and technological developments. The technological revolution that we are suffering has as a principle the energy produced by coal, oil, and gas. However, the consumption of these energy sources are limited and additionally, during the last decades have been strongly criticized due to the high CO_2 emissions released. This means that energy is an essential ingredient for the economic and social development.[1]

Besides, the energy produced by renewable energies are promising alternative supplies to limited non-renewable resources. Little by little, the use of fuel-based energy sources will be reduced and renewable solar energy, wind power, hydropower, geothermal energy and bioenergy will be settled in our life. Nevertheless, due to the intermittent availability of these type of resources, good energy storage systems have to be designed, **Figure 1.1**. Among the all systems, electrochemical energy storage systems (EESS)s seem to be the best alternative for the use of portable electronics, electric vehicles and smart grid facilities.

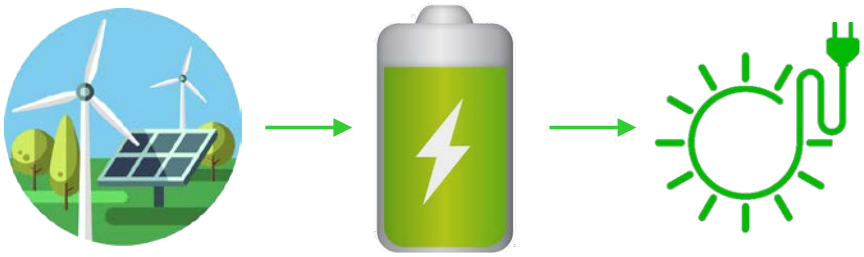

Figure 1.1. The importance of electrochemical energy storage systems.

1.2 Electrochemical energy storage systems

Design of promising energy storage devices will be one of the key points to implement renewable energy sources in our society. Depending on the application, the developed energy storage system should obey several demanded properties; i.e. light weight, flexibility, long duration, low cost, non-toxicity, safety, and it should be based on natural sources, **Figure 1.2**. During the last decades, two different effective methods have been expanded for EESSs: supercapacitors and batteries, which are distinguished by the energy storage principle. Supercapacitors store energy electrostatically in electric fields, whereas in batteries, it is stored by reversible electrochemical reactions. Supercapacitors lead to a higher power densities than batteries, which means that supercapacitors are able to release low energy but in very short times. To the contrary, batteries possess higher energy densities than supercapacitors, and they provide high amount of energy in long time.[2] Therefore, the purpose for each EESS is different.

Figure 1.2. Requirements for a good energy storage system.

Batteries have been implemented in a wide range of applications; from batteries with low energy densities in photovoltaic devices in residential areas, to energy storage systems with high energy densities, which will provide an auxiliary network service. Nowadays, lithium ion is the commonly use EESS. However, safety issues, high cost, temperature dependence, and the demand of new requirements on EESSs have led to the need of new batteries developments. Lithium metal, metal-air and lithium sulfur are some of the up-coming technologies, Figure 1.3.

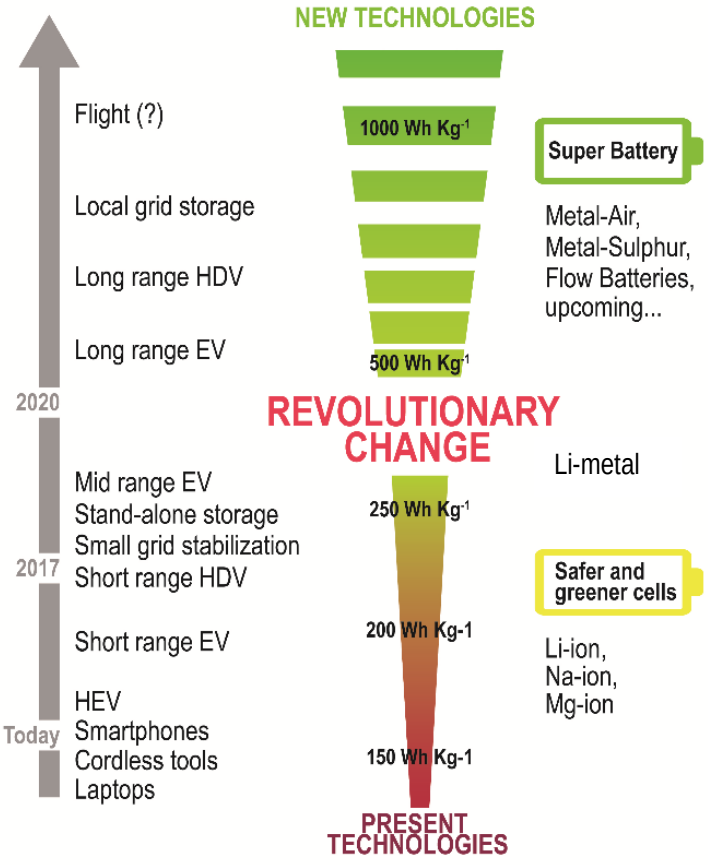

Figure 1.3. Comparison of different types of energy storage systems in terms of specific energy densities and their application. Adapted from.[3]

1.3 Battery performance – the role of the electrolyte

An electrochemical battery contains a positive electrode, cathode, and a negative electrode, anode. Between the two electrodes, the electrolyte is placed, which ensures the ion mobility between the electrodes, **Figure 1.4**. The electrolytes are considered as electronically insulating, but ionically conducting materials. As the anode and the cathode have different chemical potentials, during the discharge, electron flow occurs more negative potential (anode), to the one with more positive potential (cathode).[4] In the anode the oxidation half-reaction occurs, lose electrons, while in the cathode, the reduction half-redox reaction takes place, gain electrons. When the redox reaction is finished, the electron flow stops. In the case of rechargeable battery, when a voltage in the opposite direction is applied, the inverse current flow process happens during the charge. Electroneutrality is ensured by the ion transport across the electrolyte.[5]

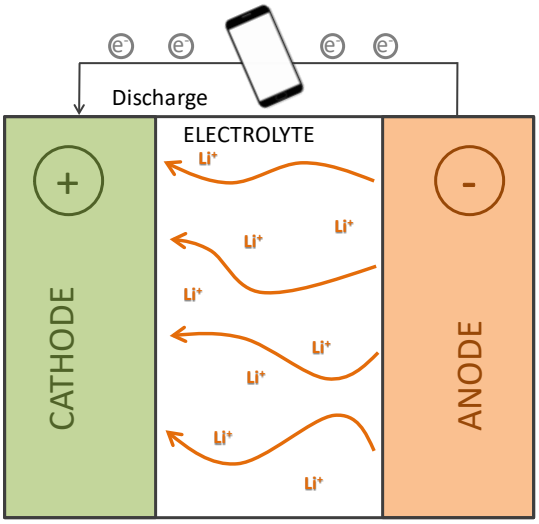

Figure 1.4. Different parts of a battery.

Generally, the commercially available batteries hold an electrolyte which is based on a salt dissolved in a liquid organic solvent. Additionally, in order to avoid the contact between the two electrodes, a separator is required. Even if liquid electrolytes offer high ionic conductivity, several characteristics have been questioned in the last years: i) flammability; ii) leakage; iii) volatility; and iv) toxicity. A successful electrolyte is expected to own multiple properties:

- Excellent ionic conductivity. The electrolyte should be a good ionic conductor and electronic insulator; it is claimed the lithium ionic conductivity rather than high anion conductivity. This factor will determine the internal impedance and electrochemical behavior at different charge/discharge rates. Cation conductivity should surpass 10^{-3} S cm^{-1} at room temperature to achieve quick charge and discharge cycles.
- High lithium transference number. A reduction of anion mobility can enhance the lithium transference number and overall battery performance, as the mobility of negatively charged anions will cause non-desired consequences.[6] A lithium transference number closed to unity can reduce concentration gradients and polarization of the cell during the charge and discharge processes.[7]
- Wide electrochemical stability window. The electrolyte should be stable between the electrodes' oxidation and reduction reactions' potentials. Meaning that an electrolyte with an electrochemical window up to 5 - 6 V *vs*. Li/Li^+ is desired for emerging technologies.
- Thermal stability. Some applications requires high temperature, thereby, the thermal stability of the electrolyte is demanded in newly elaborated electrolytes. For example, commercially available liquid organic solvents cannot work in high temperature, e.g. at 70 °C.

- Mechanical stability. A good mechanical stability is an appreciate parameter in order to avoid the use of a separator as in the case of liquid electrolytes. Additionally, ease thin film formation for a flexible battery, with the ability to adapt to different shapes is lastly requested.
- Good interfacial contact between electrolyte and electrodes. Good contact is necessary to achieve homogeneous redox reaction on the electrodes.

1.4 Types of solid electrolytes

In the last years, the research has been focused on the development of safe and non-toxic electrolytes. Different classes of electrolytes can be found in the literature to substitute the commonly used liquid organic electrolytes. The alternative solid electrolytes can be classified into two main groups, ion-conducting inorganic ceramics and ion-conducting polymer electrolytes.[8] The first discovery of solid state electrolyte dates to 1960s when the sodium ion transport in ceramic based β-alumina ($Na_2O{\cdot}11Al_2O_3$) succeeded. Ceramic electrolytes show appropriate elastic modulus, high thermal stability, wide electrochemical stability window and favored ionic conductivity and lithium transference number.[9] Several electrolytes have been developed over the years: LIPON, perovskite, garnet and alumina are some of the examples.[9-10] Although the ceramic electrolytes present several advantages, some important drawbacks cannot be avoided: i) some ceramic electrolytes are not inert in presence of moisture and CO_2, this will lead to an important chemical stability decrease and difficult processability; ii) various ceramic electrolytes can react with lithium metal anode, resulting in safety hazards; iii) poor interfacial contact provided by this type of electrolytes will provoke high interfacial resistance, and non-homogenous interfacial contact; and iv) the high cost of the material is a limitation for commercialization.[8]

Besides, solid polymer electrolytes (SPE)s can effectively overcome the problems mentioned before; SPEs show better flexibility to improve the interfacial resistance and they are more cost-effective compared to ceramic electrolytes.[8] Nevertheless, the solid polymer electrolytes provide lower ionic conductivity than ceramic electrolytes. Therefore, considering the difficulties of each one, there are still some challenges to address on this field.[8]

1.4.1 Solid Polymer Electrolyte (SPE)

The study of polymer electrolytes started with the research developed by Fenton, Parker and Wright in 1973.[11] Wright and co-workers found that poly(ethylene oxide) (PEO) was able to solvate different alkali metal ions by electrostatic forces and coordinating bonds between polar groups and metal ions.[11] In the study, a conductivity of 10^{-5} S cm^{-1} at 330 K was achieved, for highly crystalline PEO-NaSCN complex. Later, in 1980s, Armand *et al*. proposed the application of the PEO-based material for energy storage systems as SPEs.[12] The formulation strategy of SPE is the same as for liquid electrolytes, polymer electrolytes are solid solution of alkali metal salt in polymer. However, unlike liquid electrolytes, these materials are considered as safe electrolytes: generally, they are stable above 300 °C. The electrochemical properties of SPEs are affected by polymer backbone, compositions, distances between functional groups, molar mass, degree of branching and also by the nature and charge of metal cation and anion.[13]

Different from the previously mentioned conventional SPE, there is another family where there is no need of including a salt into the formulation; the negatively charged ion is anchored to the polymer backbone and the only mobile ion is the positively charged ion, the cation, which is associated with anions by electrostatic forces. With the design of single-ion conducting polymer electrolytes (SIPE)s a lithium

transference number approaching the unity is achieved. Nevertheless, the ionic conductivity is generally compromised. Since the first anionic polymer described at 1986 by Bannister *et al.*,[14] different polymeric backbones have been developed for single ion-conducting polymer electrolytes.[15] Trifuoromethylsulfonylimide (TFSI) containing anionic species, seem to be one of the most promising structures. This type of delocalized anion will provoke an improvement on electrochemical properties respect to other polymers containing low delocalized anions.[16] Among the all monomer suggested, the lithium poly(styrenesulfonyl(trifluoromethylsulfonyl) has been deeply studied.[17]

1.4.2 Gel polymer electrolytes

Generally, SPEs and SIPEs show low ionic conductivities at room temperature. Therefore, the introduction of another small molecular weight component can increase the value. In the formulation of gel polymer electrolytes, an organic solvent or an ionic liquid is therefore included. The first example of this family was published in 1975, when Feuillade and Perche added propylene carbonate into a polymer-salt formulation (copolymer of vinylidene fluoride and hexafluoropropylene with NH_4ClO_4).[18] This new formulation resulted in enhanced ionic conductivity; as ion transport mainly takes place in liquid or swollen phases. The plasticizer interacts with the polymer decreasing the intermolecular and intramolecular forces between the polymeric chains. Consequently, the rigidity of the polymer is decreased, promoting the ionic conductivity.[19] Moreover, the addition of new component can decrease the crystallinity and enhance the ion dissociation, thus, improving the ion transport. Among the all plasticizers, ionic liquids seem to be the most promising candidates, due to its high evaporation temperature; generally, above 200 °C. This new type of gel, known as ionogels, show very promising electrochemical properties as well as being considered as thermal-safe electrolytes.[20]

1.4.3 Composites polymer electrolytes

Even if great efforts have been devoted to improve the electrochemical properties of polymer and ceramic electrolytes, in both systems there are several gaps to be addressed. Due to complementary properties shown by ceramic and polymer families, composite electrolytes have been developed. The poor dielectric constant of polymer electrolytes is complemented by the introduction of ceramic fillers, which provide higher dielectric constant.[21] The dielectric constant can be adjusted by the type, size and amount of inorganic fillers implemented in the system.[22] From a polymer electrolyte point of view, in this occasion the aim will be to improve the ionic conductivity and the lithium transference number of SPEs.

1.5 Electrochemical properties

1.5.1 Ionic conductivity and ion conduction mechanism

The ionic conductivity ($\sigma = ne\mu$) is directly correlated by the concentration of charged species, elementary electric charge and the ability of the species to move in the media. All ions contribute to this measurement, the positively and negatively charged ions. Among the ions, the cation mobility is desired. The dissociation of the salt is normally associated with the lattice energy of the salt and the dielectric constant of the material. However, the dielectric constant of polymer is relatively low, and thereby, the dissociation is not ensured. Besides, in SPEs the coordination groups play an important role, where the ions tend to coordinate with them increasing the salt dissociation.

The ionic conductivity is measured by Electrochemical Impedance Spectroscopy (EIS). An AC current with a specific amplitude is applied, and the resistance of the material in a given frequency range is measured within a temperature range, between 100 °C

and 25 °C. In this analysis, how the ion conduction behaves in such temperature limit is determined. Appling the **Equation 1.1**, the ionic conductivity can be obtained.

$$R_b = \frac{l}{\sigma A}$$ **Equation 1.1.** Equation for ionic conductivity.

where l is the thickness of the membrane and A is the interfacial area between the membrane and the electrode. R_b is the resistance and it is determined by the impedance spectroscopy, by fitting by the equivalent circuit.

Due to the complexity of the SPE system and the lack of simple correlation between the structure-properties, the ion transport in the polymeric matrix, still, cannot be described in its entirety. Colby and co-workers have deeply studied the correlation between the relaxation time of the polymer backbone and the ionic conductivity, demonstrating the importance of the polymer glass transition on its conductivity.[23] However, glass transition is not easy to predict, which depends on several factors; i) polymer structure; ii) polymer type; and iii) molar mass.[24] Moreover, the system has to promote the dissociation of the anion and cation to increase the number of charge mobility. For that, the polymer is required to own some polarity, thus, the Li cation would be solvated by the polymer. Additionally, new salts have been proposed, to delocalize the negative charged ion to help the dissociation of the salt.[17, 25] Therefore, a polymer with high segmental motion and moderate polarity with the combination of a salt with low lattice energy can be appropriate candidate to promote high ionic conductivity.

Different theories have been implemented to the ionic conductivity, such as Arrhenius, Vogel-Tamman-Fulcher (VTF), William-Landel-Ferry equation, free volume model, and dynamic bond percolation (DBPM) model.[26] From all of them, the ionic

conductivity of SPEs is normally explained by Arrhenius and Vogel-Tamman-Fulcher equations.

Arrhenius equation is widely used to explain ionic conductivity mechanism of SPEs through logσ *vs.* 1000/T curve, **Equation 1.2**.

$$\sigma = \frac{\sigma_0}{T} e^{-E_A/k_B T}$$ **Equation 1.2.** Arrhenius equation.[26]

where σ_0 is related to the number of charger carrier, T is the Kelvin temperature, k_B is the Boltzmann constant, and E_A is the activation energy of the diffusion. The crucial value of this equation is the activation energy; generally, the lower E_A, the higher the ionic conductivity. When the ionic conductivity behavior in a temperature range tends to be a straight line in Arrhenius plot, the behavior is normally described by ion-hopping model.[27] The mechanism of the ion transport is based on ionic crystals, where the ions jumps to the nearest vacant place, increasing the ionic conductivity. By this equation, in the field of polymer electrolytes, the ionic conductivity of semicrystalline materials bellow the melting temperature is described.

VTF equation consists on the glass transition temperature, being more relevant to SPEs, **Equation 1.3**,[24] which was developed for pure polymeric system. Even if polymer electrolytes show solid-like macroscopic behavior, the local environment is similar to liquid-like. Thus, the ionic conductivity is normally coupled by segmental motion. This behavior can be observed at temperature above the T_g of the SPEs, SIPEs and in GPEs.

$$\sigma(T) = \sigma_0 \exp\left(-\frac{A}{T - T_0}\right)$$ **Equation 1.3.** Vogel-Tamman-Fulcher equation.[28]

where σ(T) is the ionic conductivity at certain temperature, A is the pseudo activation energy, related to the polymer segmental motion, σ_0 is the conductivity preexponential factor, and T_0 is referred to as the Vogel temperature.[29] T_0 is the glass

transition in ideal glasses, where the segmental motion or the ionic conductivity goes to zero, which is usually estimated to T_g-50.[30] Ionic conductivity based on VTF equation presences a curvature behavior in Arrhenius plot. This theory is in good agreement with free volume theory, which refers to strong dependence of polymer segmental motion in ionic conductivity. When the temperature is above T_g, the free volume is incremented, and as a consequence, the polymer segments and ions are prone to move. As a result, since the ion diffusion is considered to occur through the free volume, the ionic conductivity is increased.[31] This theory also claims the possibility to increase the free volume by introduction of plasticizers (an ionic liquid or a solvent).[32] This assumption leads to the understanding why decreasing the glass transition normally increases the ionic conductivity and vice versa.

1.5.2 Lithium transference number

First, it is necessary to define lithium transference number and lithium transport number. Transference number, refers to the fraction of the current carried by each specific specie, T_- and T_+, which is true for diluted systems, where the salt is completely dissociated. Besides, in real systems, the interactions between ions have to be assumed. As a consequence, with a salt like LiX, the formation of ion triples such as $[Li_2X]^+$ and $[LiX_2]^-$ as well as neutral species have to be considered (each specie will have their own transport number). In these systems, transport number needs to be determined. These values will be equal in diluted systems, when ion-ion pairing is avoided.

There are different techniques to measure the lithium transference number. However, the experimental determination of transference number leads to several controversies and confusions; depending on the technique employed the value may change, as the ion pairing is not considered generally.

When a high lithium transference number is measured means that the conductivity is mainly promoted by Li^+ mobility. In redox processes only lithium cation is involved; however, if high mobility of anion occurs in the system, migration in the opposite direction will occur, leading into a high gradient concentration, high polarization on the cell, and consequently, a high internal resistance will be formed.[6] Ideally, immobilized anion is desired, in which the concentration gradients are dismissed.

The most common technique to measure lithium transference number is described by Evans, Vincent and Bruce equation, which is simplified as Bruce-Vincent method,[33] Equation 1.4. A symmetric cell is polarized by applying a small potential (~10 mV) between two electrolytes until the steady state is reached. The internal resistance is measured before and after performing the polarization.

$$T_{Li^+} = \frac{I_{ss}(\Delta V - I_0 R_0)}{I_0(\Delta V - I_{ss} R_{ss})}$$ **Equation 1.4.** Equation proposed by Evans, Vincent and Bruce.

where ΔV is the applied potential difference, I_0 is the initial current, I_{ss} is the steady-state current, and R_0 and R_{ss} are the interfacial resistance before and after polarization, respectively. Bruce-Vincent equation is only true when the ion-ion paring is negligible and when only one cation and one anion are in the system. As a result, we have to take into account the accuracy of this method in the results, as in SPE systems the ion pairing may occur.

Another technique commonly used is Pulsed Field Gradient NMR (pfg-NMR).[34] NMR techniques allow to measure lithium transference number by measuring the diffusion coefficients of different species in diluted concentrations, Equation 1.5.

$$T_{Li^+} = \frac{D_+}{D_+ + D_-}$$ **Equation 1.5.** Lithium transference number by pfg-NMR.

A magnetic field is applied, and the shelf-diffusion coefficient of different species can be recorded. For example, by ^{7}Li NMR, the diffusion of lithium cation can be determined, whereas by ^{19}F NMR, the diffusion of $TFSI^-$ anion. Like that, the diffusion of the species can be determined and the transference number can be calculated. However, this method also assumes negligible ion-ion interactions.

1.5.3 Electrochemical stability window and mechanical stability

Normally, lithium batteries operate up to 4 V *vs*. Li/Li^+, therefore, an electrolyte with electrochemical stability in such a voltage range is prescribed. Additionally, to expand to emerging high voltage technologies a wider electrochemical stability is desired. Nevertheless, liquid electrolytes cannot afford high voltages, and therefore, the design of novel electrolytes is crucial for emerging devices.

Stable systems are able to form good solid electrolyte interface (SEI) layer in the interface of electrode and electrolyte during the first cycles.[35] This layer which is principally formed by the decomposition of the electrolyte's products, later helps to enhance the battery life. Thus, the electrolyte component can be tailored to form a fast and a stable SEI layer.[36]

Another important parameter is the mechanical stability of the electrolyte. If a material with an appropriate shear modulus is developed, the need of a separator is eliminated. Good mechanical properties of SPE will also provide additional properties, such as flexibility. However, this property is linked to ion transport, and one of the property can be compromised due to improvement of the other one.

1.6 Polycarbonates as polymer matrix of Solid Polymer Electrolytes (SPE)s

The chemistry of designing new polymers offers the opportunity to adjust the chemistry to different properties and applications. The choice of polymer host mainly depends on two factors: the polarity of the polymer backbone (sufficient electron donor to form coordination with cation) and low hinderance for rotation. Therefore, SPE can be implemented in different battery-technologies depending on the results, such as Li-S, Li-based and Na-based batteries. The challenges of the use of these SPEs in solid-state batteries come from the electrochemical properties. The main challenge is to find the best chemical structure candidate with high cation transport.

Poly(ethylene oxide), PEO, is the gold standard polymer among the all polymer host proposed. Since 1970s PEO has received extensive research interest.[11-12, 37] Up to now, PEO has been the irreplaceable polymer, due to its ability to solvate different lithium-based salts; such as LiBr, LiSCN, LiTFSI. In these type of low glass transition polymers, the ion conduction occurs in the amorphous phase.[38] The mechanism is leaded by the segmental motion of the coordination sites. However, it is affected by several polymer characteristics and ambient conditions: temperature, humidity, molar mass, polymer chain end-groups, salt, and therefore, physical and chemical properties.[39] Even if previously mentioned properties have a direct consequence on the electrochemical properties, mainly the research has focused on the suppression of the crystallinity of PEO (melting temperature at 60 °C). The ionic conductivity is affected by the crystalline domains of the polymer, which is more evidence at low temperature,[40] showing an ionic conductivity of 10^{-6}-10^{-7} S cm^{-1},[8] 4 orders of magnitude less than the liquid organic electrolytes.[37b] However, the absence of crystallinity will undergo to poor mechanical properties. Thus, in the direction of eliminating the crystallinity of the material and to maintain the mechanical consistency, several strategies have been studied; configuration of cross-linked

polymers[20a] and copolymers,[41] introduction of an organic solvent[42] or ionic liquid,[20a] the addition of ceramic fillers,[43] and also, the development of new salts.[44]

Besides, the lithium transference number of conventional PEO-based SPE is normally bellow 0.2. The strong coordination between ethylene oxide (EO) units and the lithium, restricts the lithium mobility, and consequently, the conduction is mainly governed by the anions.[45] This will cause low cell performance, due to the concentration gradients that will occur during the cycling. The ion mobility and lithium transference number of the PEO-SPEs have to be improved in order to be able to implement in commercially available batteries which operates at room temperature.[8]

Over the last years, the research has been focused on the development of new chemistries for SPE; polycarbonates, polysiloxanes, polyalcohols, and polyesters seem to be the most promising ones.[46] These polymers show low glass transitions, and occasionally, they do not show any crystallinity. Therefore, an improvement of ionic conductivity respect to PEO based SPEs is observed, especially, this enhancement is observed at room temperature, increasing one or two orders of magnitude and also, improving lithium transference number, above 0.5.[46]

Traditionally, solvent mixture based on cyclic and linear carbonates have been employed in Li-ion batteries. The high molecular weight analogues of this small molecules are the polycarbonates. Thus, one of the most exciting alternative is the use of polycarbonates as polymer host materials. As a result, a lot of efforts were devoted in the last 10 years to this topic. Several studies on SPE based on polycarbonates, lead to a better understanding of the correlation between chemistry and electrochemical properties. Low glass transition and the weak coordination between lithium cation and the carbonyl group of the carbonate group bring several

advantages to the electrochemical properties compared to PEO based SPEs:[46] i) improvement on ionic conductivity at room temperature, (10^{-4}-10^{-5} S cm^{-1}); ii) increase on lithium transference number, (0.5-0.6); and iii) wide electrochemical stability window (4.5-5.5 V). By FTIR analysis the favorable coordination of lithium cation with carbonyl group of the carbonate has been extensively observed; the band shifts to lower wavenumbers once it is coordinated. Moreover, within this polymer family, a new strategy has started to expand: polycarbonates seem to hold unique properties at high salt concentration,[47] which are named as "polymer-in-salt". At high salt concentration the ionic conductivity is significantly increased. If the mechanical properties of these electrolytes are improved, these new family will open new possibilities for forthcoming batteries.

Polycarbonates can be designed with carbonates groups as a part of the main chain of the polymeric backbone or as a side chain.

Main-chain polycarbonates

Aromatic polycarbonates are commercially available as engineering plastics. However, polymer electrolytes based on aromatic polymers show bad properties due to its high glass transitions, which will provoke a low ionic conductivity.[48] Nevertheless, the potential use of carbonate-based electrolyte was observed by Matsumoto and co-workers.[48b] Matsumoto *et al.* studied aromatic polycarbonates with few ethylene oxide units as a side chains; while more ethylene oxide units were incorporated in the polymer, a decrease on lithium transference number and electrochemical stability was resulted, observing the favorable effects of carbonate groups.

In order to achieve low glass transition and flexible polymers, aliphatic polycarbonates have been suggested. Poly(ethylene carbonate) (PEC) has been widely explored as a host polymer. This polycarbonate can be synthesized by two different routes: i) ring opening polymerization of 5-membered ring, which needs harsh reaction conditions due to the high stability of the ring, and consequently, results, in non-controlled structures;[49] and ii) copolymeriztion of CO_2 and epoxy ring.[50] Tominaga's group has studied the potential use of the last polymerization technique by synthesizing different polycarbonates.[50b] PEC was evaluated as polymer electrolyte by blending with different Li-salts: LiTFSI, LiBETI, $LiBF_4$, LiFSI, $LiClO_4$, and $LiCF_3SO_3$.[21a, 50b, 51] The addition of $LiClO_4$ and $LiCF_3SO_3$ to PEC, PEC-SPE showed a polyether based SPE behavior, where the ionic conductivity decreases with high salt concentrations. On these systems, a physical cross-linked effect was observed (**Figure 1.5**). Besides, with the addition of LiTFSI, LiBETI, $LiBF_4$, and LiFSI to PEC-system, a favored ionic conductivity is achieved, due to the plasticizing ability of the anion, reaching at high conductivity values at high salt concentrations. The highest ionic conductivity for 80 wt.% LiTFSI:PEC system was detected to be $5 \cdot 10^{-6}$ S cm^{-1} at 30 °C, showing a T_g of -62 °C.[52] Besides, PEC:LiFSI results also show interesting values.[21a] Similar to LiTFSI system, high salt concentration leads to improve the ionic conductivity (188 mol% LiFSI leads to $2.2 \cdot 10^{-4}$ S cm^{-1} at 60 °C and 2.510^{-5} S cm^{-1} at 30 °C). For PEC:LiTFSI and PEC:LiFSI systems 2 different mechanisms have been proposed: i) especially at low salt concentrations, the ionic conductivity closely follows the glass transition trend, i.e. the driving force of the ion mobility is the chain flexibility;[47, 53] ii) whereas at high salt concentration, when ion-ion pairing and aggregates starts to dominate the system, lithium migration decoupled from segmental motions is suggested.[21a] Therefore, percolation type polymer-in salt transport mechanism is proposed to be the dominant one at high salts contents,[54]

where there can be molten salt paths to conduct ions, and ion-hopping mechanism can occur.

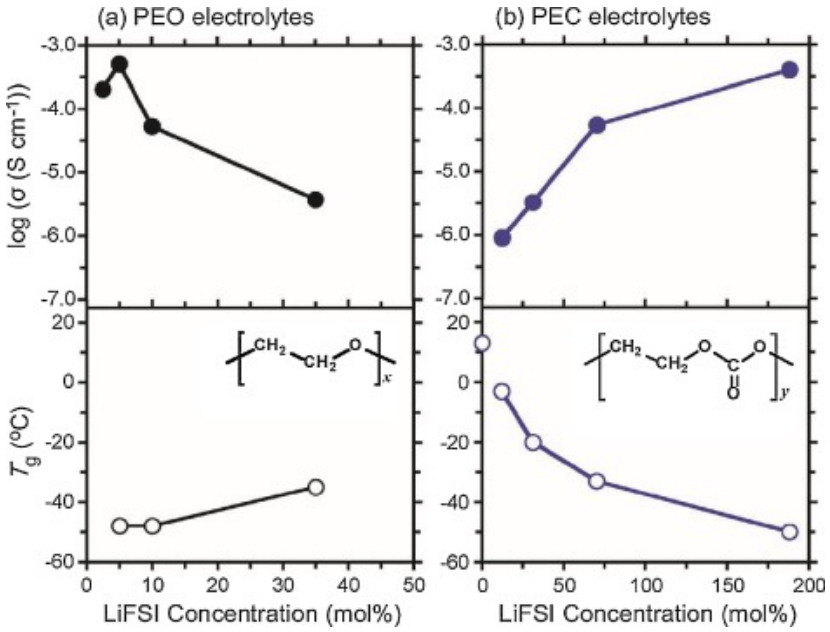

Figure 1.5. Ionic conductivity and glass transition evolution of PEO and PEC systems at different LiFSI mol%. Copyright 2019.[21a]

PEC-system, apart from showing an enhancement on ionic conductivity respect to PEO-systems, lithium transference number is significantly improved by the coordination of carbonyl groups and lithium cation.[55] As in the case of ionic conductivity the lithium transference number seems to be favored while the salt concentration is increased, reaching values as high as 0.83 at 80 °C, PEC_1LiTFSI.[21a, 53, 55] Nevertheless, at lower salt concentration PEC-SPE show higher lithium transference number than polyether-SPE, generally close to 0.5, demonstrating the evidence of carbonate groups contribution on the system.[21a]

The potential application of PEC-SPE was studied by Kimura and co-workers. $LiFePO_4$ based battery was evaluated using PEC with 80 wt.% LiFSI as electrolyte.[56] The use of 3D ordered macroporous polyimide matrix was necessary to reinforce the mechanical stability. Interestingly, high reversible capacities (120-130 mAh g^{-1}) and columbic efficiencies were observed at 30 °C.[56]

Copolymerization of CO_2 and epoxy chemistry also gives the opportunity to include different side chains.[57] Tominaga's group studied the effect on ionic conductivity by having some rigid and flexible glycidyl ether groups; possessing phenyl ether, tert-butyl ether, n-butyl ether, ethyl ether, isopropyl ether and methoxyethyl ether, **Figure 1.6**.[57c, 58] As expected rigid side chains, lead in a high T_g, and therefore, in low ionic conductivity. Besides, the flexible groups were able to increase the free volume, and consequently, the ionic conductivity. The SPE having methoxyethyl group as a side chain showed a high value of $2.2 \cdot 10^{-6}$ S cm^{-1} at 30 °C with 10 wt.% of LiTFSI.[57c]

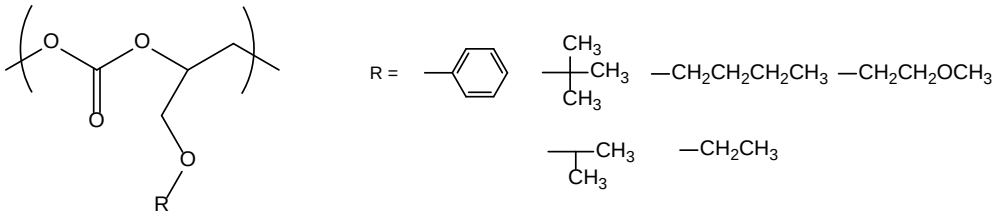

Figure 1.6. PEC with different side chains.

In another study Morioka and co-workers studied the effect of oxyethylene groups as a side chain of PEC, having one, two or three oxyethylene units.[57b] Two different behavior were concluded when LiFSI was added to the polymer. First, the T_g was increased with the increase of the salt loading, at lower salt concentration than 50 mol% of LiFSI. This trend was attributed to the polyether type SPEs behavior, where a preference coordination between Li^+ and oxyethylene groups is speculated. Besides, when the salt concentration surpasses 50 mol% LiFSI, the T_g of the SPEs

starts to decrease, showing polycarbonates based behavior. The interaction of lithium cation and oxyethylene groups, also lowered the lithium transference number, being lower for the polymer containing more oxyethylene groups.

In addition, Zhang *et al.* proposed the use of poly(propylene carbonate) as polymer electrolytes.[59] Even if this polymer shows T_g of 5 °C, higher glass transition than PEC, the conductivity was as high as $3.0 \cdot 10^{-4}$ S cm^{-1} at 20 °C with 23 wt.% of LiTFSI. However, this improvement could be affected by the cellulose-based matrix that was incorporated to reinforce the membrane. Unfortunately, data of the neat polymer electrolyte is missing to allow a comparison with other works.

Whereas ring opening polymerization of 5-membered cyclic carbonate requires harsh conditions, the 6-membered cyclic carbonates are easily polymerized.[49a] The simplest polycarbonate is named as poly(trimethylene carbonate) (PTMC). The first attempt by this type of polymer was developed by Melchiors *et al.* and dates to 1996.[60] In this study different alkali salts were combined to a triblock, composed by PEO in the middle block and poly(2,2-dimethyltrimethylene carbonate) in the extreme blocks. Due to higher PEO percentage rather than carbonate groups, the ionic conductivity was mainly through PEO, and therefore, the conductivity was not as high as for polycarbonate systems.

Additionally, PTMC is amorphous low glass transition (-15 °C) polymer, appropriate for SPE based system. Silva *et al.* reported the effect of several salts on the conductivity of PTMC: $LiCF_3SO_3$, $LiClO_4$, $LiBF_4$, $LiSbF_6$, $LiPF_6$[61] and $NaClO_4$, NaTFSI.[62]

Besides, Brandell's group studied in detail the use of this polymer in the area of polymer electrolytes. Sun *et al.* evaluated LiTFSI system with PTMC as a host polymer, **Figure 1.7**.[63] The T_g was much lower than PEC, however, the ionic conductivity trend

was more similar to polyether based SPE, where the ionic conductivity reaches a maximum while the salt concentration increases. However, the lithium transference number is improved respect to polyether based host families (0.80 at 60 °C, carbonate:Li=8),[64] meaning that the carbonate group is involved in the electrochemical properties favorably. Even though, the conductivity is not as good as PEC-systems, reasonable capacity with high efficiency was achieved using Li/$LiFePO_4$ battery at 60 °C.[65] At the first cycles the effect of the low ionic conductivity was observed in the capacity, which was gradually improved in the few first cycles, reaching up to 150 mAh g^{-1}. This limitation was overcome by adding some low molar mass PTMC to the electrode.

Ring opening polymerization also opens new strategies to developed new polycarbonate structures. Several attempts have been carried out to include functionalities which provides new properties to the host material. This approach was used by Mindemark and co-workers in different works.[66] By including heptyl ether and allyl (cross-linkable) side chain to the carbonate ring, leads to the design of new homopolymers and copolymers, Figure 1.7. From the allyl side chain the polymers were UV-polymerized to refine the molecular flexibility. Even though the glass transition is lower than PTMC's, lower ionic conductivities were achieved, from $2 \cdot 10^{-7}$ to $2 \cdot 10^{-8}$ S cm^{-1}. In order to understand the limited ionic conductivity, the coordination between alkaline salts and those carbonyl and ether groups were studied by FTIR analysis. The data was compared with PTMC, where the presence of ether groups is absence. Comparing the coordination of carbonyl groups, a minority coordination between lithium cation and ether groups was deduced. Therefore, this limited value could be attributed to the heptyl ether side chain, which is a hydrophobic molecule, and cannot provide the ion transport on the system.

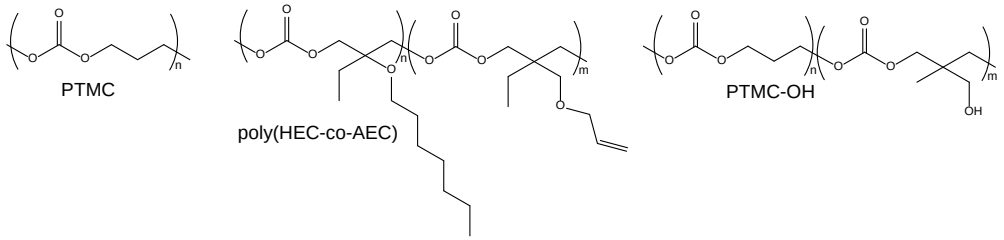

Figure 1.7. Chemical structure of (co)polymers synthesized via the ring opening polymerization of 6-member cyclic carbonates.

The functionally of the polymers can be tailored according to the final application. Mindemark *et al.* designed a polymer to improve the adhesion with inorganic substrates (Cu_2O and TiO_2).[67] This was achieved by including some hydroxyl (-OH) groups into the polymer, **Figure 1.7**. By a copolymerization between TMC and TMC-OH, necessary amount of hydroxyl groups were incorporated, 10 mol%. The ionic conductivity shown by this copolymer was comparable with PTMC:LiTFSI. However, as desired, the adhesion was improved, and 3D-nanostructured electrodes were achieved.[67]

Polycarbonates chemistry can be also combined by ether containing units in the polymeric backbone. This was developed by He *et al.*[68] via polycondensation. Using this method He and co-workers compared two polycarbonates containing diethylene oxide and triethylene oxide units between the carbonate units, PDEC and PTEC respectively. The polymers resulted in relatively low molar masses around 8,000 g mol^{-1}. Thus, when the LiTFSI was dissolved in the matrix, the membrane resulted in poor mechanical properties, and therefore, the membrane was supported by cellulose nonwoven. High ionic conductivities were analyzed at 25 °C: $1.12 \cdot 10^{-5}$ S cm^{-1} for PTEC:25 mol% LiTFSI system. Not surprisingly, the lithium transference number was between the value of polycarbonates and polyethylene oxide based systems, 0.39 at 25 °C. The potential application of the materials was tested in half cells at 25

°C using $LiFePO_4$ and a higher-voltage cathode material, $LiFe_{0.2}Mn_{0.8}PO_4$ at room temperature at 0.2C, showing good specific capacity, 130 mAh g^{-1}.

Tominaga *et al.* also designed random copolymers combining carbonate and ether groups in the polymer backbone.[38] High molecular weight copolymers were synthesized, and T_g led to decrease while the number of ether content was increased. The polycarbonates tend to incorporate between the ether units, avoiding the chelation effect, and therefore, the plasticizer effect of LiFSI was observed in the ionic conductivity tendency. This behavior was corroborated by FTIR analysis: similar coordination between carbonyl group and lithium cation as in PEC:LiFSI system was observed, which is in good agreement with the system studied by Mindemark *et al.*[66b] These systems provide higher ionic conductivity values than PEC:LiFSI in all salt concentration, showing the following values at 60 °C: $2.9 \cdot 10^{-4}$ S cm^{-1} and a lithium transference number of 0.7 where 53 % ethylene oxide units are in the system in highly concentrated system, 120 mol% LiFSI.[38b] Additionally, the potential application was tested in $LiFePO_4$ cell with good discharge capacities, close to 150 mAh g^{-1} at C/20, at 40 °C during the first cycles.

Recently, CO_2 sourced polycarbonates via polyaddition of bis(α-alkylidene carbonate)s with PEO diol of various molar masses were synthesized.[69] Regarding to the ionic conductivity of the amorphous SPE, the value was increase with the amount of ethylene oxide units. In order to improve the mechanical properties of the SPEs, a semi-interpenetrated network was prepared, leading to a reasonable ionic conductivity at room temperature $1.1 \cdot 10^{-5}$ S cm^{-1}. Even though, the lithium transference number was between PEO-SPE and PC-SPE, 0.28 at 70 °C, it was possible to cycle at 1C with a good discharge capacity of 83 mA h g^{-1} after 400 cycles, at 60 °C.

The electrochemical stability is considerably improved by the use of polycarbonates. For instance, in the case of PTMC the onset exceed to 4.5-5V *vs.* Li/Li^+. This increase could be attributed to the low hygroscopic property of the polycarbonate, which was confirmed by remaining LiOH byproduct on the system.[70] Additionally, this behavior is also consistent to a higher anodic stability of carbonate based solvents rather than ether-based solvents.[71]

Cyclic carbonate side groups

Another possible approach to include ion-coordination functional groups is as a side chain of polymer backbone. Britz *et al.* developed poly(acrylates) and poly(methacrylates) having 5-membered cyclic carbonate as functional group of the monomer (**Figure 1.8a,b**).[72] Even though, the most flexible host material was achieved by the highest number of methylene unites between the main chain and cyclic carbonate, these polymers did not provide the highest ionic conductivity when LiTFSI blends were formed. The highest ionic conductivity was determined for polymer containing the shortest number of spacer, $3.7 \cdot 10^{-6}$ S cm^{-1} at 40 °C (**Figure 1.8a**). This result is in good agreement to the conclusions developed by Mindemark *et al.* where the hydrophobic spacer did not allow the ion transport.[66b]

Additionally, having cyclic polycarbonates as a side chain, some copolymers have been developed in order to sustain new properties (**Figure 1.8c,d,e**).[73] Superionic conductivity, decoupled from segmental motion, was found in copolymer containing vinyl acetal, methoxyethylacrylate and ethylene glycol methyl ether methacrylate.

Similar side functional groups were combined with silane based polymer backbone in the work reported by Matsumoto *et al.* (**Figure 1.8f,g**).[74] Interesting ionic

conductivities comparable to PEC-system were obtained, high values at 30 °C: $1.21 \cdot 10^{-4}$ S cm^{-1} at high salt concentration (**Figure 1.8g**).

All these polymers are considered as flexible host materials. In contrast, rigid systems also show reasonable good conductivity values.[75] Cyclic carbonates as part of polymeric backbone show ionic conductivity of 10^{-7} S cm^{-1} at 40 °C with the combination of $LiCF_3SO_3$ (**Figure 1.8h**).[76] Even if this value is high for the host polymer, including some carbonate groups is able to increase the conductivity 2-4 orders of magnitude at high salt concentration (10^{-4} S cm^{-1} at room temperature) (**Figure 1.8i**).[76]

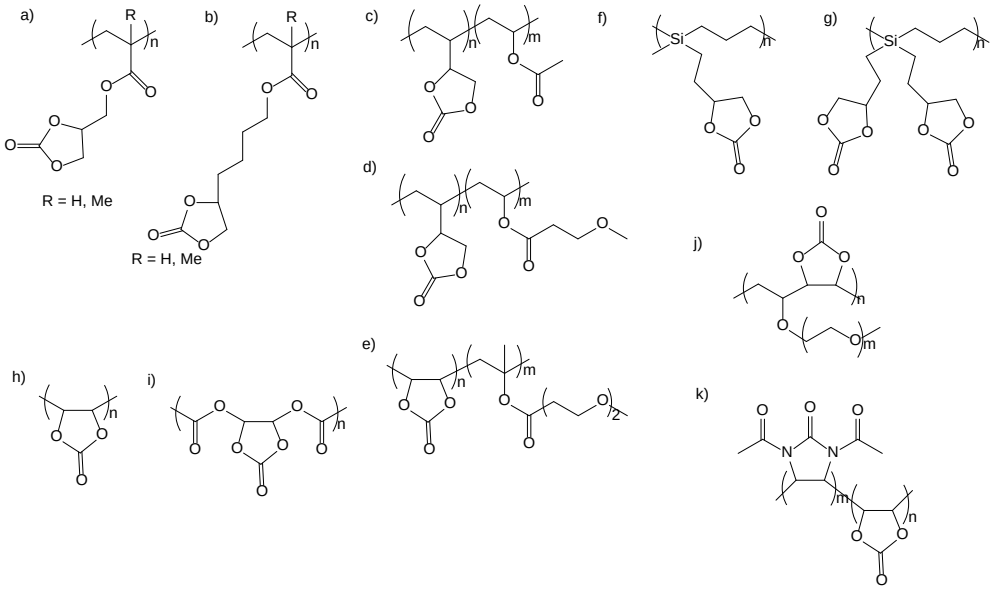

Figure 1.8. Different polymers containing carbonate groups as a side chain. Adapted from.[46]

Additionally, Chai *et al.* developed blends of rigid cyclic carbonate groups with lithium difluoro(oxolate) borate (**Figure 1.8h**).[77] This combination lead to an ionic conductivity of $2.23 \cdot 10^{-5}$ S cm^{-1} at 25 °C with the addition of 9.6 wt.% of salt. Also, it resulted in a lithium transference number of 0.57. These values were corroborated in a $LiCoO_2$/Li

cell cycling at C/10 at 50 °C, giving good stability and capacities (140-130 mAh g^{-1}) among 150 cycles at 0.1C.

In another approach ether groups were incorporate to a rigid polymer. This was leaded by Itoh *et al.*, where the combination of cyclic carbonates and ether containing side chain was synthesized (**Figure 1.8j**).[78] The similar trend as previously mentioned was relived; it was observed a preferential coordination of LiTFSI towards ether groups.[58, 66b] However, while the highest ionic conductivity was determined for the highest ether content, $1.3 \cdot 10^{-4}$ S cm^{-1} at 30 °C, the lithium transference number is compromised by the ether groups, 0.3. In another example, cyclic carbonates were combined with urea-amide group in different proportions (**Figure 1.8k**).[79] High cyclic carbonate content leads to rigid materials and Arrhenius-type temperature dependence ionic conductivity. Thus, the optimum value was successfully measured for 25 mol% urea-amide monomer: an ionic conductivity of $1.7 \cdot 10^{-6}$ S cm^{-1} at 30 °C.

1.7 Synthesis of polycarbonates via polycondensation

Historically, polycarbonates have been synthesized using three polymerization techniques, Scheme 1.1.

Scheme 1.1. Polymerization techniques for polycarbonates.

1) COPOLYMERIZATION OF EPOXY AND CO_2

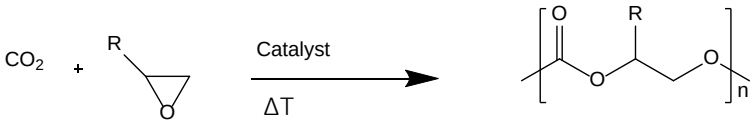

2) RING OPENING POLYMERIZATION

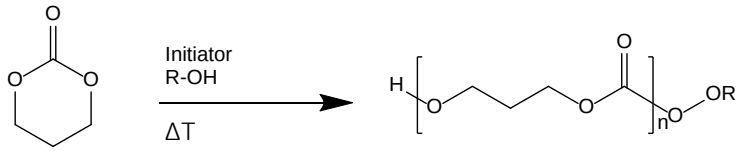

3) POLYCONDENSATION

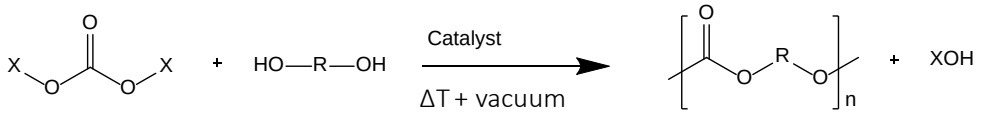

1) Copolymerization between CO_2 and epoxy. High valued compounds are synthesized from renewable and low cost resource. In the presence of a catalyst, CO_2 opens the epoxy ring leading to a control polymer structure. This polymerization is scalable; however, the yield will depend on temperature, pressure and catalyst concentration.[80]
2) Ring Opening Polymerization of cyclic carbonates. This chain propagation process, requires small concentration of initiator to achieve high molar mass polycarbonate. The number of polymer chains depends on the number of

initiator and transfer molecules (alcohol molecules) added to the polymerization.[81] In this way, a control molecular weight distribution and topology are successfully designed. However, the development of cyclic carbonates with high purity sometimes involves tedious synthetic steps.

3) Polycondensation between dicarbonates and diols. This type of polymerization is based on the condensation reaction between diols and small carbonates such as dimethylcarbonate. The polymers are formed via step-growth polymerization. This technique provides plenty of possible structures by the simply changing the diol which are commonly commercially available. The drawback of these type of polymerization is that the molar mass depends on the stoichiometry of the reagents, and besides, high temperatures and vacuum are needed.

1.7.1 Analysis of different catalysts used in the polycondensation reaction of aliphatic polycarbonates

The discovery of polycarbonates dates to 1898, when Einhorn disclosed the transformation of hydroquinone and resorcinol derivatives into polymeric materials.[82] However, at the beginning of the 20th century the limited solubility of this polymer and its difficult processing avoided its study.

In 1953, the first aromatic polycarbonates were commercialized by Bayer and were widely used as engineering plastics, owing to their outstanding high impact, low scratch- and temperature-resistance.[83] Traditionally, polycarbonates were synthesized by interfacial polycondensation, between phosgene and sodium salts of bisphenol-A at 20-40 °C and atmospheric pressure. Weak organic bases, such as trimethylamine, were employed to accelerate the polycondensation reaction and achieved high molecular weights. Continuous restriction on the use of phosgene

derivatives, have pushed both industry and academia to develop phosgene free synthesis of polycarbonates. In this sense, phosgene has been replaced by dimethyl carbonate or diphenyl carbonate.

Polycarbonate synthesis can be successfully performed through the polycondensation of dimethyl carbonate (DMC) or diphenyl carbonate (DPC) with a diol in a two-step process (Scheme 1.2). The first reaction step consists on initial condensation, the temperature is maintained at 100-130 °C over a period of 1-24 h until the equilibrium is reached. In this stage, hydroxyl and carbonate end groups react eliminating methanol/phenol, leading to low molar mass oligomers (< 1,000 $g.mol^{-1}$). In the second step, the chain growth takes place by transesterification between hydroxyl and methyl/phenyl carbonate end groups or between two methyl/phenyl carbonate end groups in the presence of transesterification catalyst. High temperatures (150-350 °C) and high vacuum are required to proceed the reaction and to remove all unreacted monomers and the by-products (alcohol based molecules). The mole ratio of this polymerization is crucial to enhance the conversion of the first step and to obtain high molecular weight polycarbonates during the second step. The aim is to increase the number of methyl/phenyl carbonate end-groups for the transesterification reaction, which are more reactive compared to hydroxyl groups. This can be achieved with an excess of dimethyl/diphenyl carbonate amount.[84]

Scheme 1.2. General route for the synthesis of polycarbonates via step-growth polymerization. Adapted from ref.[84-85]

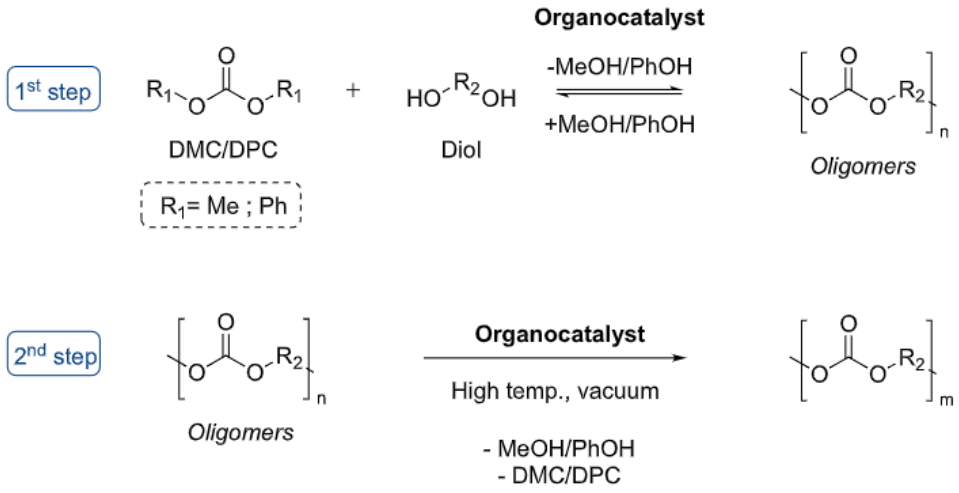

This methodology not only avoids the use of chlorinated reagents but is also performed in bulk avoiding the employment of organic solvents and hindering the formation of cyclic carbonate side products. Nevertheless, the reactivity of these two linear carbonates is much lower than historically used toxic phosgene reagent. Therefore, the reaction must take place at higher temperature (150-350 °C) and reduced pressure, with the required addition of catalysts. Alkali metals, such as NaH or NaOH, have dominated the field of polycarbonates obtained by step-growth polymerizations.[86]

New efforts in polycarbonate synthesis were oriented toward the discovery of novel organocatalysts to achieve high molecular weights. There are three ways to activate the reaction: i) increasing the electrophilicity of the carbonate; ii) increasing the nucleophilicity of the alcohol; and iii) through a nucleophilic activation of the carbonate.[87] Several classes of organic compounds, including tertiary amines, strong bases such as guanidines and amidines, *N*-heterocyclic carbenes and thiourea

derivatives have been investigated in polycarbonate synthesis, as point out in the following Figure 1.9.

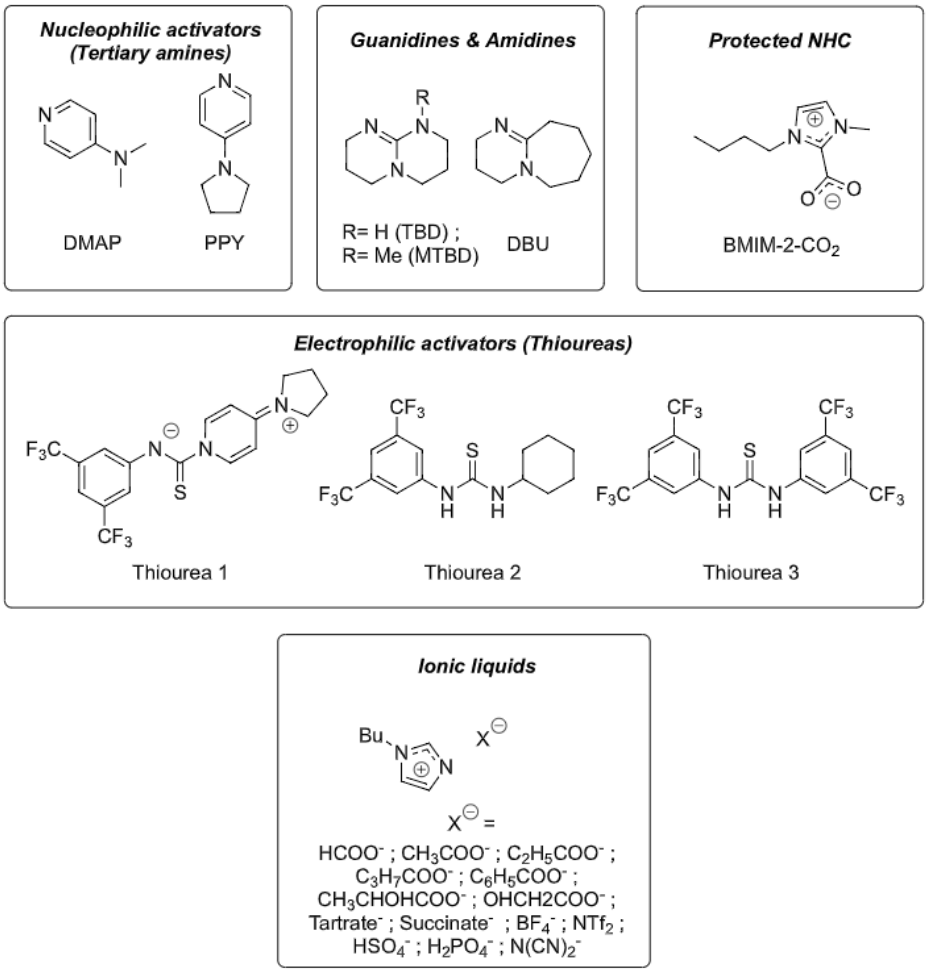

Figure 1.9. Organic bases used as catalysts for step-growth polymerization of polycarbonates. Adapted from.[88] *Cyclic guanidines and amidines:* TBD, MTBD, and DBU,[85, 89] *N-heterocyclic carbenes:* protected NHC,[90] *Nucleophilic activator:* PPY,[85, 91] DMAP,[84-86, 91-92] *Electrophilic activators:* Thioureas,[85] *Dual catalyst based on ionic compounds:* tetraethyl ammonium hydroxide,[93] imidazolium-based ionic liquids.[94]

Still the achievement of high molecular weight polycarbonates by organocatalyzed step-growth polymerization remains an issue. While metal-based catalysed polymerization leads to molecular weights higher than 100 kg mol^{-1} (M_n = 150 kg mol^{-1} using NaH),[86b] it is indeed more problematic to reach molar masses higher than 80 kg mol^{-1} from organocatalysts. Imidazolium-based ionic liquids and DMAP prove the most attractive compounds in this context.

1.7.2 Pre-screening of organocatalysts used in this thesis for the synthesis of Polycarbonates

In this thesis polycondensation was chosen as the synthetic method to prepare innovative polycarbonates to be used in solid polymer electrolytes. Before to start developing innovative polycarbonates, the polycondensation conditions and the catalyst were evaluated. As a first reaction model, dimethyl carbonate (DMC), diethylene glycol as a diol and DMAP as an organocatalyst were chosen. Based on previous works, DMAP was selected for being one of the most promising and easy handling catalyst.[85] A distillation set up with cooling system under nitrogen was employed to optimize the mole ratio of the polycondensation. The first step was carried out at 130 °C during 4 h and the condensation of the DMC and ethylene glycol-hydroxyl end group takes place in competition with some evaporation of the DMC. For the second step, the reaction was heated up until 180 °C and the high vacuum was controlled: during the first 13 h the vacuum was maintained at 2 kPa and later, it was kept bellow <0.1 kPa which was left in such conditions 8 hours.

Scheme 1.3. Scheme of model polycondensation reaction.

Five model reactions were carried out by changing the reagents stoichiometry, mole ratios of DMC:diethylene glycol:DMAP: 1.5:1:0.01, 2:1:0.01, 2.5:1:0.01, 3:1:0.01, 5:1:0.01. The molar mass of the polymerization was followed by GPC in THF based on PS standard, **Figure 1.10**, and it was taken as an indication of successful polymerizations. From the graph, how the molar mass is affected by the molar ratio can be observed. The first observation is that the polymerization did not happen with low excess of DMC (1.5:1:0.01), where the complete evaporation of DMC may occurred. Besides, at higher DMC mole ratios than 1.5:1:0.01, the molar mass was progressively increased in the second step, until a plateau was detected, **Figure 1.10**, where the molar mass was constant. Consequently, the reaction's yield was also affected by the mole ratio, **Table 1.1**; when a higher excess of DMC was employed, the higher was the yield. Taking into account the molar masses and the yields, the mole ratio of 3:1:0.01 (DMC:diol:DMAP) seemed to be the optimum ratio for this type of system.

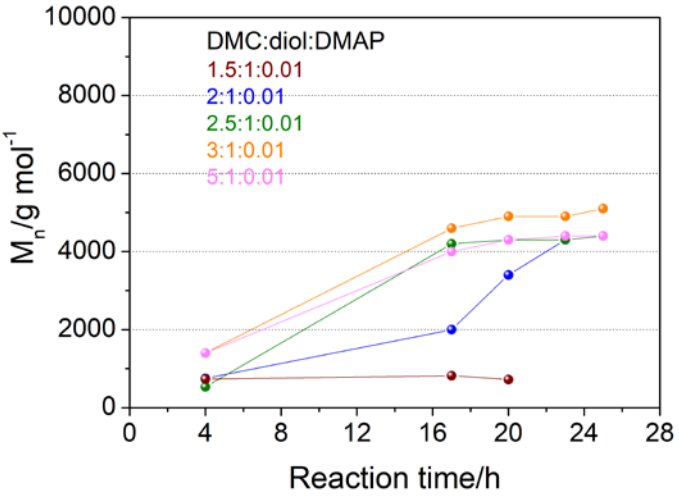

Figure 1.10. Effect of molar ratio on M_n among the polycondensation.

Table 1.1. Yields of polymerization using different mole ratios.

DMC:diol:DMAP	1.5:1:0.01	2:1:0.01	2.5:1:0.01	3:1:0.01	5:1:0.01
YIELD:	---	59 %	73 %	82 %	85 %

The next step was to evaluate different organcoatalysts and its effect on the polymerization with the mole ratio of DMC:diethylene glycol:catalyst - 3:1:0.01. The following different acid, basic and neutral catalysts were evaluated, **Figure 1.11**; commercially available basic catalysts: DMAP, TBD, and DBU, commercially available acid catalysts: MSA, p-TSA, dodecyl benzene and triflic acid, and some catalysts were synthesized: MSA:TBD 1:1, MSA:TBD 2:1 and MSA:TBD 1:2, as described by Basterretxea and co-workers.[95]

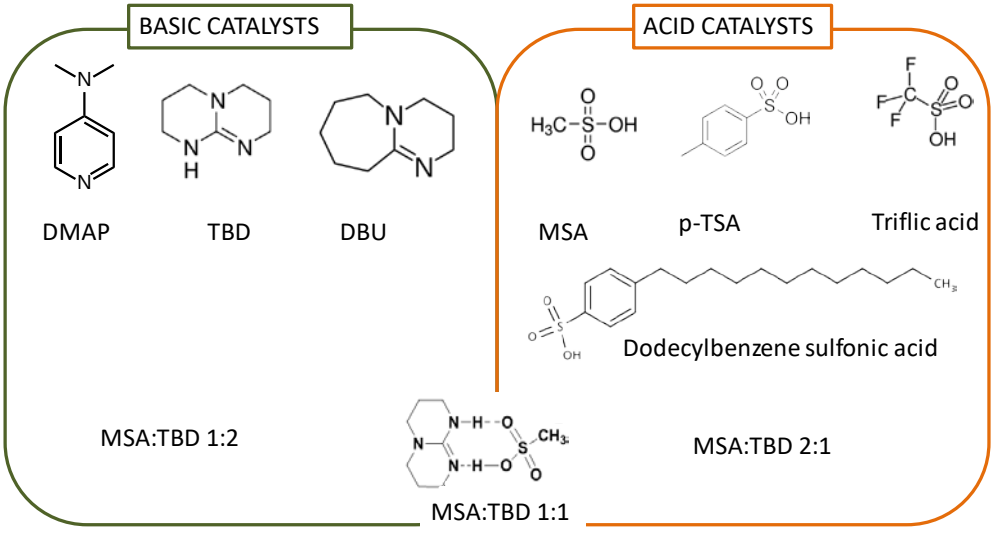

Figure 1.11. Chemical structure of the pre-screened organocatalysts.

From the GPC data, **Figure 1.12**, the effectiveness of the basic catalyst can be clearly observed. All of the basic catalysts were able to catalyse the polycondensation of the polycarbonates, even if differences between them could be observed. According to the experiments, DMAP, TBD, MSA:TBD 1:1 and MSA:TBD 1:2 were the most promising ones. Besides, there were not significant differences on yields between different basic catalysed polymerizations, **Table 1.2**.

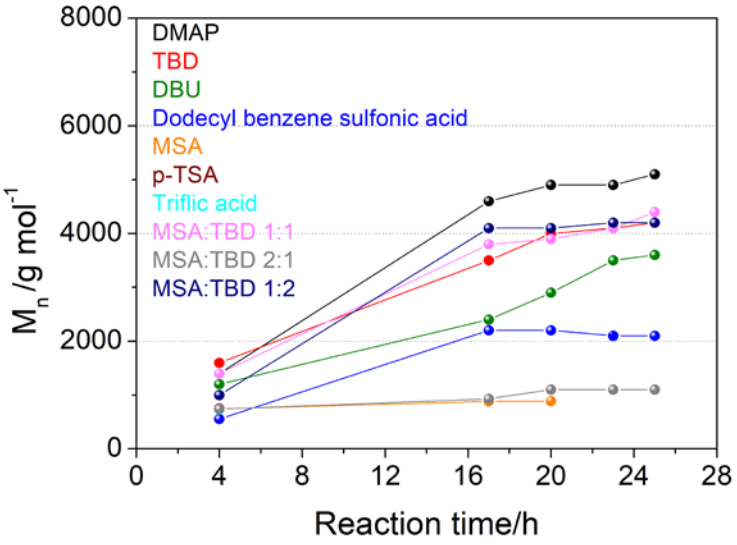

Figure 1.12. Effect of organocatalyst on M_n among the polycondensation.

Table 1.2. Yields of different organocatalyzed polymerization.

CATALYST	DMAP	TBD	DBU	MSA:TBD 1:2	MSA:TBD 1:1
YIELD:	82 %	85 %	73 %	90 %	84 %

While basic catalysts worked effectively, none of the acid-catalysts was able to catalyse the polymerization. As can be observed from the ^{1}H-NMR, **Figure 1.13**, different catalytic activity in the first 4 hours of polymerization between the acid and basic catalysts could be observed: in the case of acid-catalysts the formation of the carbonate links was avoided or retarded, restricting the polymerization. As the proton attributed to –COOC<u>H</u>$_2$– cannot be detected for the polymers catalysed by acid organocatalysts.

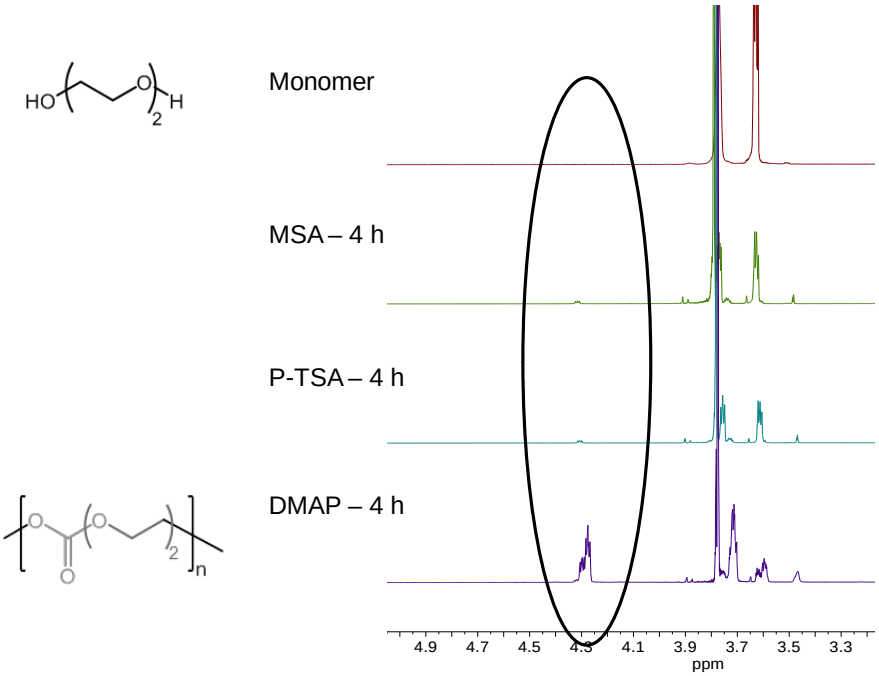

Figure 1.13. ^{1}H NMR spectra. Differences on the catalysts' activity in the first 4 hours of polymerization. NMR carried out in $CDCl_3$.

As a conclusion, commercially available DMAP was chosen for the following polymerizations, being the most promising organocatalyst regarding molar mass and yield. In the **Scheme 1.4** the mechanism of DMAP as nucleophilic activation is described. In presence of DMAP the carbonyl group will show a nucleophilic

character. Thanks to the nucleophilic activation, an alcohol group can attack the carbonyl group, forming a carbonate group.

Scheme 1.4. Proposed nucleophilic activation mechanism of DMAP in the polymerization of polycarbonates. Adapted from ref.[91a]

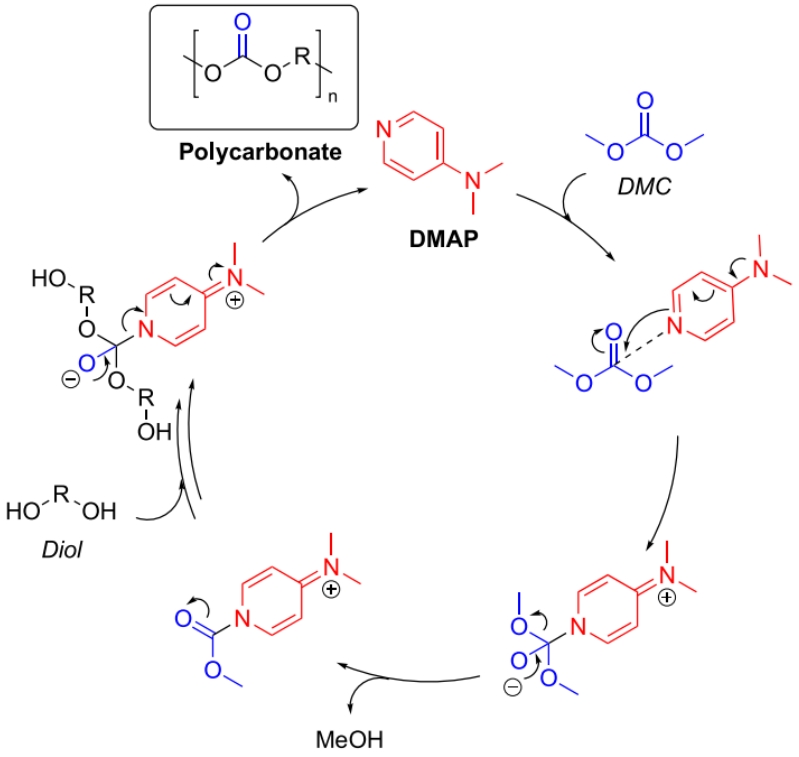

The set up that was used during the PhD was different. The polymerizations were carried out in schlenk flasks. Consequently, the mole ratio of DMC:diol:DMAP was again calculated, being 2:1:0.01 the estimated ratio. Also, the reaction time and conditions were adapted. The first step last 4 h and the temperature was maintained at 130 °C, and for the second step, the temperature was increased up to 180 °C and the high vacuum was applied directly (<0.1 Pa). For the last step the polymerization was run overnight.

1.8 Motivation and objectives of the PhD thesis

The continuous research on polymer electrolytes will lead us into a promising energy storage system. Up to now, PEO has been extensively explored polymer matrix in solid polymer electrolytes for lithium batteries. However, recently, polycarbonate-SPEs show considerable enhancements respect to PEO-SPEs, such as improved lithium conductivity and electrochemical stability. The main objective of this thesis is to evaluate and compare new polycarbonates' structures as SPEs in lithium batteries. For this purpose, the versatile and simple polycondensation technique was chosen as synthetic tool to develop innovative polycarbonates. This synthetic method allowed to easily change the functionality of the diol and the properties of the polycarbonates. During our work, three different polycarbonate families have been successfully synthesized and characterized, which are described in 3 different chapters.

Following the first chapter about the introduction of the polymer electrolytes, and once the best organocatalyst have been selected for the polymerization, in the second chapter, the versatility of polycondensation for the synthesis of linear aliphatic polycarbonates is demonstrated. Homopolymers and copolymers containing different methylene units are shown, and the effect of chemical structure and thermal properties in the electrochemical properties are discussed. This study is complemented by the evaluation of aliphatic homopolymers as solid polymer electrolytes in batteries.

In chapter 3, a variety of poly(ethylene oxide carbonates) are described as promising SPEs. On these polycarbonates, the number of ethylene oxide (EO) is varied between the carbonate groups. Thereby, the effect of EO units and carbonate groups on electrochemical properties was investigated. Moreover, the chemistry of the most promising poly(ethylene oxide carbonate) is modified to improve the mechanical

properties, in order to be able to further characterized the electrochemical properties. The promising PEO/PC polymer was further evaluated in lithium battery full cells.

During the chapter 4, the design of single ion conducting polymer electrolytes is discussed. In the synthesis, a new single-ion conducting sulfonamide diol monomer is introduced in the PEO-PC backbone. This allowed a direct comparison of the electrochemical characterization, ion mobility and symmetric cell performance of single ion conducting polymer electrolyte with the analogous conventional SPE.

In the last chapter, the most relevant conclusions are highlighted.

1.9 References

1. (a) Asafu-Adjaye, J., The relationship between energy consumption, energy prices and economic growth: time series evidence from Asian developing countries. *Energy Economics* 2000, *22* (6), 615-625; (b) Lee, C.-C., Energy consumption and GDP in developing countries: A cointegrated panel analysis. *Energy Economics* 2005, *27* (3), 415-427.

2. Halper, M. S.; Ellenbogen, J. C., Supercapacitors: A brief overview. *The MITRE Corporation, McLean, Virginia, USA* 2006, 1-34.

3. http://www.hiu-batteries.de/battery-research-center-in-germany/research/electrochemistry/electrochemistry-for-batteries/research/.

4. Tarascon, J.-M.; Armand, M., Issues and challenges facing rechargeable lithium batteries. In *Materials For Sustainable Energy: A Collection of Peer-Reviewed Research and Review Articles from Nature Publishing Group*, World Scientific: 2011; pp 171-179.

5. Long, L.; Wang, S.; Xiao, M.; Meng, Y., Polymer electrolytes for lithium polymer batteries. *Journal of Materials Chemistry A* 2016, *4* (26), 10038-10069.

6. (a) Doyle, M.; Fuller, T. F.; Newman, J., The importance of the lithium ion transference number in lithium/polymer cells. *Electrochimica Acta* **1994,** *39* (13), 2073-2081; (b) Thomas, K. E.; Sloop, S. E.; Kerr, J. B.; Newman, J., Comparison of lithium-polymer cell performance with unity and nonunity transference numbers. *Journal of Power Sources* **2000,** *89* (2), 132-138.

7. Song, J. Y.; Wang, Y. Y.; Wan, C. C., Review of gel-type polymer electrolytes for lithium-ion batteries. *Journal of Power Sources* **1999,** *77* (2), 183-197.

8. Fergus, J. W., Ceramic and polymeric solid electrolytes for lithium-ion batteries. *Journal of Power Sources* **2010,** *195* (15), 4554-4569.

9. Cao, C.; Li, Z.-B.; Wang, X.-L.; Zhao, X.-B.; Han, W.-Q., Recent Advances in Inorganic Solid Electrolytes for Lithium Batteries. *Frontiers in Energy Research* **2014,** *2* (25).

10. Knauth, P., *Inorganic Solid Li Ion Conductors: An Overview*. 2009; Vol. 180, p 911-916.

11. Fenton, D. E.; Parker, J. M.; Wright, P. V., Complexes of alkali metal ions with poly(ethylene oxide). *Polymer* **1973,** *14* (11), 589.

12. (a) Armand, M. B.; Duclot, M. J.; Rigaud, P., Polymer solid electrolytes: Stability domain. *Solid State Ionics* **1981,** *3*, 429-430; (b) Armand, M., Polymer solid electrolytes - an overview. *Solid State Ionics* **1983,** *9*, 745-754; (c) Armand, M. B., Polymer Electrolytes. *Annual Review of Materials Science* **1986,** *16* (1), 245-261.

13. Rivas, B. L.; Pereira, E. D.; Moreno-Villoslada, I., Water-soluble polymer–metal ion interactions. *Progress in Polymer Science* **2003,** *28* (2), 173-208.

14. Bannister, D. J.; Davies, G. R.; Ward, I. M.; McIntyre, J. E., Ionic conductivities for poly(ethylene oxide) complexes with lithium salts of monobasic and dibasic acids and blends of poly(ethylene oxide) with lithium salts of anionic polymers. *Polymer* **1984,** *25* (9), 1291-1296.

15. Zhang, H.; Li, C.; Piszcz, M.; Coya, E.; Rojo, T.; Rodriguez-Martinez, L. M.; Armand, M.; Zhou, Z., Single lithium-ion conducting solid polymer electrolytes: advances and perspectives. *Chemical Society Reviews* **2017,** *46* (3), 797-815.

16. (a) Porcarelli, L.; Manojkumar, K.; Sardon, H.; Llorente, O.; Shaplov, A. S.; Vijayakrishna, K.; Gerbaldi, C.; Mecerreyes, D., Single Ion Conducting Polymer Electrolytes Based On Versatile Polyurethanes. *Electrochimica Acta* **2017,** *241* (Supplement C), 526-534; (b) Ma, Q.; Zhang, H.; Zhou, C.; Zheng, L.; Cheng, P.; Nie, J.; Feng, W.; Hu, Y.-S.; Li, H.; Huang, X.; Chen, L.; Armand, M.; Zhou, Z., Single Lithium-Ion Conducting Polymer Electrolytes Based on a Super-Delocalized Polyanion. *Angewandte Chemie International Edition* **2016,** *55* (7), 2521-2525.

17. Meziane, R.; Bonnet, J.-P.; Courty, M.; Djellab, K.; Armand, M., Single-ion polymer electrolytes based on a delocalized polyanion for lithium batteries. *Electrochimica Acta* **2011,** *57*, 14-19.

18. Feuillade, G.; Perche, P., Ion-conductive macromolecular gels and membranes for solid lithium cells. *Journal of Applied Electrochemistry* **1975,** *5* (1), 63-69.

19. Honary, S.; Orafai, H., The Effect of Different Plasticizer Molecular Weights and Concentrations on Mechanical and Thermomechanical Properties of Free Films. *Drug Development and Industrial Pharmacy* **2002,** *28* (6), 711-715.

20. (a) Porcarelli, L.; Gerbaldi, C.; Bella, F.; Nair, J. R., Super soft all-ethylene oxide polymer electrolyte for safe all-solid lithium batteries. *Scientific reports* **2016,** *6*, 19892; (b) Eshetu, G. G.; Mecerreyes, D.; Forsyth, M.; Zhang, H.; Armand, M., Polymeric ionic liquids for lithium-based rechargeable batteries. *Molecular Systems Design & Engineering* **2019,** *4* (2), 294-309.

21. (a) Tominaga, Y.; Yamazaki, K., Fast Li-ion conduction in poly(ethylene carbonate)-based electrolytes and composites filled with TiO2 nanoparticles. *Chemical Communications* **2014,** *50* (34), 4448-4450; (b) Weston, J. E.; Steele, B. C. H., Effects of inert fillers on the mechanical and electrochemical properties of lithium salt-poly(ethylene oxide) polymer electrolytes. *Solid State Ionics* **1982,** *7* (1), 75-79.

22. Li, Z. H.; Zhang, H. P.; Zhang, P.; Li, G. C.; Wu, Y. P.; Zhou, X. D., Effects of the porous structure on conductivity of nanocomposite polymer electrolyte for lithium ion batteries. *Journal of Membrane Science* **2008,** *322* (2), 416-422.

23. (a) Dou, S.; Zhang, S.; Klein, R. J.; Runt, J.; Colby, R. H., Synthesis and Characterization of Poly(Ethylene Glycol)-Based Single-Ion Conductors. *Chemistry of Materials* 2006, *18* (18), 4288-4295; (b) Roach, D. J.; Dou, S.; Colby, R. H.; Mueller, K. T., Nuclear magnetic resonance investigation of dynamics in poly(ethylene oxide)-based lithium polyether-ester-sulfonate ionomers. *The Journal of Chemical Physics* 2012, *136* (1), 014510; (c) Zhang, S.; Dou, S.; Colby, R. H.; Runt, J., Glass transition and ionic conduction in plasticized and doped ionomers. *Journal of non-crystalline solids* 2005, *351* (33-36), 2825-2830; (d) Fragiadakis, D.; Dou, S.; Colby, R. H.; Runt, J., Molecular mobility and Li+ conduction in polyester copolymer ionomers based on poly (ethylene oxide). *The Journal of chemical physics* 2009, *130* (6), 064907.

24. Angell, C. A., Polymer electrolytes—Some principles, cautions, and new practices. *Electrochimica Acta* 2017, *250*, 368-375.

25. (a) Porcarelli, L.; Shaplov, A. S.; Salsamendi, M.; Nair, J. R.; Vygodskii, Y. S.; Mecerreyes, D.; Gerbaldi, C., Single-Ion Block Copoly(ionic liquid)s as Electrolytes for All-Solid State Lithium Batteries. *ACS Applied Materials & Interfaces* 2016; (b) Zhang, H.; Oteo, U.; Zhu, H.; Judez, X.; Martinez-Ibañez, M.; Aldalur, I.; Sanchez-Diez, E.; Li, C.; Carrasco, J.; Forsyth, M.; Armand, M., Enhanced Lithium-Ion Conductivity of Polymer Electrolytes by Selective Introduction of Hydrogen into the Anion. *Angewandte Chemie International Edition* 2019, *58* (23), 7829-7834; (c) Oteo, U.; Martinez-Ibañez, M.; Aldalur, I.; Sanchez-Diez, E.; Carrasco, J.; Armand, M.; Zhang, H., Improvement of the Cationic Transport in Polymer Electrolytes with (Difluoromethanesulfonyl)(trifluoromethanesulfonyl)imide Salts. *ChemElectroChem* 2019, *6* (4), 1019-1022.

26. Laidler, K. J., The development of the Arrhenius equation. *Journal of Chemical Education* 1984, *61* (6), 494.

27. Ratner, M., Aspects of the Theoretical Treatment of Polymer Solid Electrolytes: Transport Theory and Models. *Applied Science* 1987, *23*, 173-236.

28. Abraham, K. M.; Jiang, Z.; Carroll, B., Highly Conductive PEO-like Polymer Electrolytes. *Chemistry of Materials* 1997, *9* (9), 1978-1988.

29. Gu, G.; Bouvier, S.; Wu, C.; Laura, R.; Rzeznik, M.; Abraham, K., 2-Methoxyethyl (methyl) carbonate-based electrolytes for Li-ion batteries. *Electrochimica acta* 2000, *45* (19), 3127-3139.

30. MacCallum, J. R.; Vincent, C. A., *Polymer electrolyte reviews*. Springer Science & Business Media: 1989; Vol. 2.

31. Miyamoto, T.; Shibayama, K., Free-volume model for ionic conductivity in polymers. *Journal of Applied Physics* 1973, *44* (12), 5372-5376.

32. (a) MacFarlane, D. R.; Zhou, F.; Forsyth, M., Ion conductivity in amorphous polymer/salt mixtures. *Solid State Ionics* 1998, *113-115*, 193-197; (b) Forsyth, M.; Meakin, P.; MacFarlane, D. R., 13C NMR spin–lattice relaxation times as a probe of local polymer dynamics in plasticized polyethers. *Journal of Materials Chemistry* 1997, *7* (2), 193-201.

33. Evans, J.; Vincent, C. A.; Bruce, P. G., Electrochemical measurement of transference numbers in polymer electrolytes. *Polymer* 1987, *28* (13), 2324-2328.

34. Zugmann, S.; Fleischmann, M.; Amereller, M.; Gschwind, R. M.; Wiemhöfer, H. D.; Gores, H. J., Measurement of transference numbers for lithium ion electrolytes via four different methods, a comparative study. *Electrochimica Acta* 2011, *56* (11), 3926-3933.

35. Pinson, M. B.; Bazant, M. Z., Theory of SEI formation in rechargeable batteries: capacity fade, accelerated aging and lifetime prediction. *Journal of the Electrochemical Society* 2013, *160* (2), A243-A250.

36. Pang, Q.; Liang, X.; Shyamsunder, A.; Nazar, L. F., An In Vivo Formed Solid Electrolyte Surface Layer Enables Stable Plating of Li Metal. *Joule* 2017, *1* (4), 871-886.

37. (a) Di Noto, V.; Lavina, S.; Giffin, G. A.; Negro, E.; Scrosati, B., Polymer electrolytes: Present, past and future. *Electrochimica Acta* 2011, *57*, 4-13; (b) Quartarone, E.; Mustarelli, P., Electrolytes for solid-state lithium rechargeable

batteries: recent advances and perspectives. *Chemical Society Reviews* 2011, *40* (5), 2525-2540.

38. (a) Morioka, T.; Nakano, K.; Tominaga, Y., Ion-Conductive Properties of a Polymer Electrolyte Based on Ethylene Carbonate/Ethylene Oxide Random Copolymer. *Macromolecular Rapid Communications* 2017, *38* (8), 1600652-n/a; (b) Tominaga, Y.; Nakano, K.; Morioka, T., Random copolymers of ethylene carbonate and ethylene oxide for Li-Ion conductive solid electrolytes. *Electrochimica Acta* 2019, *312*, 342-348.

39. Devaux, D.; Bouchet, R.; Glé, D.; Denoyel, R., Mechanism of ion transport in PEO/LiTFSI complexes: Effect of temperature, molecular weight and end groups. *Solid State Ionics* 2012, *227*, 119-127.

40. Berthier, C.; Gorecki, W.; Minier, M.; Armand, M. B.; Chabagno, J. M.; Rigaud, P., Microscopic investigation of ionic conductivity in alkali metal salts-poly(ethylene oxide) adducts. *Solid State Ionics* 1983, *11* (1), 91-95.

41. Gomez, E. D.; Panday, A.; Feng, E. H.; Chen, V.; Stone, G. M.; Minor, A. M.; Kisielowski, C.; Downing, K. H.; Borodin, O.; Smith, G. D., Effect of ion distribution on conductivity of block copolymer electrolytes. *Nano letters* 2009, *9* (3), 1212-1216.

42. Pitawala, H.; Dissanayake, M.; Seneviratne, V.; Mellander, B.-E.; Albinson, I., Effect of plasticizers (EC or PC) on the ionic conductivity and thermal properties of the (PEO) 9 LiTf: Al 2 O 3 nanocomposite polymer electrolyte system. *Journal of Solid State Electrochemistry* 2008, *12* (7-8), 783-789.

43. (a) Takeda, Y.; Imanishi, N.; Yamamoto, O., Developments of the advanced all-solid-state polymer electrolyte lithium secondary battery. *Electrochemistry* 2009, *77* (9), 784-797; (b) Xi, J.; Qiu, X.; Zhu, W.; Tang, X., Enhanced electrochemical properties of poly (ethylene oxide)-based composite polymer electrolyte with ordered mesoporous materials for lithium polymer battery. *Microporous and mesoporous materials* 2006, *88* (1-3), 1-7.

44. Mazor, H.; Golodnitsky, D.; Rosenberg, Y.; Peled, E.; Wieczorek, W.; Scrosati, B., Solid composite polymer electrolytes with high cation transference number. *Israel Journal of Chemistry* 2008, *48* (3-4), 259-268.

45. Meyer, W. H., Polymer electrolytes for lithium-ion batteries. *Advanced materials* 1998, *10* (6), 439-448.

46. Mindemark, J.; Lacey, M. J.; Bowden, T.; Brandell, D., Beyond PEO—Alternative host materials for Li+-conducting solid polymer electrolytes. *Progress in Polymer Science* 2018, *81*, 114-143.

47. Kimura, K.; Motomatsu, J.; Tominaga, Y., Correlation between Solvation Structure and Ion-Conductive Behavior of Concentrated Poly(ethylene carbonate)-Based Electrolytes. *The Journal of Physical Chemistry C* 2016, *120* (23), 12385-12391.

48. (a) Spiegel, E. F.; Adamic, K. J.; Williams, B. D.; Sammells, A. F., Solvation of lithium salts within single-phase dimethyl siloxane bisphenol-A carbonate block copolymer. *Polymer* 2000, *41* (9), 3365-3369; (b) Matsumoto, M.; Uno, T.; Kubo, M.; Itoh, T., Polymer electrolytes based on polycarbonates and their electrochemical and thermal properties. *Ionics* 2013, *19* (4), 615-622.

49. (a) Tomita, H.; Sanda, F.; Endo, T., Reactivity comparison of five- and six-membered cyclic carbonates with amines: Basic evaluation for synthesis of poly(hydroxyurethane). *Journal of Polymer Science Part A: Polymer Chemistry* 2001, *39* (1), 162-168; (b) Rokicki, G., Aliphatic cyclic carbonates and spiroorthocarbonates as monomers. *Progress in Polymer Science* 2000, *25* (2), 259-342.

50. (a) Xu, J.; Feng, E.; Song, J., Renaissance of aliphatic polycarbonates: New techniques and biomedical applications. *Journal of Applied Polymer Science* 2014, *131* (5); (b) Tominaga, Y.; Nanthana, V.; Tohyama, D., Ionic conduction in poly(ethylene carbonate)-based rubbery electrolytes including lithium salts. *Polymer Journal* 2012, *44*, 1155.

51. Tominaga, Y.; Yamazaki, K.; Nanthana, V., Effect of anions on lithium ion conduction in poly (ethylene carbonate)-based polymer electrolytes. *Journal of the Electrochemical Society* 2015, *162* (2), A3133-A3136.

52. Tominaga, Y.; Nanthana, V.; Tohyama, D., Ionic conduction in poly(ethylene carbonate)-based rubbery electrolytes including lithium salts. *Polym J* 2012, *44* (12), 1155-1158.

53. Okumura, T.; Nishimura, S., Lithium ion conductive properties of aliphatic polycarbonate. *Solid State Ionics* 2014, *267*, 68-73.

54. Forsyth, M.; Sun, J.; Macfarlane, D. R.; Hill, A. J., Compositional dependence of free volume in PAN/LiCF3SO3 polymer-in-salt electrolytes and the effect on ionic conductivity. *Journal of Polymer Science Part B: Polymer Physics* 2000, *38* (2), 341-350.

55. Kimura, K.; Matsumoto, H.; Hassoun, J.; Panero, S.; Scrosati, B.; Tominaga, Y., A QuaternaryPoly(ethylene carbonate)-Lithium Bis(trifluoromethanesulfonyl)imide-Ionic Liquid-Silica Fiber Composite Polymer Electrolyte for Lithium Batteries. *Electrochimica Acta* 2015, *175*, 134-140.

56. Kimura, K.; Yajima, M.; Tominaga, Y., A highly-concentrated poly(ethylene carbonate)-based electrolyte for all-solid-state Li battery working at room temperature. *Electrochemistry Communications* 2016, *66*, 46-48.

57. (a) Konieczynska, M. D.; Lin, X.; Zhang, H.; Grinstaff, M. W., Synthesis of Aliphatic Poly(ether 1,2-glycerol carbonate)s via Copolymerization of CO2 with Glycidyl Ethers Using a Cobalt Salen Catalyst and Study of a Thermally Stable Solid Polymer Electrolyte. *ACS Macro Letters* 2015, *4* (5), 533-537; (b) Morioka, T.; Ota, K.; Tominaga, Y., Effect of oxyethylene side chains on ion-conductive properties of polycarbonate-based electrolytes. *Polymer* 2016, *84*, 21-26; (c) Tominaga, Y.; Shimomura, T.; Nakamura, M., Alternating copolymers of carbon dioxide with glycidyl ethers for novel ion-conductive polymer electrolytes. *Polymer* 2010, *51* (19), 4295-4298.

58. Nakamura, M.; Tominaga, Y., Utilization of carbon dioxide for polymer electrolytes [II]: Synthesis of alternating copolymers with glycidyl ethers as novel ion-conductive polymers. *Electrochimica Acta* 2011, *57*, 36-39.

59. Zhang, J.; Zhao, J.; Yue, L.; Wang, Q.; Chai, J.; Liu, Z.; Zhou, X.; Li, H.; Guo, Y.; Cui, G.; Chen, L., Safety-Reinforced Poly(Propylene Carbonate)-Based All-Solid-State Polymer Electrolyte for Ambient-Temperature Solid Polymer Lithium Batteries. *Advanced Energy Materials* 2015, *5* (24), 1501082.

60. Melchiors, M.; Keul, H.; Höcker, H., Preparation and properties of solid electrolytes on the basis of alkali metal salts and poly(2,2-dimethyltrimethylene carbonate)-block-poly(ethylene oxide)-block-poly(2,2-dimethyltrimethylene carbonate). *Polymer* 1996, *37* (9), 1519-1527.

61. (a) Smith, M. J.; Silva, M. M.; Cerqueira, S.; MacCallum, J. R., Preparation and characterization of a lithium ion conducting electrolyte based on poly(trimethylene carbonate). *Solid State Ionics* 2001, *140* (3), 345-351; (b) Silva, M. M.; Barros, S. C.; Smith, M. J.; MacCallum, J. R., Characterization of solid polymer electrolytes based on poly(trimethylenecarbonate) and lithium tetrafluoroborate. *Electrochimica Acta* 2004, *49* (12), 1887-1891; (c) Silva, M. M.; Barbosa, P.; Evans, A.; Smith, M. J., Novel solid polymer electrolytes based on poly (trimethylene carbonate) and lithium hexafluoroantimonate. *Solid state sciences* 2006, *8* (11), 1318-1321; (d) Barbosa, P. C.; Rodrigues, L. C.; Silva, M. M.; Smith, M. J., Characterization of pTMCnLiPF6 solid polymer electrolytes. *Solid State Ionics* 2011, *193* (1), 39-42.

62. Mindemark, J.; Mogensen, R.; Smith, M. J.; Silva, M. M.; Brandell, D., Polycarbonates as alternative electrolyte host materials for solid-state sodium batteries. *Electrochemistry Communications* 2017, *77*, 58-61.

63. Sun, B.; Mindemark, J.; Edström, K.; Brandell, D., Polycarbonate-based solid polymer electrolytes for Li-ion batteries. *Solid State Ionics* 2014, *262*, 738-742.

64. Sun, B.; Mindemark, J.; V. Morozov, E.; Costa, L. T.; Bergman, M.; Johansson, P.; Fang, Y.; Furó, I.; Brandell, D., Ion transport in polycarbonate based solid polymer

electrolytes: experimental and computational investigations. *Physical Chemistry Chemical Physics* 2016, *18* (14), 9504-9513.

65. Sun, B.; Mindemark, J.; Edström, K.; Brandell, D., Realization of high performance polycarbonate-based Li polymer batteries. *Electrochemistry Communications* 2015, *52*, 71-74.

66. (a) Mindemark, J.; Imholt, L.; Brandell, D., Synthesis of high molecular flexibility polycarbonates for solid polymer electrolytes. *Electrochimica Acta* 2015, *175*, 247-253; (b) Mindemark, J.; Imholt, L.; Montero, J.; Brandell, D., Allyl ethers as combined plasticizing and crosslinkable side groups in polycarbonate-based polymer electrolytes for solid-state Li batteries. *Journal of Polymer Science Part A: Polymer Chemistry* 2016, *54* (14), 2128-2135.

67. Mindemark, J.; Sun, B.; Brandell, D., Hydroxyl-functionalized poly(trimethylene carbonate) electrolytes for 3D-electrode configurations. *Polymer Chemistry* 2015, *6* (26), 4766-4774.

68. He, W.; Cui, Z.; Liu, X.; Cui, Y.; Chai, J.; Zhou, X.; Liu, Z.; Cui, G., Carbonate-linked poly(ethylene oxide) polymer electrolytes towards high performance solid state lithium batteries. *Electrochimica Acta* 2017, *225*, 151-159.

69. Ouhib, F.; Meabe, L.; Mahmoud, A.; Eshraghi, N.; Grignard, B.; Thomassin, J.-M.; Aqil, A.; Boschini, F.; Jérôme, C.; Mecerreyes, D.; Detrembleur, C., CO2-sourced polycarbonates as solid electrolytes for room temperature operating lithium batteries. *Journal of Materials Chemistry A* 2019, *7* (16), 9844-9853.

70. Xu, C.; Sun, B.; Gustafsson, T.; Edström, K.; Brandell, D.; Hahlin, M., Interface layer formation in solid polymer electrolyte lithium batteries: an XPS study. *Journal of Materials Chemistry A* 2014, *2* (20), 7256-7264.

71. Xu, K., Nonaqueous liquid electrolytes for lithium-based rechargeable batteries. *Chemical Reviews* 2004, *104* (10), 4303-4417.

72. Britz, J.; Meyer, W. H.; Wegner, G., Blends of Poly(meth)acrylates with 2-Oxo-(1,3)dioxolane Side Chains and Lithium Salts as Lithium Ion Conductors. *Macromolecules* 2007, *40* (21), 7558-7565.

73. Wang, Y.; Fan, F.; Agapov, A. L.; Saito, T.; Yang, J.; Yu, X.; Hong, K.; Mays, J.; Sokolov, A. P., Examination of the fundamental relation between ionic transport and segmental relaxation in polymer electrolytes. *Polymer* 2014, *55* (16), 4067-4076.

74. Matsumoto, K.; Kakehashi, M.; Ouchi, H.; Yuasa, M.; Endo, T., Synthesis and Properties of Polycarbosilanes Having 5-Membered Cyclic Carbonate Groups as Solid Polymer Electrolytes. *Macromolecules* 2016, *49* (24), 9441-9448.

75. Kaplan, M. L.; Rietman, E. A.; Cava, R. J.; Holt, L. K.; Chandross, E. A., Crown ether enhancement of ionic conductivity in a polymer-salt system. *Solid State Ionics* 1987, *25* (1), 37-40.

76. Wei, X.; Shriver, D. F., Highly Conductive Polymer Electrolytes Containing Rigid Polymers. *Chemistry of Materials* 1998, *10* (9), 2307-2308.

77. Chai, J.; Liu, Z.; Ma, J.; Wang, J.; Liu, X.; Liu, H.; Zhang, J.; Cui, G.; Chen, L., In Situ Generation of Poly (Vinylene Carbonate) Based Solid Electrolyte with Interfacial Stability for LiCoO2 Lithium Batteries. *Advanced Science* 2017, *4* (2), 1600377.

78. Itoh, T.; Fujita, K.; Inoue, K.; Iwama, H.; Kondoh, K.; Uno, T.; Kubo, M., Solid polymer electrolytes based on alternating copolymers of vinyl ethers with methoxy oligo(ethyleneoxy)ethyl groups and vinylene carbonate. *Electrochimica Acta* 2013, *112*, 221-229.

79. Mitsuda, H.; Uno, T.; Kubo, M.; Itoh, T., Solid Polymer Electrolytes Based on Poly(1,3-diacetyl-4-imidazolin-2-one). *Polymer Bulletin* 2006, *57* (3), 313-319.

80. (a) Klaus, S.; Lehenmeier, M. W.; Anderson, C. E.; Rieger, B., Recent advances in CO2/epoxide copolymerization—new strategies and cooperative mechanisms. *Coordination Chemistry Reviews* 2011, *255* (13-14), 1460-1479; (b) Inoue, S.; Koinuma, H.; Tsuruta, T., Copolymerization of carbon dioxide and epoxide. *Journal of Polymer Science Part B: Polymer Letters* 1969, *7* (4), 287-292.

81. (a) Helou, M.; Miserque, O.; Brusson, J.-M.; Carpentier, J.-F.; Guillaume, S. M., Ultraproductive, Zinc-Mediated, Immortal Ring-Opening Polymerization of Trimethylene Carbonate. *Chemistry – A European Journal* 2008, *14* (29), 8772-

8775; (b) Nuyken, O.; Pask, S. D., Ring-Opening Polymerization—An Introductory Review. *Polymers* 2013, *5* (2), 361-403.

82. Einhorn, A., Ueber die Carbonate der Dioxybenzole. *Justus Liebigs Annalen der Chemie* 1898, *300* (2), 135-155.

83. Schobert, H. H.; Song, C., Chemicals and materials from coal in the 21st century. *Fuel* 2002, *81* (1), 15-32.

84. Meabe, L.; Sardon, H.; Mecerreyes, D., Hydrolytically degradable poly(ethylene glycol) based polycarbonates by organocatalyzed condensation. *European Polymer Journal* 2017, *95*, 737-745.

85. Sun, J.; Kuckling, D., Synthesis of high-molecular-weight aliphatic polycarbonates by organo-catalysis. *Polymer Chemistry* 2016, *7* (8), 1642-1649.

86. (a) Haba, O., Itakura, I., Ueda, M. and Kuze, S., Synthesis of polycarbonate from dimethyl carbonate and bisphenol-a through a non-phosgene process. *J. Polym. Sci. A Polym. Chem.* 1999, *37*, 2087–2093; (b) Park, J. H.; Jeon, J. Y.; Lee, J. J.; Jang, Y.; Varghese, J. K.; Lee, B. Y., Preparation of High-Molecular-Weight Aliphatic Polycarbonates by Condensation Polymerization of Diols and Dimethyl Carbonate. *Macromolecules* 2013, *46* (9), 3301-3308; (c) Zhu, W.; Huang, X.; Li, C.; Xiao, Y.; Zhang, D.; Guan, G., High-molecular-weight aliphatic polycarbonates by melt polycondensation of dimethyl carbonate and aliphatic diols: synthesis and characterization. *Polymer International* 2011, *60* (7), 1060-1067.

87. Cornille, A.; Auvergne, R.; Figovsky, O.; Boutevin, B.; Caillol, S., A perspective approach to sustainable routes for non-isocyanate polyurethanes. *European Polymer Journal* 2017, *87*, 535-552.

88. Bossion, A.; Heifferon, K. V.; Meabe, L.; Zivic, N.; Taton, D.; Hedrick, J. L.; Long, T. E.; Sardon, H., Opportunities for organocatalysis in polymer synthesis via step-growth methods. *Progress in Polymer Science* 2018.

89. (a) Mutlu, H.; Ruiz, J.; Solleder, S. C.; Meier, M. A. R., TBD catalysis with dimethyl carbonate: a fruitful and sustainable alliance. *Green Chemistry* 2012, *14* (6), 1728-1735; (b) Hult, D.; Garcia-Gallego, S.; Ingverud, T.; Andren, O. C. J.;

Malkoch, M., Degradable high Tg sugar-derived polycarbonates from isosorbide and dihydroxyacetone. *Polymer Chemistry* 2018.

90. (a) Bigot, S.; Kébir, N.; Plasseraud, L.; Burel, F., Organocatalytic synthesis of new telechelic polycarbonates and study of their chemical reactivity. *Polymer* 2015, *66*, 127-134; (b) Naik, P. U.; Refes, K.; Sadaka, F.; Brachais, C.-H.; Boni, G.; Couvercelle, J.-P.; Picquet, M.; Plasseraud, L., Organo-catalyzed synthesis of aliphatic polycarbonates in solvent-free conditions. *Polymer Chemistry* 2012, *3* (6), 1475-1480.

91. (a) Nederberg, F.; Connor, E. F.; Möller, M.; Glauser, T.; Hedrick, J. L., New Paradigms for Organic Catalysts: The First Organocatalytic Living Polymerization. *Angewandte Chemie International Edition* 2001, *40* (14), 2712-2715; (b) Dove, A. P., Organic Catalysis for Ring-Opening Polymerization. *ACS Macro Letters* 2012, *1* (12), 1409-1412.

92. (a) Meabe, L.; Huynh, T. V.; Lago, N.; Sardon, H.; Li, C.; O'Dell, L. A.; Armand, M.; Forsyth, M.; Mecerreyes, D., Poly(ethylene oxide carbonates) solid polymer electrolytes for lithium batteries. *Electrochimica Acta* 2018, *264*, 367-375; (b) Meabe, L.; Lago, N.; Rubatat, L.; Li, C.; Müller, A. J.; Sardon, H.; Armand, M.; Mecerreyes, D., Polycondensation as a Versatile Synthetic Route to Aliphatic Polycarbonates for Solid Polymer Electrolytes. *Electrochimica Acta* 2017, *237*, 259-266.

93. Bi, F. L.; Xi, Z. H.; Zhao, L., Reaction Mechanisms and Kinetics of the Melt Transesterification of Bisphenol-A and Diphenyl Carbonate. *International Journal of Chemical Kinetics* 2018.

94. (a) Eo, Y. S.; Rhee, H.-W.; Shin, S., Catalyst screening for the melt polymerization of isosorbide-based polycarbonate. *Journal of Industrial and Engineering Chemistry* 2016, *37*, 42-46; (b) Ma, C.; Xu, F.; Cheng, W.; Tan, X.; Su, Q.; Zhang, S., Tailoring Molecular Weight of Bioderived Polycarbonates via Bifunctional Ionic Liquids Catalysts under Metal-Free Conditions. *ACS Sustainable Chemistry & Engineering* 2018, *6* (2), 2684-2693.

95. Basterretxea, A.; Gabirondo, E.; Jehanno, C.; Zhu, H.; Flores, I.; Müller, A. J.; Etxeberria, A.; Mecerreyes, D.; Coulembier, O.; Sardon, H., Polyether Synthesis by Bulk Self-Condensation of Diols Catalyzed by Non-Eutectic Acid–Base Organocatalysts. *ACS Sustainable Chemistry & Engineering* 2019, *7* (4), 4103-4111.

CHAPTER 2.

Synthesis and characterization of aliphatic polycarbonates as solid polymer electrolytes

CHAPTER 2.

Synthesis and characterization of aliphatic polycarbonates as solid polymer electrolytes

2.1 Introduction

Aliphatic polycarbonates based SPEs have shown promising ionic conductivity values, good electrochemical stability and high lithium transference number.[1] In those works, the aliphatic carbonates have been synthesized mainly using two main routes: i) ring-opening polymerization (ROP) of cyclic carbonates,[1a, 2] and ii) copolymerization between CO_2 and epoxides.[3] Although these synthetic routes are successful, they suffer from some limitations and synthetic difficulties for chemical modifications. For instance, the chemical structure of the studied aliphatic polycarbonates as host materials is limited to the availability of cyclic monomers. In the case of ROP, usually trimethylene carbonate is employed, which leads to three-carbon spacer, and

regarding epoxide rings, induce two-carbon spacer. In order to study the effect of spacer between the carbonate units polycondensation technique has to be employed.

Polycarbonates having ethylene oxide links between carbonate groups, synthesized through polycondensation, have been proposed by He and co-workers.[4] In the same direction, in this chapter, we present the synthesis of a series of aliphatic polycarbonates by simple melt polycondensation employing organocatalysis.[5] This synthetic method offers the possibility of designing great variety of aliphatic polycarbonates by adjusting the chemical structure of the commercially available aliphatic diol. Using this method, first of all, a series of eight different aliphatic polycarbonates are developed, ranging from 4 to 12 methylene units between the carbonate groups. Once the chemical structure and thermal properties are discussed, the possibilities of this synthetic method are explored; a series of copolymer families are carefully developed. Finally, how the number of methylene units and LiTFSI concentration affects the electrochemical properties of homopolymers are evaluated.

2.2 Results and discussion

2.2.1 Synthesis and characterization of aliphatic homopolycarbonates having between 4 and 12 methylene groups

Aliphatic polycarbonates have gained great attention in the last decade in the area of solid polymer electrolytes. The low glass transition and high lithium cation mobility due to the weak coordination with carbonate groups has provoked the interest in this polymer family. Thus, following the polycondensation synthetic route depicted in Scheme 2.1, eight different aliphatic polycarbonates were obtained as light-brownish

solids, with a yield between 85 and 90 %. Thus, 1,4-butanediol, 1,5-pentanediol, 1,6-hexanediol, 1,7-heptanediol, 1,8-octanediol, 1,9-nonanediol, 1,10-decanediol, 1-12-dodecanediol, led to aliphatic polycarbonates named as: P4C, P5C, P6C, P7C, P8C, P9C, P10C, P12C, respectively.

Scheme 2.1. Polycondensation route to obtain eight aliphatic polycarbonates.

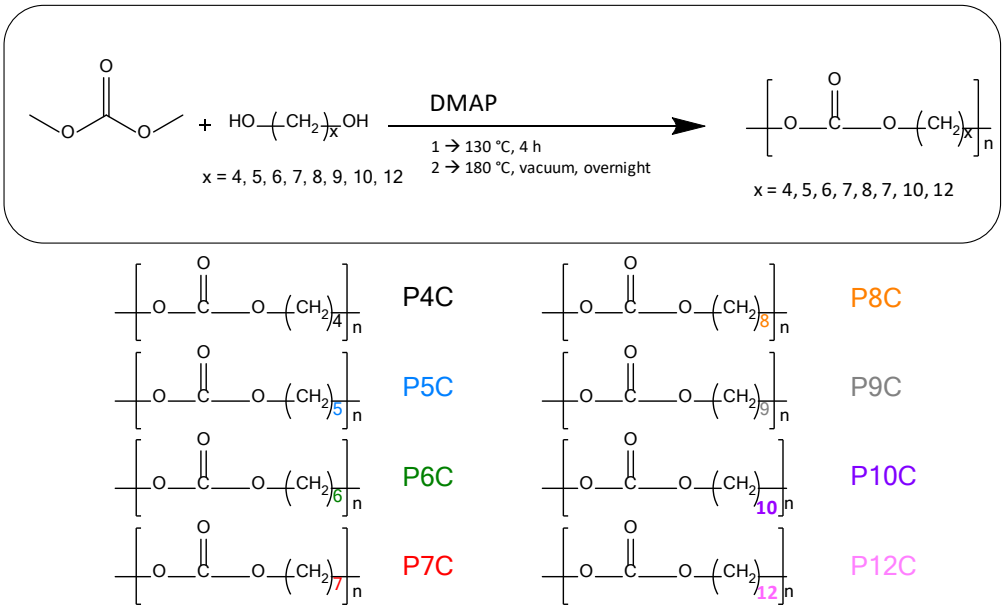

Firstly, in order to confirm the chemical structure, the aliphatic polycarbonates were characterized by NMR. **Figure 2.1** shows a representative example of the ^{1}H NMR and ^{13}C NMR of P6C. The NMRs of the other aliphatic polycarbonates are shown in the **Appendix Figure A1, A2**. The ^{1}H NMR spectrum shows signals at 4.12, 1.68 and 1.41 ppm, which are attributed to the methylene protons of the polymer backbone. Furthermore, the small signal at 3.78 ppm assigned to methoxy groups, indicates that the polymer is terminated by methoxy functionality. The ^{13}C NMR spectrum shows the signal of the carbonyl group at 155.34 ppm, confirming the chemical nature of

the carbonate polymer. Moreover, the signals at 67.78, 28.56 and 25.39 ppm are attributed to the different methylene carbons of the polymer backbone.

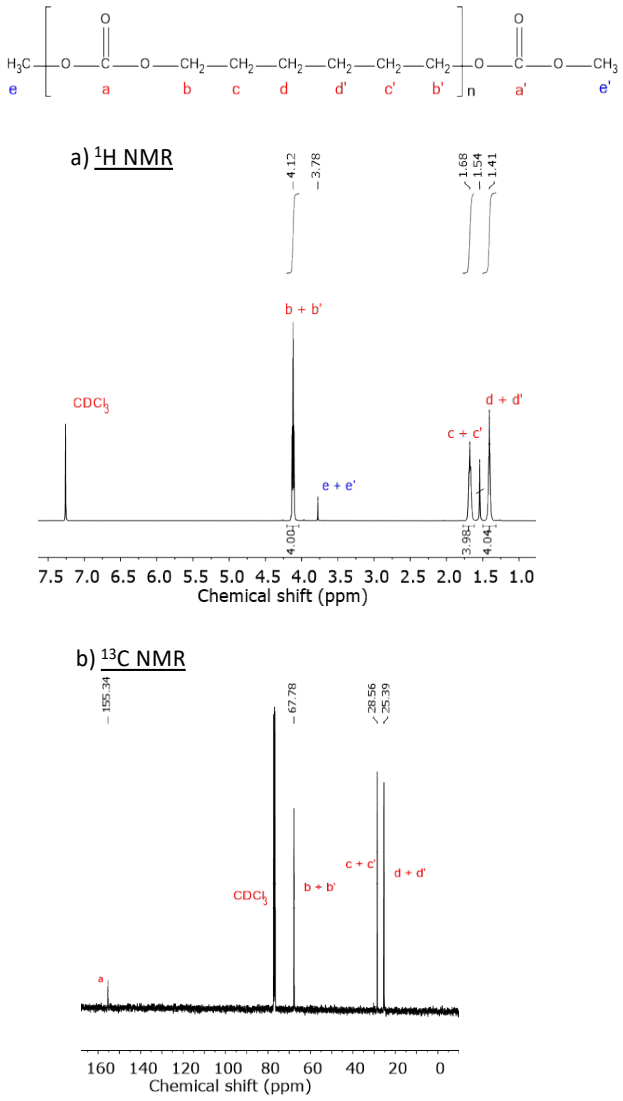

Figure 2.1. Representative a) ^{1}H NMR, and b) ^{13}C NMR spectra of poly(hexamethylene carbonate), P6C.

Table 2.1 summarizes the absolute molar masses measured by GPC/SEC and thermal properties measured by DSC of the aliphatic polycarbonates. The molar masses determined by multiangle light-scattering detector, showed values between 8,000 and 43,000 g mol^{-1}, which are common values for polycondensation polymers.[5] Although there is not a clear reason, experimentally we observed that, the smaller the diol, the higher the molar mass of the aliphatic polycarbonates.

Table 2.1. Results of the molar masses and thermal characterization of aliphatic polycarbonates.

Homopolymers	M_n (mol g^{-1})[1]	Đ	T_g (°C)[d]	T_m (°C)[a]	T_m (°C)[c]	T_c (°C)[b]	ΔH_m (J g^{-1})[c]
P4C	43,300	1.6	-36	55	55	27	47
P5C	27,700	1.6	-43	47	--	--	--
P6C	25,100	1.7	-50	51	46	40	44
P7C	14,800	1.5	-50	47	43	34	57
P8C	15,300	1.4	-54	57	56	42	40
P9C	16,100	1.5	-48	51	51	42	82
P10C	8,000	1.5	-37	57	56	48	83
P12C	8,100	1.6	-37	63	64	58	99

[1] Molar masses measured by multiangle light scattering. [a] The data is recorded from the DSC measurements in the first heating scan. [b] The data recorded from the first cooling scan. [c] The data is recorded from the DSC measurements in the second heating scan. Heating and cooling scan rates: 20 K min^{-1} and 2 K min^{-1} respectively. [d] Data measured during the 3rd heating scan at 20 K min^{-1}, after performing a ballistic cooling.

Next, the crystallization and glass transition of the different aliphatic polycarbonates were characterized by Differencial Scanning Calorimetry (DSC). The DSC thermograms are shown in the Figure 2.2 and melting temperature (T_m), crystallization temperature (T_c) and glass transition temperature (T_g) were determined for all the samples. As a

first observation, in the first scan, all the aliphatic polycarbonates were semicrystalline polymers, showing melting temperatures between 47 and 63 °C. It is worth to note, that these polycarbonates show different behavior; most of the aliphatic polycarbonates used so far as host materials, they were amorphous,[1a] whereas these are semicrystalline materials. Furthermore, it was noticed that there is a change in the melting temperature with the number of CH_2 on the repetitive unit: the polymers which have an odd number of CH_2 moieties (P5C, P7C and P9C) show a lower melting temperature than the ones having even number of CH_2 (P4C, P6C, P8C, P10C and P12C). Same observations have already been reported, which has been coined as odd-even effect.[6] Additionally, the trend on T_m can be clearly noted, **Figure 2.2b**, which increases when increasing the methylene units number. The same trend is observed for crystallization temperature, a higher value is observed for even number of units, and also the value is increased with CH_2 units. According to the ΔH_m the behavior is similar to the melting/crystallization temperatures; it is higher with the even ones and lower with odd ones, while the value is also increasing when the repeating unit has higher number of CH_2. On the other hand, aliphatic polycarbonates showed glass transition temperatures between -36 and -54 °C, **Table 2.1**. T_g is usually related to the CH_2 moieties on the repetitive unit. As it has been previously reported,[6] in our case also, the T_g slightly decreases with an increase in the CH_2 number in the repeating unit, until the value 8 is reached, beyond in which the T_g starts to increase.

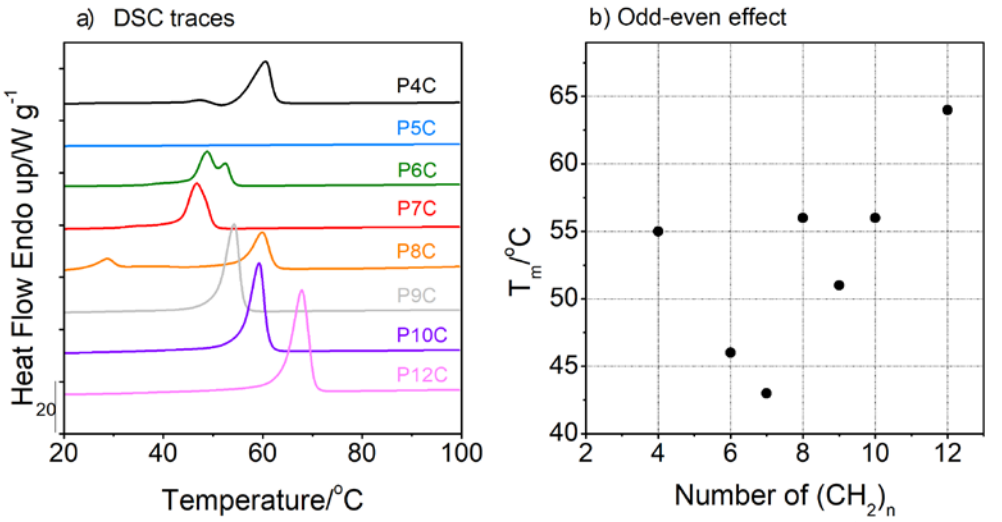

Figure 2.2. a) DSC traces of the aliphatic polycarbonates obtained during the 2nd heating scan at 20 K min^{-1}, and b) graphical representation comparing the relationship between the T_m value and the number of methylene groups of the 2nd heating scan at 20 K min^{-1}.

2.2.2 Potential use of polycondensation on the synthesis of copolymers

The advantage of the versatile melt polycondensation was proved by the successful synthesis of a series of copolymers. The monomers, 1,4-butanediol, 1,7-heptanediol, and 1,12-dodecanediol were selected from the previous section.[7] The homopolymers where chosen according to the melting temperature: 1,7-heptanediol characterized as the lowest melting temperature, and 1,4-butanediol and 1,12-dodecanediol defined as the highest melting temperatures of the family. The combination of different diols in the synthesis was successfully achieved following the same procedure as for the homopolymers. With this method a series of different copolymers poly(heptane-co-dodecane carbonate) P7C-P12C, poly(butane-co-dodecane carbonate) P4C-P12C and poly(heptane-co-butane carbonate) P7C-P4C were synthesized (Scheme 2.2).

Scheme 2.2. Polycondensation of diols and dimethyl carbonate leading to random aliphatic polycarbonate copolymers.

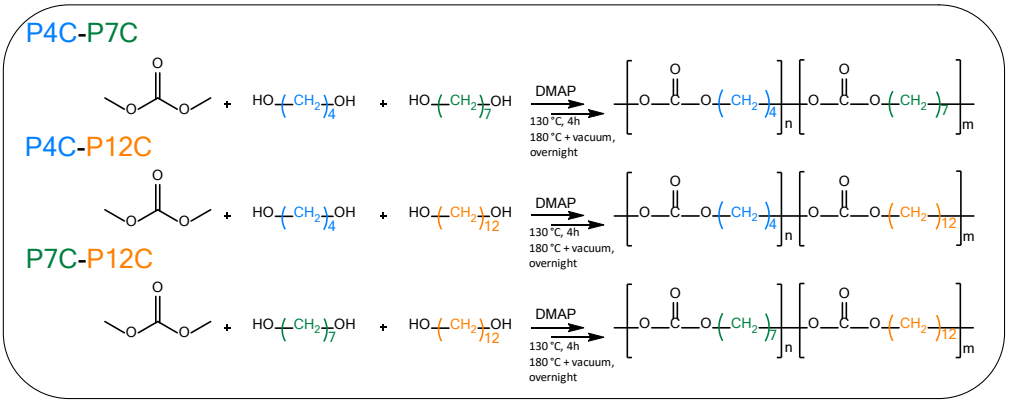

The chemical characterization of the copolymers was carried out by ^{1}H NMR, ^{13}C NMR, and GPC. The molar composition of the copolymers was determined ^{1}H NMR technique. As an illustrative example, the obtained P4C-P7C random copolymer with an initial monomer feed of 60:40 mol% is depicted in **Figure 2.3**. The peak attributed to 3 C**H**$_2$ methylene units in the middle of the repetitive unit corresponding to 1,7-heptanediol, integrates to 6 protons. In this way, the value of the rest of the areas could be estimated with respect to that area, and thereby, the mol ratio of the repetitive units could be easily calculated. All the synthesized copolymers were analysed using similar methodology and further information is provided in **Appendix Figure A3, A4**. Even if the initial feed was 60:40 mol% of 1,4-butanediol and 1,7-heptanediol, respectively, the final composition of copolymer is determined by integrating the areas of ^{1}H NMR spectrum, 66:44 mol%. The composition of the 24 copolymers synthesized are shown in **Table 2.2**. Even if the initial monomer ratio and the final composition in the copolymer are not exactly the same, the final composition is related to the monomer feed.

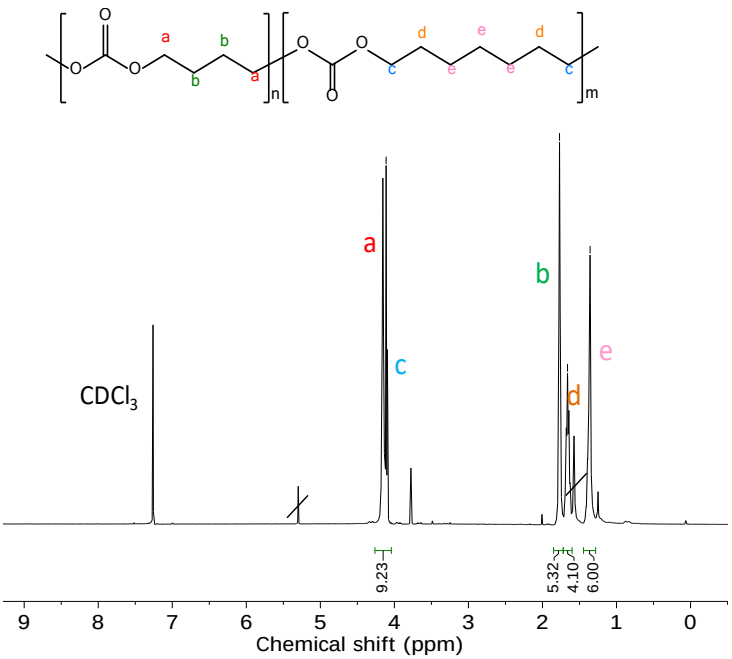

Figure 2.3. ^{1}H NMR of P4C-P7C 60:40 mol% in $CDCl_3$.

Table 2.2. Chemical characterization of copolymers: P7C-P12C, P4C-P12C and P4C-P7C.

Initial monomer feed %		Copolymer composition (^{1}H NMR)		GPC (PS standard)		Randomnes (^{13}C NMR)
Heptane-diol	Dodecane-diol	P7C	P12C	M_n (g mol^{-1})	Đ	R
95	05	95	5	17,000	1.8	0.64
90	10	90	10	13,000	1. 7	0.65
80	20	82	18	14,000	1.6	0.89
70	30	67	33	9,200	1.9	1.13
60	40	56	44	20,000	1,6	1.02
50	50	43	57	13,000	1,7	0.98
40	60	40	60	26,000	1,4	1.15
20	80	16	84	19,000	1,6	0.79

Butane-diol	Dodecane-diol	P4C	P12C	M_n (g mol^{-1})	Đ	R
95	05	94	6	11,000	1.6	0.77
90	10	88	12	12,000	1.3	0.96
85	15	82	18	6,000	1.7	1.09
80	20	67	33	14,000	1.6	1.07
60	40	55	45	11,000	1.5	1.09
50	50	43	57	23,000	1.6	1.01
40	60	34	66	15,000	1.6	1.06
20	80	17	83	16,000	1.5	1.03
Butane-diol	Heptane-diol	P4C	P7C	M_n (g mol^{-1})	Đ	R
95	05	92	8	11,000	1.5	0.71
90	10	85	15	17,000	1.4	0.72
80	20	75	25	22,000	1.6	0.76
60	40	66	44	11,000	1.4	1.02
40	60	33	67	11,000	1.6	1.04
20	80	21	79	6,000	1.6	0.99
10	90	10	90	18,000	1.6	0.92
05	95	6	94	15,000	1.6	0.62

The commoner distributions in the copolymer (random / blocky / alternate) is a fundamental factor, which will significantly affect the final properties such as crystallinity or biodegradation rate. The degree of randomness (R) of the copolymers is defined using the three different **Equation 2.1**, **2.2**, and **2.3**, and it is measured by ^{13}C NMR analysis.[8] **Figure 2.4** shows the ^{13}C NMR of P4C-P7C 60:40 mol% structure. The signals around 155 and 67 ppm, which are split in three and four peaks, are attributed to the carbonyl and –O<u>C</u>H$_2$– carbon resonance, respectively. A correct assignation of the peaks can lead to determine different dyad sequences of the copolymers, and consequently, the chemical structure of the copolymer. In this occasion, the split of carbonyl resonance is evaluated to determine the

microstructure of the copolymer (**Appendix Figure A5-A7**). The degree of the randomness can be obtained applying the following equations:

$$R = \frac{1}{L_{nP4C}} + \frac{1}{L_{nP7C}} \quad \text{Equation 2.1.}$$

$$L_{nP4C} = \frac{f_{P4C-P7C} + 2f_{P4C-P4C}}{f_{P4C-P7C}} \quad \text{Equation 2.2.}$$

$$L_{nP7C} = \frac{f_{P4C-P7C} + 2f_{P7C-P7C}}{f_{P4C-P7C}} \quad \text{Equation 2.3.}$$

where $f_{P4C\text{-}P4C}$, $f_{P4C\text{-}P47}$, and $f_{P7C\text{-}P7C}$ describe the dyads fraction, whereas L_{nP4C} and L_{nP4C} determines the number-average sequence length of the repetitive units.

The carbonyl resonance of P4C-P7C (60:40 mol%) is split in 3 peaks at 155.50, 155.42, and 155.33 ppm, corresponding to the dyads P7C-P7C ($f_{P7C\text{-}P7C}$), P4C-P7C ($f_{P4C\text{-}P7C}$), and P4C-P4C ($f_{P4C\text{-}P4C}$), respectively (**Figure 2.4**). Based on the relative integrated areas and using **Equations 2.1-2.3**, the microstructure of the copolymers is calculated. Considering that in block copolymers R equals to 0, in random copolymers R equals to 1, and in alternate copolymers R equals to 2, the microstructure of the copolymer is deduced (**Table 2.2-2.3**). This value in most of the cases is close to 1, which confirms the random nature of the samples.

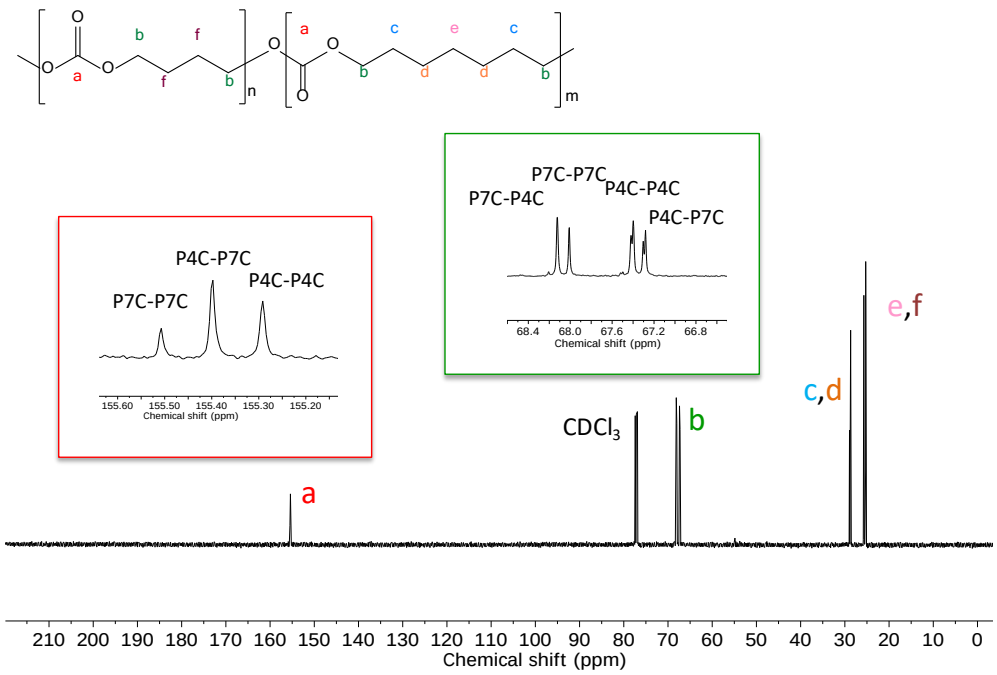

Figure 2.4. ^{13}C NMR analysis of P4C-P7C 60:40 mol% in $CDCl_3$. The signals of –O<u>C</u>OO- and -OCOO<u>C</u>H_2- zoomed, 155.60 – 1555.20 ppm and 68.4 – 66.8 ppm zoomed, respectively.

The molar mass has a direct effect on the thermal properties of the material. Therefore, the molar mass of the material was carefully determined by GPC in THF, using narrow PS standards. A similar M_n value between the copolymers was found, close to 15,000 g mol^{-1} (**Table 2.1-2.3**). The polydispersities obtained by GPC measurements are common values in polycondensation based synthesis, values between 1.3 and 2.0. These similar results allow to compare the properties of the different polycarbonates.

2.2.3 Electrochemical characterization of solid polymer electrolytes based on aliphatic homopolycarbonates

The eight homopolymers were evaluated as matrix for polymer electrolytes by adding LiTFSI salt to them in order to have mobile ions. The Arrhenius plots of the synthesized polycarbonates containing 30 wt.% of LiTFSI are presented in **Figure 2.5a**. The lowest ionic conductivity at room temperature was showed by P4C, $4 \cdot 10^{-7}$ S cm^{-1}, and the highest value observed was $6 \cdot 10^{-6}$ S cm^{-1} given by P7C. The rest of polycarbonates showed intermediate values following the series as: P7C > P12C > P9C = P6C > P10C > P8C > P5C = P4C. At 100 °C the SPEs based on P4C showed the lowest a value of $9 \cdot 10^{-5}$ S cm^{-1} and the highest value was obtained now for P12C with a value of $5 \cdot 10^{-4}$ S cm^{-1}. Although there is a slight trend which indicates that the higher the number of methylene groups the higher the ionic conductivity, several exceptions to this rule are observed. Besides, molar mass takes an important role in these results; P10C and P12C have the lowest value, showing one of the best values, which could be attributed to fewer entanglements. Moreover, these results are also linked to the DSC measurements, **Figure 2.5b**. Generally, the ionic conductivity is higher when the T_g is lower, except, where the melting point of the polymer is observed at low temperatures. All glass transitions of the SPEs were characterized, showing values of -51 °C for P4C, -36 °C/P5C, -52 °C/P6C, -54 °C/P7C, -44 °C/P8C, -41 °C/P9C, -59 °C/P10C and -58 °C/P12C. Although there are some exceptions, some relationship between high ionic conductivity and low T_g can be drawn. On the other hand, the ionic conductivity of P8C, P10C and P12C at room temperature is affected by the semicrystallinity.

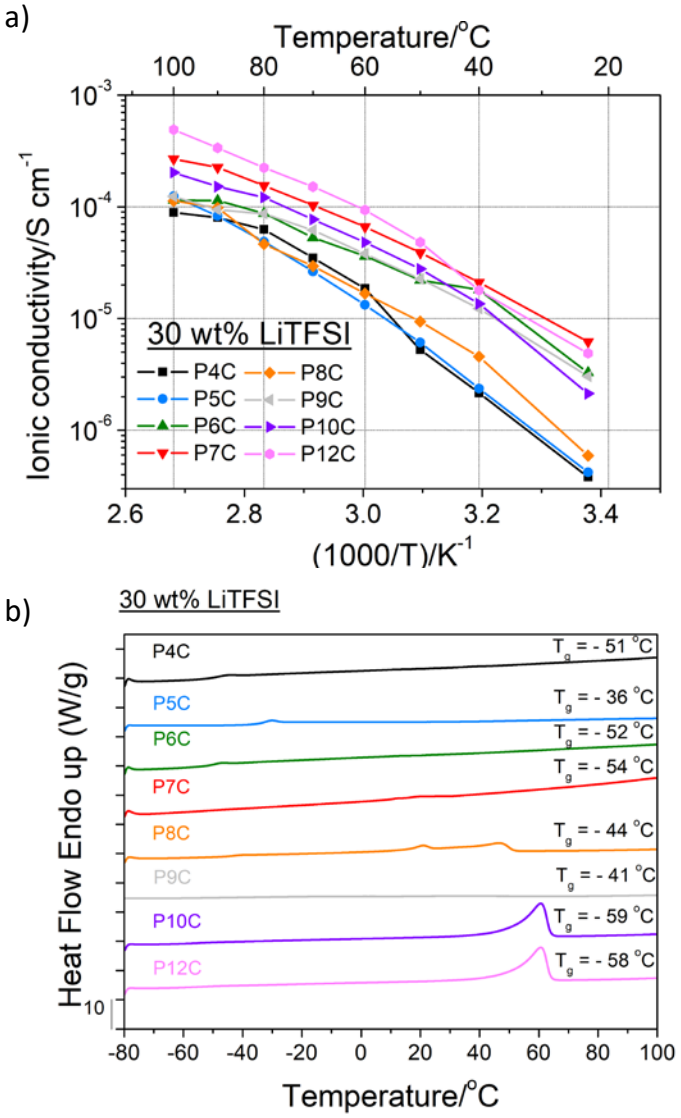

Figure 2.5. Aliphatic polycarbonates with 30 wt.% of LiTFSI. a) Arrhenius plot of solid polymer electrolytes, and b) DSC traces obtained during the 2nd heating scan at 20 K min^{-1}.

To further investigate the nature of the aliphatic polycarbonate and its influence on the ionic conductivity of the SPEs, several SPEs were formulated by different amounts of LiTFSI. The variation of the ionic conductivity, the coordination of lithium ion with

the carbonate group and, thereby the T_g were studied for three selected polycarbonates. For these experiments, we selected the aliphatic polycarbonates which showed the highest values of ionic conductivity such as P7C and P12C, and one of the lowest one, P5C. Solid polymer electrolytes based on P5C, P7C and P12C were blended with five salt concentrations: 20 wt.%, 30 wt.%, 40 wt.%, 60 wt.% and 80 wt.% of LiTFSI. The temperature dependence Arrhenius plot of the ionic conductivity for P5C-LiTFSI, P7C-LiTFSI and P12C-LiTFSI are shown in **Figure 2.6**.

As a first general observation, the highest conductivity values were obtained for P12C SPEs, then for P7C and the lowest for P5C. Two different effects of the salt addition were detected. In the case of P5C and P7C the maximum values of ionic conductivity were obtained SPEs containing between 20 and 30 wt.% of LiTFSI while by adding more salt, the ionic conductivity decreases. SPEs of P5C-20 wt.% LiTFSI and P7C-30 wt.% LiTFSI, showed an ionic conductivity of $2 \cdot 10^{-6}$ and $6 \cdot 10^{-6}$ S cm^{-1} respectively at room temperature, **Figure 2.6a,b**. A possible explanation for this behavior was found in the DSC thermograms, showed in **Figure 2.7a,b**. In the cases of P5C-SPE and P7C-SPE, the SPEs were amorphous electrolytes. P5C-SPE, beyond 20 and 30 wt.%, the glass transition clearly increases, from -40 °C to -35 °C. In these samples, the salt is acting as a physical cross-linker, decreasing the ion mobility.

On the other hand, in regards to P12C, the highest ionic conductivity was shown by the highest salt concentration, **Figure 2.6c**. The ionic conductivity values were significantly increased, from $3 \cdot 10^{-7}$ S cm^{-1} with 20 wt.% of LiTFSI, until $1 \cdot 10^{-4}$ S cm^{-1} with 80 wt.% of LiTFSI at 25 °C. It is worth to note that the value of $1 \cdot 10^{-4}$ S cm^{-1} at room temperature reported here, represents one of the highest conductivity values reported so far for polycarbonates, i.e. PEC-LiFSI (188 mol.%) shows ionic conductivity around 10^{-5} S cm^{-1}.[9] However, this polymer electrolyte cannot be considered as a free-

standing membrane, due to the low molar mass of P12C (8,100 g mol^{-1}), a viscous material is obtained. Moreover, DSC traces pronounced a different P12C-SPEs behavior respected to P5C-SPE and P7C-SPE. At low salt concentration, P12C-SPEs were semicrystalline, and by the addition of the salt the melting enthalpy is decreased, **Figure 2.7c,** and the glass transition of P12C-SPEs is not affected by the amount of salt. Herein, the trend of this ionic conductivity can be due to several factors: i) the decrease of crystallinity with the addition of salt can increase the ionic mobility, especially at room temperature; and ii) long hydrophobic spacers between the carbonyl groups can affect the solubility of the salt, thereby, the behavior/mechanism of ionic conductivity could be different. A similar trend with long hydrophobic spacers have been coined by Olmedo and co-workers.[10] Moreover, in order to prove the effect of molar mass on electrochemical properties, P12C with 23,900 g mol^{-1} was synthesized. As a result, a decrease on ionic conductivity was observed: with high molar mass P12C, 23,900 g mol^{-1}, and 80 wt.% LiTFSI, the ionic conductivity decreases significantly, $3 \cdot 10^{-6}$ S cm^{-1}.

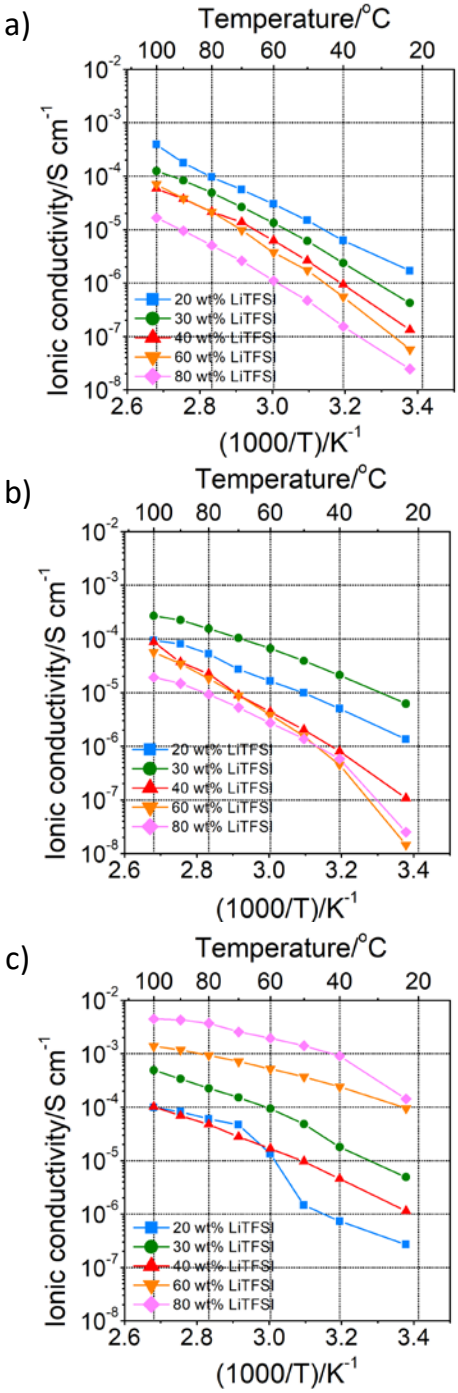

Figure 2.6. Ionic conductivity analysis of LiTFSI - SPEs: a) P5C, b) P7C, and c) P12C.

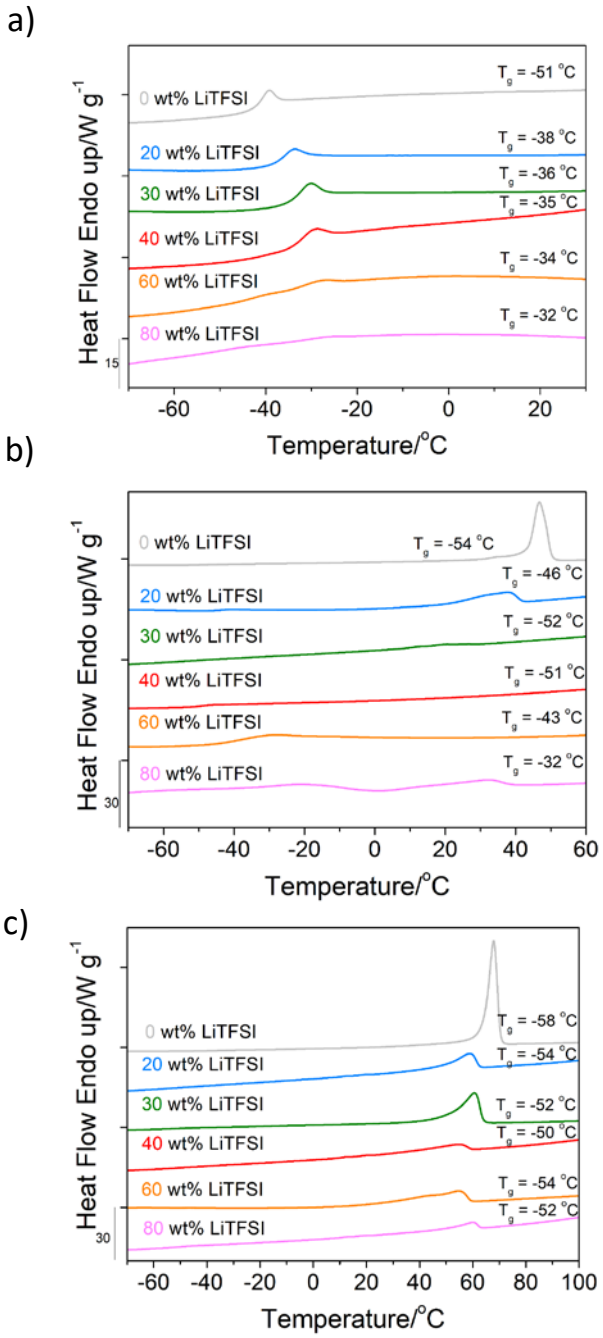

Figure 2.7. DSC analysis of LiTFSI - SPEs: a) P5C, b) P7C, and c) P12C. 2nd heating scan at 20 K min.

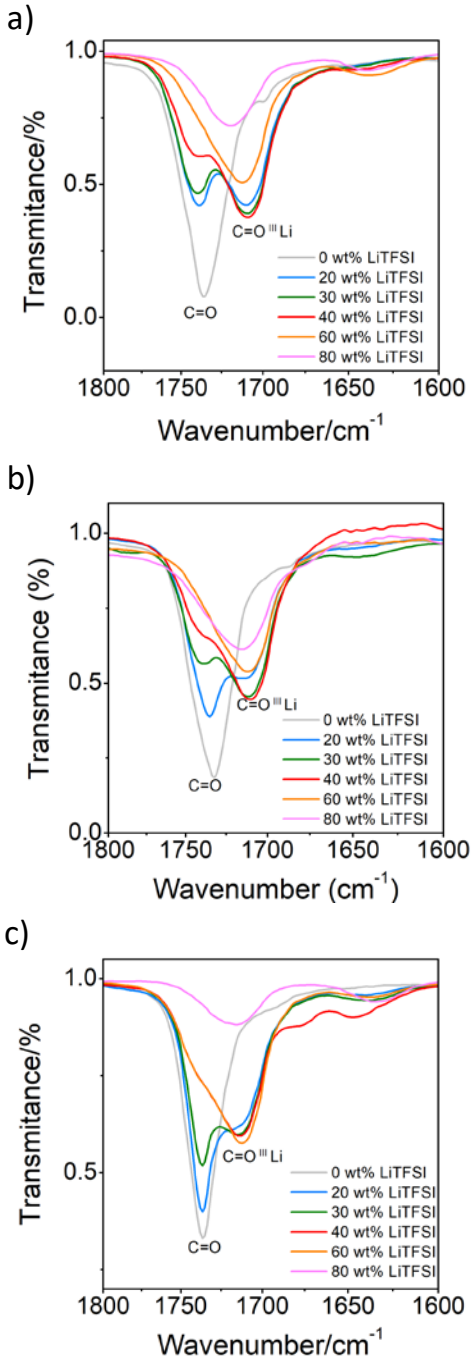

Figure 2.8. FTIR-ATR analysis of LiTFSI - SPEs: a) P5C, b) P7C, and c) P12C.

In previous works, the FTIR spectra demonstrated how lithium cation is able to coordinate with carbonyl group of the carbonate chemistry.[9b, 11] The FTIR spectra of P5C, P7C, and P12C with different amounts of LiTFSI are shown in **Figure 2.8**. The neat homopolymers showed one single carbonyl stretching at 1740 cm^{-1}. At low salt concentrations two vibrations of carbonyl group can be distinguished in all the SPEs; free carbonyl group at 1740 cm^{-1} and carbonyl group coordinated with the lithium cation around 1710 cm^{-1}. However, at high salt concentrations, mainly the vibration of coordinated carbonyl group appears. This new band at lower wavenumber is associated to the coordination between the lithium cation and the polycarbonate backbone.

Electrochemical stability window of P12C (80 wt.% LiTFSI) was evaluated by cyclic voltammetry at 60 °C, which is depicted on **Figure 2.9**. According to anodic limit of the polymer was found to be stable up to 4 V *vs.* Li/Li^+. Besides, during the cathodic scan, reversible peaks at -0.33 and 0.16 vs. Li/Li^+ corresponds to lithium plating/stripping, confirming the capability of the polymer to transport lithium ions. Moreover, the two strong redox peaks at 0.79 and 1 V vs. Li/Li^+ in cathodic scan seem to be reversible, which could be attributed to some impurities at the electrode surface.

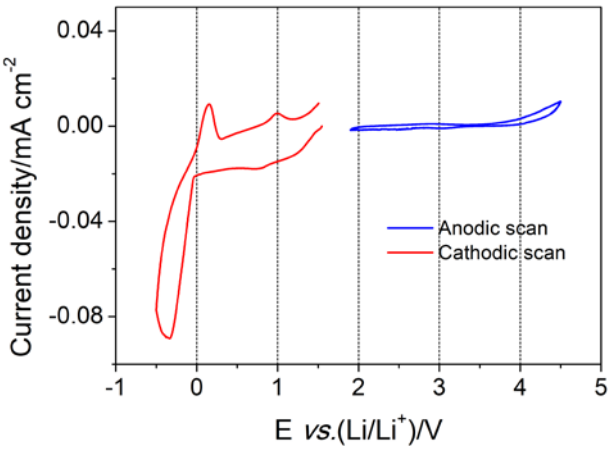

Figure 2.9. Electrochemical stability window obtained by CV at 0.5 mV s^{-1} for P12C, 80 wt.% LiTFSI at 60 °C.

2.3 Conclusions

In this chapter, we showed the versatility of polycondensation to obtain a variety of new aliphatic homopolymers and copolymers. We successfully proved the ability of this method to tune the polycarbonates chemical structure, by simply changing the structure of commercially available diol. In all the cases homogeneous molar masses (15,000 g mol^{-1}) and pure polymers were developed. According to the DSC analysis the effect of chemical structure on thermal properties were discussed, where an odd-even effect for the homopolymers was observed. We have to highlight that, these polycarbonates are semicrystalline materials, the opposite that was observed so far for poly(ethyelene carbonate) and poly(trimethylene carbonate).

The use of aliphatic homopolymers was evaluated as host materials of solid polymer electrolytes by dissolving different LiTFSI concentrations in the matrix. The results indicate that structure of the polycarbonate, molar mass of the polymer and the amount of salt affect glass transition temperature, crystallinity, and consequently, ionic conductivity. A higher ionic conductivity was characterized for the

polycarbonate containing higher methylene units, being poly(dodecamethylene carbonate) with 80 wt.% of LiTFSI the highest, which displayed an excellent ionic conductivity value of $1 \cdot 10^{-4}$ S cm^{-1} at room temperature and an electrochemical stability window up to 4 V. This high value of poly(dodecamethylene carbonate) can be attributed to the structure of the polymer; the addition of LiTFSI leads unique properties due to crystallinity and long hydrophobic spacer. Using other host polymers (few methylene units), the behavior was different; the addition of the salt leads to amorphous materials; high LiTFSI concentrations increases the glass transition temperature, and thereby, a lower ionic conductivity values were observed.

Altogether, polycondensation strategy offers several advantages to engineer polycarbonates. The desired final properties can be adjusted by selecting the correct diol. Regarding to the electrochemical properties, the structure of the polycarbonate will influence on the trend of the ionic conductivity.

2.4 Experimental part

2.4.1 Materials

Dry dimethyl carbonate (99+ %) and 4-dimethilaminopyridine (DMAP) (99%) were purchased from Across Organics. 1,4-butanediol (99+%), 1,5-pentanediol (98%), 1,7-heptanediol (95%), 1,8-octanediol (99+%), 1,9-nonanediol (99%), 1,10-decanediol (99%) and 1,12-dodecandeiol (98%) were supplied by Across Organics and 1,6-hexanediol (99%) by Sigma-Aldrich. All diols and DMAP were dried for 5 h prior to use. Lithium bis(trifluoromethane)sulfonimide (LiTFSI) (99.9%) was supplied from Solvionic. Tetrahydrofuran (GPC grade) was obtained from Scharlab, dry acetonitrile (ACN) (99.9%) from Across Organics, dichloromethane (DCM) (Cerfified AR for Analysis) and methanol (MeOH) (Certified AR for Analysis) from Fisher Scientific,

toluene (HPLC grace) from Sigma-Aldrich and deuterated chloroform (99.8%) from Deutero GmbH.

2.4.2 Aliphatic homopolymer synthesis

The chemical route used in this work was similar to the one previously reported.[5] Essentially, DMC, diol and the organocatalyst, DMAP, were added into a schlenk flask, where the flask was connected to the vacuum line. A 2:1:0.01 molar ratio of DMC:diol:DMAP was used. P6C: DMC (8 mL, 95 mmol, 2 eq.), 1,6-hexanediol (5.6 g, 47.5 mmol, 1 eq), DMAP (57.9 mg, 0.475 mmol, 0.01 eq). The temperature was raised and kept isothermally at 130 °C for 4 h. Then again, the temperature was increased until 180 °C and high vacuum was applied. The reaction was left overnight. The high vacuum was necessary in the second step to remove the MeOH produced during the first step and to evaporate the excess DMC added to the flask. All the polymers were dissolved in dichloromethane and purified by precipitation in cold methanol, obtaining a yield around 85 % in all the cases. The polymers were characterized by ^{1}H NMR and ^{13}C NMR. The following example is given for P6C. ^{1}H NMR ($CDCl_3$ 500 MHz): δ = 4.12 (t, OCOOC**H**$_2$, 4H), 1.68 (m, OCOOCH$_2$C**H**$_2$, 4 H) and 1.41 (m, OCOOCH$_2$CH$_2$C**H**$_2$, 4 H). ^{13}C NMR ($CDCl_3$ 500 MHz): δ = 155.34 (O**C**OO), 67.78 (OCOO**C**H$_2$), 28.56 (OCOOCH$_2$**C**H$_2$), 25.39 (OCOOCH$_2$CH$_2$**C**H$_2$).

2.4.3 Copolymer synthesis

As in the case of homopolymers, in the first step, dried reagents were introduced in a 50 mL of schlenk, flask which was placed in an oil bath at 130 °C, over 4 h. During the second step the temperature was raised at 180 °C and high vacuum was applied overnight. Using this methodology 3 different polycarbonates families were synthesized, changing the structure of diols and the mol ratio of diols. For all polycarbonates a mol ratio of DMC:diol:DMAP 2:1:0.01 was used. For instance, P4C-

P7C 60:40 mol% was synthesized using the following amounts of reactants: DMC (8 mL, 95 mmol, 2 eq.), diols (1 eq.): 1,4-butanediol (2.57 g, 28.48 mmol, 0.60 eq.), 1,7-heptanediol (2.51 g, 18.99 mmol, 0.4 eq), DMAP (57.9 mg, 0.475 mmol, 0.01 eq.). Once the reaction was stopped, the polymers were dissolved in dichloromethane and powdered in cold methanol, yield above 85 %. The disappearance of the monomers was confirmed by ^{1}H NMR. The final composition of the polymer was characterized by ^{1}H NMR ($CDCl_3$, 400 MHz), as an example P4C:P7C, δ= 4.15 (t, OCOOC**H₂**, 4H (P4C)), 4.11 (t, OCOOC**H**$_2$, 4H (P7C)), 1.77 (t, $OCOOCH_2C$**H**$_2$, 4H (P4C)), 1.66 (t, $OCOOCH_2C$**H**$_2$, 4H (P7C)), 1.36 (t, $OCOOCH_2CH_2C$**H**$_2C$**H**$_2C$**H**$_2CH_2CH_2OCOO$, 6H (P7C)). The yield of the polymerization was determined by gravimetric (yield = 85 %).

2.4.4 Preparation of solid polymer electrolytes

Solid polymer electrolytes were prepared by solvent casting method from solution in anhydrous ACN (0.3 g of polymer/salt in 0.5 mL dry ACN). The solutions were directly casted onto the stainless steel spacers. First, ACN was removed under vacuum at room temperature during 24 h, and then after, the evaporation was completed inside of an argon filled glovebox, increasing the temperature up to 60 °C and applying vacuum for another 24 h. The samples were sandwiched between two stainless steel (SS) electrodes (average surface area = 2.01 cm^2) in a coin cell CR2016 assembled in an argon-filled glove box (M-Braun).

To perform the electrochemical stability window study the polymer electrolyte, P12C 80 wt.% LiTFSI, was prepared directly casting on stainless steel or copper disk, the solvent was removed as it has been explained previously.

2.4.5 Characterization methods

^{1}H and ^{13}C Nuclear Magnetic Resonance (NMR) spectra were recorded on Bruker spectrometers at 500 MHz at room temperature, using deuterated chloroform.

The absolute molar masses of homopolycarbonates were analyzed by SEC/MALS/RI. The equipment was composed of a LC20 pump (Shimadzu) coupled to a DAWN Heleos multiangle (18 angles) light scattering laser photometer equipped with an He–Ne laser (λ = 658 nm) and an Optilab Rex differential refractometer (λ = 658 nm), (all from Wyatt Technology Corp., USA). Separation was carried out using three columns in series (Styragel HR2, HR4, and HR6; with pore sizes from 10 2 to 10 6 Å). Filtered toluene was used for the calibration of the 90° scattering intensity. The detectors at angles other than 90° in the MALS instrument were normalized to the 90° detector using a standard (PS 28 770 g mol^{-1}; Polymer Labs), which is small enough to produce isotropic scattering, at a flow rate of THF through the detectors of 1 mL min^{-1}. In addition, the same standard and conditions were used to perform the alignment (interdetector delay volume) between concentration and light-scattering detectors and the band-broadening correction for the sample dilution between detectors. The analyses were performed at 35 °C and THF was used as a mobile phase at a flow rate of 1 mL min^{-1}. $\partial n/\partial C$ was measured being around 0.06 mg mL^{-1} for all the homopolymers. The absolute molar mass was calculated from the RI/MALS data using the Debye plot (with first-order Zimm formalism) by using the ASTRA software version 6.0.3 (Wyatt Technology, USA).

Besides, molar mass distributions of the copolymers were measured by size exclusion chromatography (SEC). Samples were diluted in THF (GPC grade) to a concentration of approximately 5 mg mL^{-1} and filtered through a 0.45 mm nylon filter. The SEC set up consisted of a pump (LC-20A, Shimadzu), an autosampler (Waters 717), a differential refractometer (Waters 2410) and three columns in series (Styragel HR2, HR4, and HR6 with pore sizes ranging from 102 to 106 Å). Chromatograms were obtained in THF (GPC grade) at 35 °C using a flow rate of 1 mL min^{-1}. The equipment

was calibrated using narrow polystyrene standards ranging from 595 to $3.95 \cdot 10^{-6}$ g mol^{-1} (5^{th} order universal calibration).

A Perkin Elmer 8500 DSC equipped with an Intracooler III was employed in this study to characterize thermal properties. All the experiments were performed under ultrapure nitrogen flow and the instrument was calibrated with dodecane, indium and tin standards. Samples of 5 mg were used. Measurements were performed by placing the samples in sealed aluminum pans. The samples were first heated at a rate of 20 K min^{-1}, from 25 °C to 100 °C and they were left 3 min at 100 °C to avoid the influence of thermal history, in order to be able to compare the crystallization/melting temperature afterwards. Subsequently, it was cooled down to -80 °C at a rate of 2 K min^{-1}. Once again, it was heated up until 100 °C at 20 K min^{-1} after waiting during 3 min at -80 °C. In order to determine the glass transition temperature, it was performed a ballistic cooling at the data was recorded during the heating scan at 20 K min^{-1}.

Attenuated Total Reflectance Fourier Transform Infrared Spectroscopy measurements (ATR-FTIR) were conducted on a Bruker ALPHA Spectrometer.

All electrochemical measurements were carried out on a VMP3 (Biologic, Claix, France) potentiostat. Ionic conductivity of the polymer electrolytes was determined by AC impedance spectroscopy over the frequency range from 100 mHz to 1 MHz with an amplitude of 10 mV. The conductivities were analyzed in a temperature range down from 100 °C to 25 °C.

Electrochemical stability window was determined applying cyclic voltammetry (CV) of the polymer electrolyte at 60 °C. The anodic limit was evaluated between open circuit potential (OCV) and 4.5 V *vs*. Li/Li^+ at a constant rate of 0.5 m Vs^{-1}. On the other hand,

the anodic scan was determined between OCV and -0.5 V *vs* .Li/Li^+ using the same scan rate. The polymer electrolyte was sandwiched between a metal lithium disk and a working electrode. Metallic lithium served as a reference and counter electrode. Besides, stainless steel disk was used as working electrode during anodic stability study, whereas copper disks for cathodic measurements. The samples were sealed in CR2032 coin cells.

2.5 References

1. (a) Sun, B.; Mindemark, J.; Edström, K.; Brandell, D., Polycarbonate-based solid polymer electrolytes for Li-ion batteries. *Solid State Ionics* **2014,** *262*, 738-742; (b) Mindemark, J.; Lacey, M. J.; Bowden, T.; Brandell, D., Beyond PEO—Alternative host materials for Li+-conducting solid polymer electrolytes. *Progress in Polymer Science* **2018,** *81*, 114-143.

2. Mindemark, J.; Sun, B.; Törmä, E.; Brandell, D., High-performance solid polymer electrolytes for lithium batteries operational at ambient temperature. *Journal of Power Sources* **2015,** *298*, 166-170.

3. (a) Tominaga, Y.; Shimomura, T.; Nakamura, M., Alternating copolymers of carbon dioxide with glycidyl ethers for novel ion-conductive polymer electrolytes. *Polymer* **2010,** *51* (19), 4295-4298; (b) Nakamura, M.; Tominaga, Y., Utilization of carbon dioxide for polymer electrolytes [II]: Synthesis of alternating copolymers with glycidyl ethers as novel ion-conductive polymers. *Electrochimica Acta* **2011,** *57*, 36-39; (c) Morioka, T.; Ota, K.; Tominaga, Y., Effect of oxyethylene side chains on ion-conductive properties of polycarbonate-based electrolytes. *Polymer* **2016,** *84*, 21-26.

4. He, W.; Cui, Z.; Liu, X.; Cui, Y.; Chai, J.; Zhou, X.; Liu, Z.; Cui, G., Carbonate-linked poly(ethylene oxide) polymer electrolytes towards high performance solid state lithium batteries. *Electrochimica Acta* **2017,** *225*, 151-159.

5. Sun, J.; Kuckling, D., Synthesis of high-molecular-weight aliphatic polycarbonates by organo-catalysis. *Polymer Chemistry* **2016,** *7* (8), 1642-1649.

6. Su, W.; Feng, J.; Wang, H.-F.; Zhang, X.-Z.; Zhuo, R.-X., Controllable preparation of poly(alkylene carbonate)s and observation on their structure-related odd–even effect. *Polymer* 2010, *51* (5), 1010-1015.

7. Meabe, L.; Lago, N.; Rubatat, L.; Li, C.; Müller, A. J.; Sardon, H.; Armand, M.; Mecerreyes, D., Polycondensation as a Versatile Synthetic Route to Aliphatic Polycarbonates for Solid Polymer Electrolytes. *Electrochimica Acta* 2017, *237*, 259-266.

8. Zhang, J.; Zhu, W.; Li, C.; Zhang, D.; Xiao, Y.; Guan, G.; Zheng, L., Effect of the biobased linear long-chain monomer on crystallization and biodegradation behaviors of poly(butylene carbonate)-based copolycarbonates. *RSC Advances* 2015, *5* (3), 2213-2222.

9. (a) Tominaga, Y.; Nanthana, V.; Tohyama, D., Ionic conduction in poly(ethylene carbonate)-based rubbery electrolytes including lithium salts. *Polym J* 2012, *44* (12), 1155-1158; (b) Kimura, K.; Motomatsu, J.; Tominaga, Y., Correlation between Solvation Structure and Ion-Conductive Behavior of Concentrated Poly(ethylene carbonate)-Based Electrolytes. *The Journal of Physical Chemistry C* 2016, *120* (23), 12385-12391; (c) Tominaga, Y.; Yamazaki, K., Fast Li-ion conduction in poly(ethylene carbonate)-based electrolytes and composites filled with TiO2 nanoparticles. *Chemical Communications* 2014, *50* (34), 4448-4450; (d) Tominaga, Y., Ion-conductive polymer electrolytes based on poly(ethylene carbonate) and its derivatives. *Polym J* 2017, *49* (3), 291-299.

10. Olmedo-Martínez, J. L.; Meabe, L.; Basterretxea, A.; Mecerreyes, D.; Müller, A. J., Effect of Chemical Structure and Salt Concentration on the Crystallization and Ionic Conductivity of Aliphatic Polyethers. *Polymers* 2019, *11* (3), 452.

11. Mindemark, J.; Imholt, L.; Montero, J.; Brandell, D., Allyl ethers as combined plasticizing and crosslinkable side groups in polycarbonate-based polymer electrolytes for solid-state Li batteries. *Journal of Polymer Science Part A: Polymer Chemistry* 2016, *54* (14), 2128-2135.

CHAPTER 3.

Synthesis and characterization of poly(ethylene oxide carbonate) materials as solid polymer electrolytes

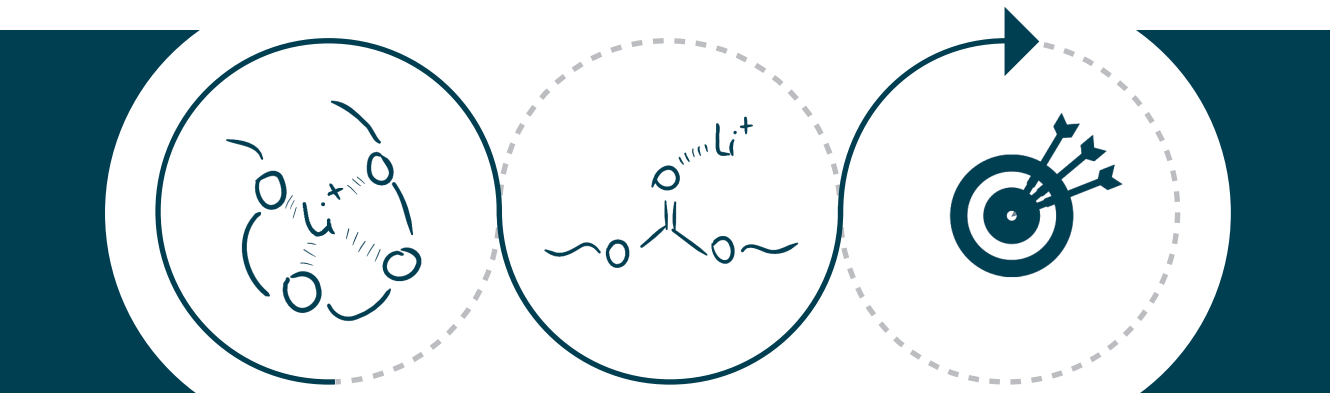

CHAPTER 3.

Synthesis and characterization of poly(ethylene oxide carbonate) materials as solid polymer electrolytes

3.1 Introduction

Since the first report about ionic conductivity of salts in poly(ethylene oxide) (PEO) by Wright in 1973,[1] several generations of PEO-SPEs for lithium batteries have been explored, due to its ability to solvate different types of salt. However, limited ionic conductivity and low lithium transference number of PEO led the batteries to operate at 70 °C. In the last decades, several attempts can be found in the literature in order to improve the PEO based SPEs properties; such as the incorporation of different types of salt,[2] chemical functionalization,[3] single-ion conducting polyelectrolytes.[4]

block copolymers,[4a, 5] introduction of inorganic nanoparticles or nanofillers,[6] or corss-linked PEO networks.[7]

The main limitation of lithium conduction in PEO-SPE performance come from the high crystallinity and strong coordination between ethylene oxide (EO) units and lithium cation.[8] Alternative to this type of host polymer, polycarbonates have been proposed; where usually crystallinity is absent and the weak coordination between carbonate and lithium promotes the lithium conduction. However, if carbonate groups and ethylene oxide (EO) units are alternated along the backbone, the crystallization of the EO units could be restricted, strong interation between ion-polymer can be interrupted, and additionally, low glass transition should be achieved.[9]

Thus, He and co-workers proposed the synthesis of two polycarbonates having two and three EO links via polycondensation,[10] showing promising properties, an ionic conductivities in the range of 10^{-5} S cm^{-1} at room temperature after addition of cellulose nanofibers. In another studies, Tominaga et. al. reported the copolymerization between CO_2 and different epoxies having ethylene carbonate and EO links in the final polymer.[9b, 11] In this example, the polycarbonates having few EO units and carbonate groups showed an ionic conductivity in the range of 10^{-4} S cm^{-1} at 60 °C with high LiFSI content (120 mol%). Following this promising combination, in this chapter we further explored the combination of the two lithium friendly chemical groups: ethylene oxide and carbonate. We envision to provide three properties to the SPEs: i) a decrease on glass transition respect to polycarbonate due to the incorporation of EO units, and thereby, an enhancement on chain mobility and the ionic conductivity;[12] ii) a restriction of crystalline EO phase formation by the inlclusion of carbonate groups; and iii) a favourable coordination between lithium cation and

the carbonate group, which will promote the lithium conductivity, and therefore the lithium transfer number at room temperature.

Thus, in this chapter, we synthesized a series of eight different poly(ethylene oxide)/carbonate, PEO-PC, with different proportion of EO and carbonate groups by the polycondensation between poly(ethylene oxide) end-capped diol and dimetyl carbonate. The aim of this work, is to optimize the composition of the PEO-PC to investigate how the chemical structure and lithium salt concentration affect the electrochemical properties. Therefore, the ammount of EO units was varied from 2 to 45 between each carbonate group. However, the mechanical properties of this linear and low glass transition polymer needed to be improved. Thus, the mechanical properties of the best candidate for SPE were improved by engineering a PEO-PC copolymer including a pendant methacrylic cross-linkable unit. The electrochemical properties and lithium diffusion of these free-standing PEO-PC films were evaluated. Finally, the transport ability of lithium was tested in a lithium symmetric cell. Due to its promising properties, preliminary tests of these SPEs in a solid-state cell, Lithium-SPE-NMC, were carried out.

3.2 Results and discussion

3.2.1 Synthesis and physicochemical characterization of poly(ethylene oxide carbonates) (PEO_X-PC)

In the previous chapter we tested the versatile synthetic method of melt polycondensation to synthesize functional aliphatic polycarbonates. In this chapter, different low molecular weight poly(ethylene oxide) diols were used as monomers with dimethyl carbonate in the polycondensation process. The synthetic route towards poly(ethylene oxide carbonate) based polymers is depicted in Scheme 3.1. It

shows the synthesis of eight different polymers, containing between 2 and 45 EO units between each carbonate links. This synthetic approach benefits from the commercial availability of poly(ethylene glycol) diols of different lengths. The different PEO_x-PC polymers were synthesized in 2 steps reaction involving high temperature and vacuum. Using this method, PEO_x-PC copolymers have been synthesized with different number of EO units (between 2 and 45): PEO_2-PC, PEO_3-PC, PEO_4-PC, PEO_6-PC, PEO_{13}-PC, PEO_{22}-PC, PEO_{34}-PC and PEO_{45}-PC.

Scheme 3.1. Synthetic route to different poly(ethylene oxide carbonates) (PEO_x-PC).

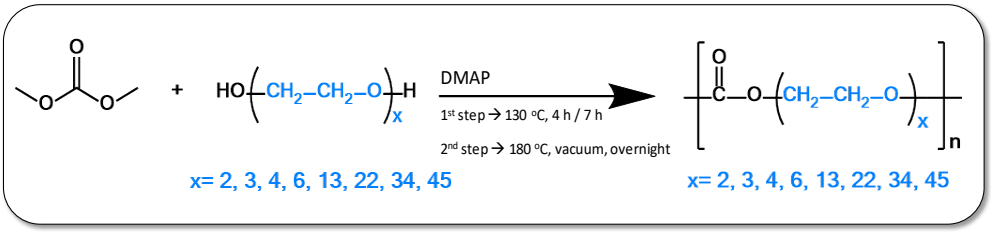

Figure 3.1a shows the ^1H NMR spectrum of PEO_2-PC. The signal at 4.29 ppm is attributed to the protons next to the carbonate group, whereas the signal at 3.73 ppm is assigned to the protons next to the oxygen. ^1H NMR and ^{13}C NMR spectra of the all the polymers are shown in **Appendix Figure A8-A9**. Both spectra confirmed the formation of the PEO_x-PC polymers showing the expected peaks of the methylene groups close to the carbonates and the disappearance of the corresponding monomer signals. As expected, the intensity of the carbonyl signal of the carbonate group in ^{13}C NMR spectra (**Appendix Figure A9**) varies depending on the composition of the PEO_x-PC polymers and the theoretical ratio between carbonate group and EO units. More clearly, the presence of the carbonate group was confirmed by FTIR-ATR with the high intensity band appearing at 1740 cm^{-1}, **Figure 3.1b**.

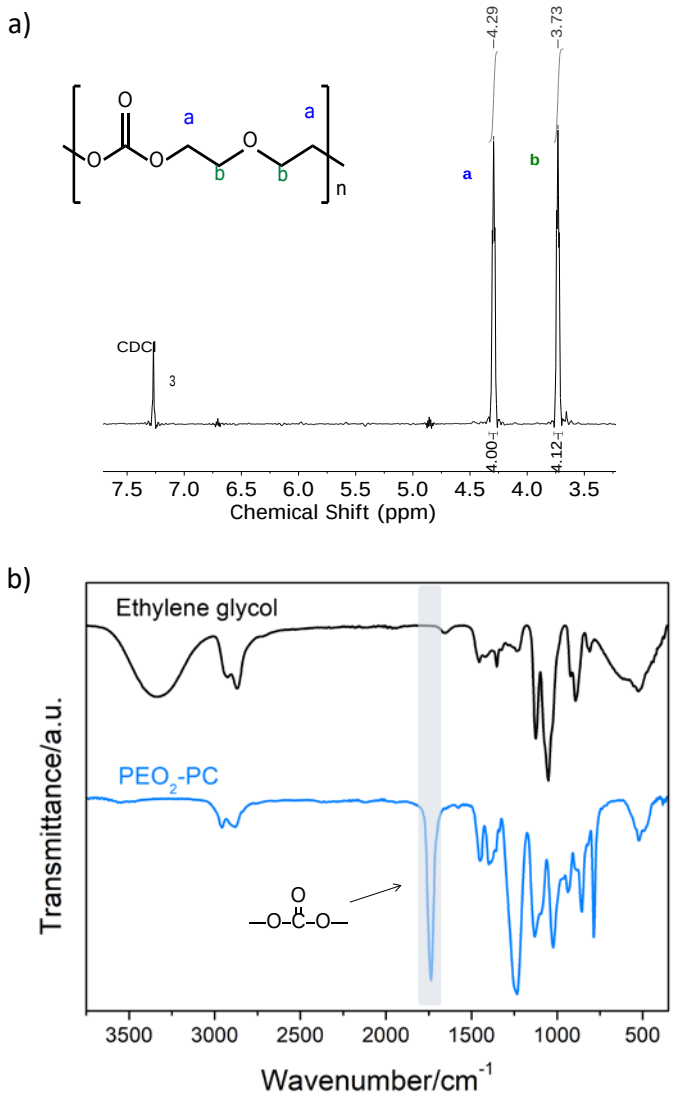

Figure 3.1. a) ^{1}H NMR spectrum of PEO_2-PC polymer, and b) FTIR-ATR of ethylene glycol (the monomer) and the resulting PEO_2-PC polymer.

Several polycarbonates were designed having different EO lengths *vs.* carbonate ratios in order to investigate the structure-properties relationship, **Table 3.1.** The molar masses of the PEO_x-PC polymers were characterized by size exclusion chromatography having a light scattering detector. The polymers showed values of

molar masses in the range of 47,600 and 8,300 g mol^{-1}, and dispersities around 1.5. It is worth noting that the obtained values of molar masses and dispersities are typical of polycondensation processes.

Table 3.1. Physical properties of PEO_X-PC.

Polymer	M_n (g mol^{-1})	Đ	T_g (°C)[d]	T_c (°C)[a]	T_m (°C)[b]	ΔH_m [b] (J g^{-1})
PEO_2-PC	47,600	1.4	-21	--	--	--
PEO_3-PC	35,800	1.6	-36	--	--	--
PEO_4-PC	32,400	1.4	-40	$8_{(cold\ T_c)}$	52	59
PEO_6-PC	21,900	1.5	-53	--	--	--
PEO_{13}-PC	21,900	1.6	-49	13	29	81
PEO_{22}-PC	14,700	1.5	-52	30	38	113
PEO_{34}-PC	22,500	1.7	-55	37	46	112
PEO_{45}-PC	8,300	1.5	-55	39	50	147

[a] The data were recorded from the DSC measurements in the first cooling scan. [b] The data were recorded from the DSC measurements in the second heating scan. Cooling and heating scan rates: 2 K min^{-1} and 20 K min^{-1} respectively. [d] Data measured during the 3rd heating scan at 20 K min^{-1}, after performing fast cooling scan at 50 K min^{-1}.

Differential scanning calorimetry (DSC) was used to determine the thermal properties of polycarbonates, which are summarized in **Table 3.1** and shown in **Figure 3.2**. Not, surprisingly the glass transition temperature (T_g) decreases significantly with high amount of the EO units between the carbonate groups. This same behaviour, where EO induces to decrease the T_g, have been reported for other polycarbonates having EO units.[12] The highest T_g is observed in the case of the short PEO_2-PC, -21 °C and the lowest for long PEO_{45}-PC, -55 °C. On the other hand, polycarbonates containing few EO groups do not presences any crystallinity, PEO_2-PC, PEO_3-PC and PEO_6-PC. Besides, PEO_4-PC shows a crystallization process during the heating scan, which is known as a cold crystallization. In the case of higher length of EO units, the polymers

show crystallinity during the cooling scan, and the crystallization temperature (T_c) increases with the PEO length from 8 to 39 °C. As a result, the melting temperature (T_m) of the PEO_x-PC polymers increases when the EO content is higher showing values between 29 and 52 °C. Meanwhile, the enthalpy of the melting (ΔH_m) also increases with the number of EO groups, demonstrating that more crystalline EO phase in the case of higher amount of EO units.

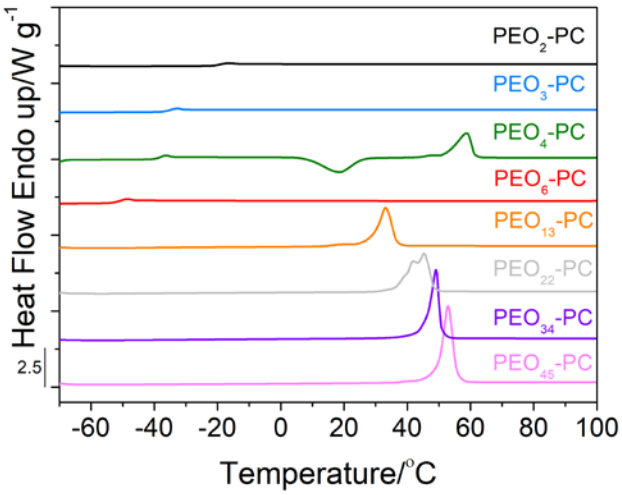

Figure 3.2. DSC traces of PEO_X-PC. DSC traces obtained in the 2nd heating scan at 20 K min^{-1}.

3.2.1.1 Ionic conductivity of poly(ethylene oxide carbonates) having LiTFSI as solid polymer electrolytes

In this work we have incorporated carbonate links within the poly(ethylene oxide) chains to improve PEO properties as a solid polymer electrolyte. Thus, in order to verify this hypothesis, we first have compared the ionic conductivity of the precursor PEO_{34} diol and the resulting PEO_{34}-PC formulated as SPEs by mixing with 30 wt.% LiTFSI. As it can be seen in **Figure 3.3**, the ionic conductivity is improved with the addition of few carbonate groups in the polymeric chain, especially at room temperature which is in good accordance to our expectations. The value given by the low molecular wegiht precursor diol, PEO_{34}, is $1.4 \cdot 10^{-5}$ S cm^{-1}, whereas the PEO_{34}-PC shows a value of $3.7 \cdot 10^{-5}$ S cm^{-1}.

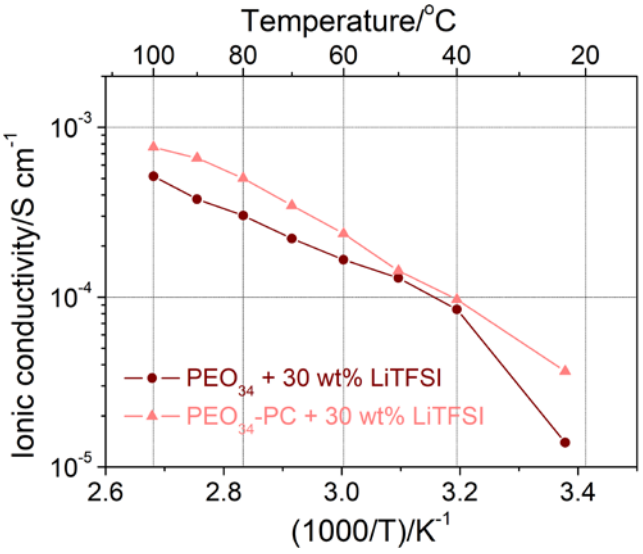

Figure 3.3. Arrhenius plot of ionic conductivity for poly(ethylene glycol) (1500 g mol^{-1}), PEO_{34}, and the corresponding polycarbonate PEO_{34}-PC (22,500 g mol^{-1}).

Once we confirmed the beneficial effect of the carbonate group, the relationship between ionic conductivity and thermal properties of the eight different PEO_x-PC polymers was investigated. The ionic conductivity values of polycarbonates containing 30 wt.% LiTFSI are represented in Arrhenius plot, **Figure 3.4a**, which are measured by impedance spectroscopy in the temperature interval between 100 and 25 °C. In all cases the expected typical Vogel-Tammann-Fulcher (VTF) behaviour is observed. We have to point out that most of them are soft solid and sticky materials. The ionic conductivity generally increases with the content of EO units between carbonate groups. **Figure 3.4b** shows the DSC curves of the different solid polymer electrolytes. As it can be seen, the measurements showed that the lowest T_g value of -48 °C was consistent with the polymer showing the highest ionic conductivity, PEO_{34}-PC. On the contrary, the electrolyte assigned with highest T_g value of -32 °C, showed the lowest ionic conductivity, PEO_2-PC. In addition, the crystalline domains were suppressed or decreased with the addition of 30 wt.% of LiTFSI, only PEO_{45}-PC was a semicrystalline material, which may explain why this material does not show the highest conductivity value at 25 °C. Thus, it seems that the ionic conductivity is compromised between the amounts of EO units and carbonates groups. It seems that both characters in the polymer have a crucial role, being both of them fundamental for the improvement of the ionic conductivity. EO units brings crystallinity to system, restricting the ionic conductivity, thus, there is an optimum number of EO units, which is 34. From these results, we can suspect to increase the crystallinity of the polymer electrolytes with higher amount of EO units, more than 45. To highlight, the highest ionic conductivity value at 25 °C was observed for the case of PEO_{34}-PC showing a value of $3.7 \cdot 10^{-5}$ S cm^{-1}.

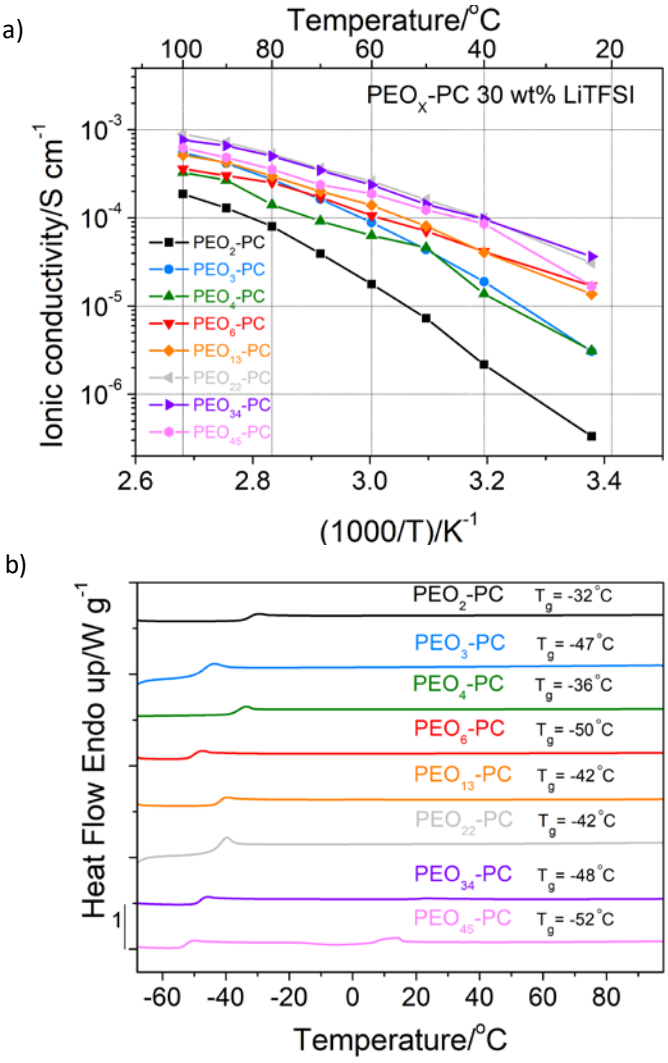

Figure 3.4. Analysis of PEO$_x$-PC with 30 wt.% LiTFSI: a) Arrhenius plot of ionic conductivity, and b) DSC traces recorded in the 2nd heating scan at 20 K min^{-1}.

Next, we investigated the effect of the ratio between polymer and salt concentration. For this purpose a series of SPEs were formulated varying LiTFSI amount on PEO$_6$-PC and PEO$_{34}$-PC, **Figure 3.5** and **Figure 3.6** respectively. In both cases, when the salt content is varied the tendency is similar and the highest ionic conductivity values are

obtained for the SPEs with 30 wt.% lithium salt. In regards to PEO_6-PC, all polymer electrolytes are amorphous, and thus, the ionic conductivity is only restricted by the glass transition (**Figure 3.5**). For this system also, the increase of lithium salt provokes an increase in T_g which limits the ion dynamics. For this polymer electrolyte family, 30 wt.% LiTFSI (O/Li mole ratio of 17) is the SPE with the highest ionic conductivity, showing a value of $2 \cdot 10^{-5}$ S cm^{-1} at room temperature.

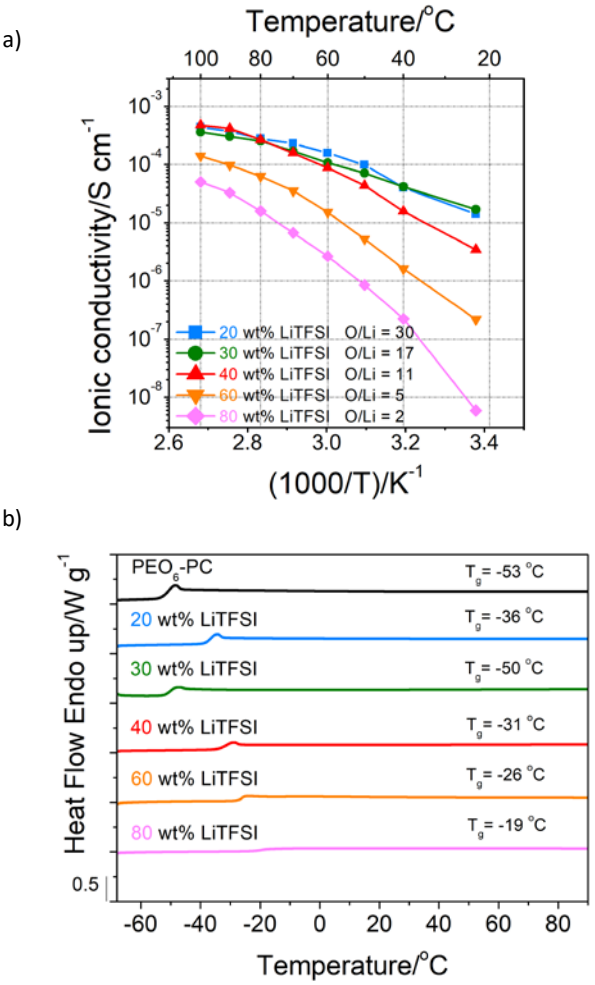

Figure 3.5. Analysis of PEO_6-PC with different wt.% LiTFSI: 20 wt.%, 30 wt.%, 40 wt.%, 60 wt.%, 80 wt.%. a) Arrhenius plot of ionic conductivity, and b) DSC traces of the corresponding polycarbonates obtained in the 2nd heating scan at 20 K min^{-1}.

In the case of PEO_{34}-PC, with low salt concentration (20 wt.% LiTFSI) the ion movement is restricted at low temperature by the crystallinity of the polymer, which is shown in the DSC curves of **Figure 3.6b.** Apparently, once the salt concentration increases, the salt suppresses the crystallinity and the T_g increases. Thus, at high contents of lithium salt, the dynamics are limited by the increased glass transition of the SPE, being more similar behavior to PEO-SPEs. In order to confirm this trend, we calculate the activation energy using VTF **Equation 3.1**, **Table 3.2**. Where A is the pseudo activation energy, σ_0 is the conductivity pre-exponential factor and T_0 is referred to as the Vogel temperature, the glass transition in ideal glasses, however, usually it is estimated to T_g-50. The values obtained from VTF equation are in good accordance to the ionic conductivity trend; the lowest activation energies (2.49-1.19 KJ mol^{-1}) are shown by the SPEs giving the highest ionic conductivities. It can be concluded that the activation energy is limited by the glass transition, higher activation energy (7.11-14.49 kJ mol^{-1}) is needed by the SPE with higher glass transition. The optimum mole ratio of 1:16 (**Equation 3.2**), corresponding to 30 wt.% of LiTFSI for PEO_{34}-PC, shows an ionic conductivity of $3.7 \cdot 10^{-5}$ S cm^{-1} at room temperature. PEO_{34}-PC:SPE having 20 wt.% LiTFSI shows a technologically useful high value of $2.4 \cdot 10^{-4}$ S cm^{-1} at 70 °C, which is similar to PEO_{34}-PC with 30 wt.% LiTFSI at the same temperature, $3.5 \cdot 10^{-4}$ S cm^{-1}, **Figure 3.6a**.

It is worth noting that these values are comparable to those PEO_2-PC ($3.81 \cdot 10^{-6}$ S cm^{-1}) and PEO_3-PC ($1.12 \cdot 10^{-5}$ S cm^{-1}) with the cellulose nonwoven substrate at 25 °C, previously reported.[10] However, these SPEs do not have any substrate to improve the mechanical and electrochemical properties.

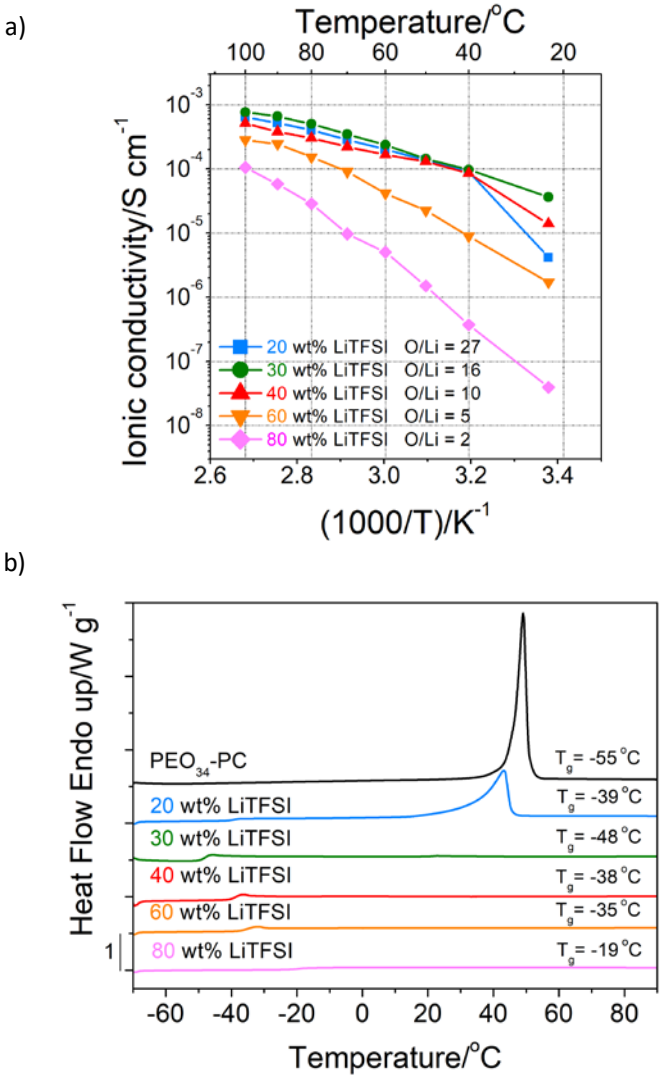

Figure 3.6. Analysis of PEO_{34}-PC with different wt.% LiTFSI : 20 wt.%, 30 wt.%, 40 wt.%, 60 wt.% and 80 wt.%. a) Arrhenius plot of ionic conductivity, and b) DSC traces of the corresponding polycarbonates obtained in the 2nd heating scan at 20 K min^{-1}.

$$\sigma = \sigma_0 \, exp\left(-\frac{A}{T-T_0}\right)$$ **Equation 3.1.** Vogel–Tamman–Fulcher (VTF) equation.[13]

Table 3.2. Activation energies calculated from VTF equation.

PEO_{34}-PC	20 wt.% LiTFSI	30 wt.% LiTFSI	40 wt.% LiTFSI	60 wt.% LiTFSI	80 wt.% LiTFSI
E_A (kJ mol^{-1})	2.49	1.33	1.19	7.11	14.49

$$\frac{O}{Li} mole\ ratio = nO \times \frac{\frac{g_{polymer}}{M_{w_{polymer}}}}{\frac{g_{salt}}{M_{w_{salt}}}}$$ **Eqaution 3.2.** O/Li mole ratio calculation.

3.2.1.2 Chemical characterization of PEO_{34}-PC by FTIR and solid state NMR

It is well known that the lithium ions coordinate with carbonyl groups, while ethylene oxide groups chelate and trap lithium ions.[14] Thus, a higher ionic conductivity and lithium transference number is usually measured when carbonyl groups are on the system.[9b] **Figure 3.7** shows the FTIR spectra of the previous SPEs (PEO_{34}-PC) in order to investigate this coordination between the lithium and the carbonate group. Without any salt in the media a sharp band is observed between 1740-1745 cm^{-1}. However, when the salt LiTFSI is incorporated to the SPE, the stretching vibration mode for the carbonyl group becomes broad and it shifts to lower wavenumbers (1725 cm^{-1}). This shift in stretching frequency occurs due to the coordination between the carbonyl group and the lithium cation, which is more pronounced with higher LiTFSI concentrations.

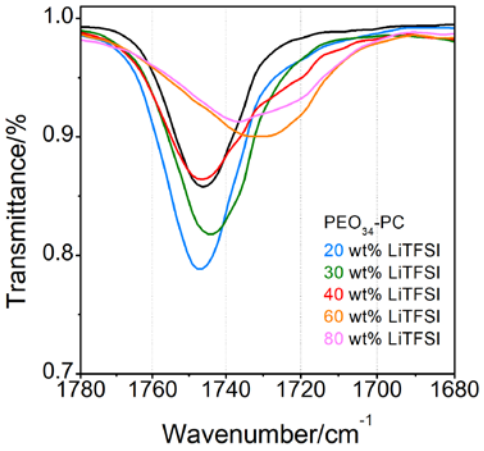

Figure 3.7. FTIR-ATR study on the coordination between Li cation and carbonyl groups of PEO_{34}-PC with different wt.% LiTFSI.

To get a further insight into the ion dynamics in these SPEs ^{7}Li NMR and ^{19}F NMR studies were performed for PEO_{34}-PC in order to study the local motion as a function of salt concentration. **Figure 3.8** shows the ^{7}Li and ^{19}F spectrum of PEO_{34}-PC based polymer electrolytes at different LiTFSI concentrations, ranging between 20 wt.% and 80 wt.% LiTFSI. Owing to solid and sticky nature of the solid polymer electrolytes, there was some difficulty to get the sample uniformly distributed within the 5 mm NMR tubes, thus, resulting in magnetic field shimming having to be carried out on each sample individually. This will affect the line-shapes and potentially cause some errors in the absolute values of the observed chemical shifts. If we observed to **Figure 3.8**, in the 80 wt.% LiTFSI sample, a second ^{7}Li and ^{19}F signal appears at a higher shift, respect to the other samples. Although we considered that this signal could arise from the shimming effects, we measured different longitudinal relaxation times (see **Figure 3.9**) which indicate that they indeed represent two different lithium sites.

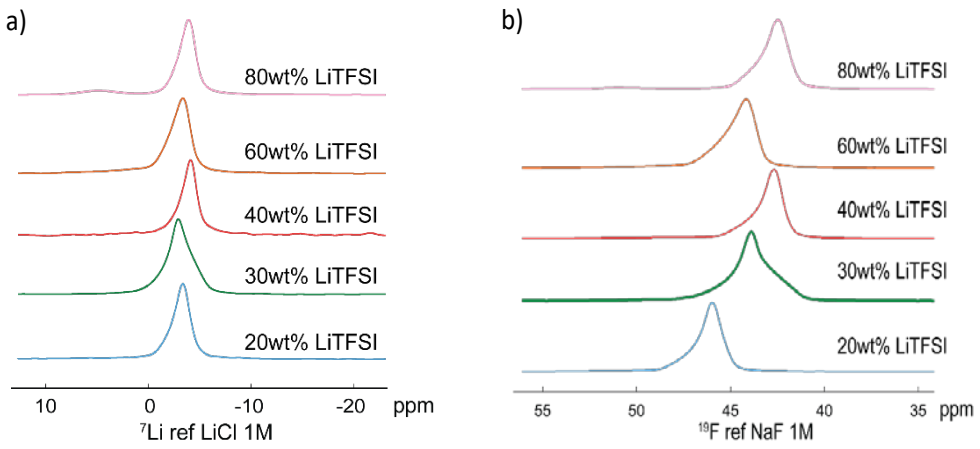

Figure 3.8. a) ^{7}Li NMR spectrum of PEO_{34}-PC at 343.15 K of different wt.% LiTFSI samples, and b) ^{19}F NMR spectrum of PEO_{34}-PC at 343.15 K of different wt.% LiTFSI samples.

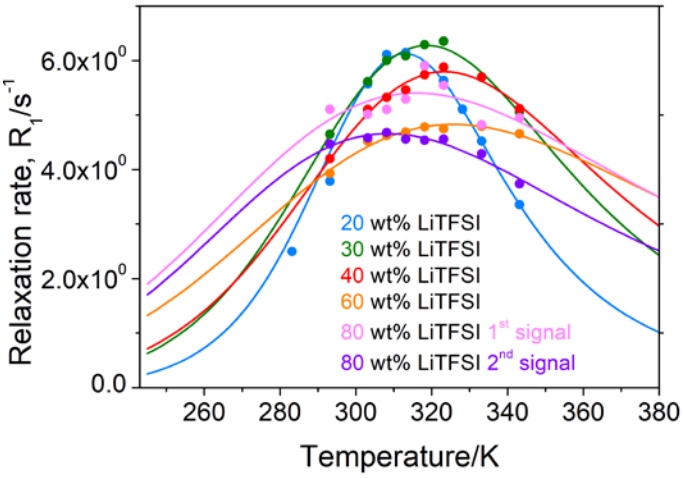

Figure 3.9. The ^{7}Li longitudinal relaxation rates (R_1) for PEO_{34}-PC of different wt.% LiTFSI samples. The lines are fitted by the BPP model.

The ^{7}Li relaxation rates ($R_1 = T_1^{-1}$) for the different wt.% LiTFSI samples are shown in **Figure 3.9**. These data were fitted using the Bloembergen, Purcell and Pound (BPP)[15] model for nuclear spin relaxation. We expect that in these polymers the quadrupolar

interaction will be the dominant mechanism for ^{7}Li longitudinal relaxation, hence, we use:[16]

$$\frac{1}{T_1} = \frac{4\pi\langle C_Q^2\rangle}{50}\left[\frac{\tau_c}{1+\omega_0^2\tau_c^2} + \frac{4\tau_c}{1+\omega_0^2\tau_c^2}\right]$$ **Equation 3.3.** Bloembergen, Purcell and Pound (BPP).[15]

C_Q is the quadrupolar coupling constant, which is sensitive to the symmetry of the local Li^+ environment (specifically the electric field gradient), and τ_c is the correlation time. The latter mechanism can be assumed to be thermally activated and thus will show Arrhenius behavior:

$$\tau_c = \tau_0 exp\left(\frac{E_A}{RT}\right)$$ **Equation 3.4.** Arrhenius equation.

where E_A is the activation energy, R is the gas constant, τ_0 is the correlation time at infinite temperature. The parameters extracted from the relaxation measurements using this model are shown in **Table 3.3** together with the τ_c value calculated for 343 K.

Table 3.3. The parameters extracted from the ^{7}Li T_1 NMR relaxation measurements by using **Equation 3.3**.

PEO_{34}-PC	C_Q (kHz)	τ_c (ns) at 343.15 K	E_A (kJ mol^{-1})[a]
20 wt.% LiTFSI	25.21±0.46	1.47±0.03	37.73±0.69
30 wt.% LiTFSI	25.52±0.47	2.52±0.05	27.53±0.51
40 wt.% LiTFSI	24.51±0.45	3.12±0.06	24.49±0.45
60 wt.% LiTFSI	22.38±0.41	3.82±0.07	17.20±0.32
80 wt.% LiTFSI (1st signal)	23.67±0.44	3.20±0.06	16.59±0.31
80 wt.% LiTFSI (2nd signal)	21.98±0.40	2.63±0.05	17.68±0.33

The activation energies extracted from the T_1 data show that the lower LiTFSI concentrations have E_A approaching 40 kJ mol^{-1} whereas at concentrations higher than 40 wt.% LiTFSI the value is almost halved. This reflects faster/favorable reorientational dynamics around the Li^+ at higher concentrations. The τ_c values were determined as a function of temperature using the T_1 fitting parameters and are plotted in **Figure 3.10**. At lower temperatures, the τ_c for the 20 wt.% LiTFSI sample is longer than at higher concentrations, but the trend is changed at higher temperatures with the 20 wt.% LiTFSI sample overall having the shortest τ_c at temperatures above 310 K which suggests faster dynamics, while 60 wt.% has the longest τ_c over almost the entire temperature range which suggests slower dynamics.

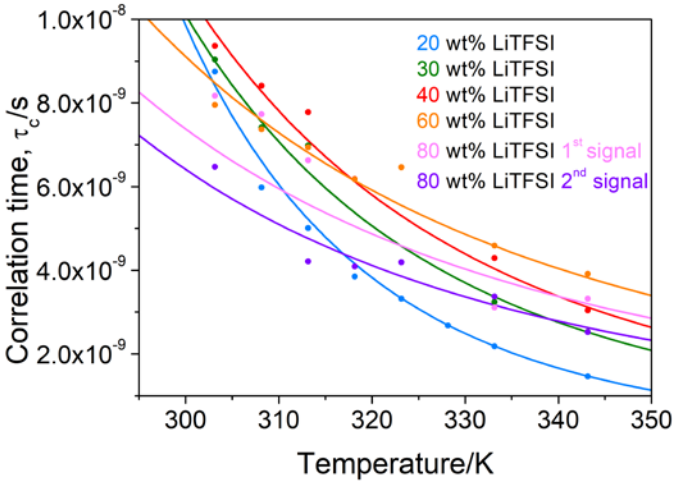

Figure 3.10. τ_c plots with temperatures for different PEO_{34}-PC samples.

The decrease in activation energies in longitudinal relaxation measurements can be explained as motion of lithium at nanosecond timescale get favour at higher lithium concentrations. This decrease with increasing salt concentration may occur as a result of an increase in ion clustering, which can be facilitated by an exchange in the

coordination environment, which is in good agreement with the new signal of ^{7}Li and ^{19}F NMR spectrum.

At this timescale, the relaxation mechanism is expected to be the fluctuation of the coordinating or near neighbour species such as the polymer or the anions. Hence, this activation energy lowering could be explained from fluctuations in ion-ion interactions. To our knowledge, the vehicular mechanism is one of the mechanisms to provide the ionic conductivity for the polymer electrolyte system,[17] as many authors have observed the coupling of the polymer chain mobility and the ionic conductivity.[18] Therefore, we believe that at high salt concentration the lithium motion can relate to lithium vibration/fluctuation or lithium hopping, changing the mechanism respect to low salt concentrations, from vehicular to structural rearrangement. This has been observed through simulations in related ionomer[19] and ionic liquid systems and correlates with a change in mechanism of dynamics from vehicular to structural rearrangement.[20] In our system, when we increase the salt concentration the glass transition is increased, therefore, the lower activation energy at 80 wt.% LiTFSI can come from the structural rearrangement.

The C_Qs are comparable for 20 wt.% LiTFSI and 30 wt.% LiTFSI, and then are seen to decrease with increasing LiTFSI content, suggesting an increase in the average symmetry of the lithium environments most likely due to a different coordination environment.

The appearance of another signal in ^{7}Li spectrum for 80 wt.% LiTFSI sample can be explained by the existence of Li clusters (Li bounded by TFSI-anions) at high LiTFSI concentration, owing to the appearance of one signal when the LiTFSI concentration is lower than the 80 wt.%. Thus, we expect that the appearance of the new signal (named as 1st signal) in highly concentrated samples can be assigned for LiTFSI

clusters. The correlation time is slightly higher for the 1st signal than the 2nd one, suggesting slower local dynamics for the LiTFSI clusters or a more restricted local environment with fewer fluctuations.

The results of ^{7}Li NMR and ionic conductivity are fundamental for a better understanding of the systems; from the NMR analysis we can determine how fast the local motions are in the electrolyte, and the results measured by electrochemical impedance spectroscopy, are analyzing the overall longer range ion motions in the system. From both of them, several environments on the electrolyte can be determined. At high salt content electrolytes, PEO_{34}-PC 80 wt.% LiTFSI, interestingly, 2 different signals are observed, which have a different C_Q and E_a from the T_1 relaxation measurements and thus, it reflects two different environments in the system. Compared to the high salt content electrolytes, the correlation times determined from the T_1 fitting, in case of the lower LiTFSI concentrations, are higher, meaning faster local motions. These low salt content electrolytes do not show two different signals on the ^{7}Li and ^{19}F NMR.

3.2.1.3 Lithium diffusion coefficient measurements by NMR

The ^{7}Li diffusion coefficients are fitted to the Stejskal-Tanner equation. γ is the gyromagnetic ration of the interest nucleus, D is the diffusion coefficients ($m^2\,s^{-1}$), D is the gradient pulse duration (s), δ is the diffusion duration (s) and g is the gradient strength ($G\,m^{-1}$). S is the signal intensity observed at g gradient strength while S(0) is the maximum signal intensity. The ^{7}Li diffusion coefficients measurements are performed at 70°C, it is observed that it decreases with increasing LiTFSI content from 20 wt.% to 60 wt.%. Then they increase to their highest values for the first and the second signal at 80 wt.%, (see **Figure 3.11** for details). This observation is consistent with the ionic conductivity for LiTFSI concentrations ranging from 20 to 60 wt.%, but

not for the case of 80 wt.%. The highest diffusion values corresponds to the first signal of for 80 wt.% LiTFSI. These results can be explained by the basic difference between diffusion and ionic conductivity measurements. For the diffusion measurements we observe a mean diffusion value for every mobile species containing ^{7}Li. These species may consist of the Li coordinated (through Li···O interaction), clusters of Li with $TFSI^-$ anions, and can potentially include neutral clusters. Moreover, it is possible that the majority of the Li^+ is undergoing slow translational diffusion with coefficient values too slow to measure by NMR. For the ionic conductivity measurement, only charged species are taken into account which means the Li^+ itself and $(Li)_n$-$(TFSI)_m$ ($n \neq m$).

$$\frac{S}{S(0)} = \exp[-\gamma^2 D\delta^2 \left(\Delta - \frac{1}{3}\delta\right) g^2$$ **Equation 3.5.** Stejskal-Tanner equation.[21]

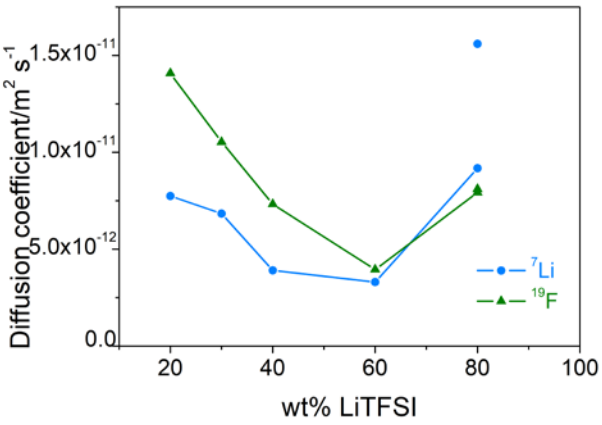

Figure 3.11. Diffusion measurements of different PEO_{34}-PC containing different wt.% LiTFSI.

3.2.2 Synthesis and physicochemical characterization of cross-linked polycarbonate: PEO_{34}-PC 10 wt.% MA

Based on the previous work, we observed that both structures (ethylene oxide and carbonate groups) play an important role in the electrochemical behaviour. Specially, the polycarbonate with 34 EO units gave reasonable improved values. However, the low molar mass of the polymer and the plasticizing ability of LiTFSI led in poor mechanical properties. Therefore, next, we have incorporated cross-linkable methacrylic groups in order to developed a free standing SPE, based on polycarbonate containing 34 EO units, **Scheme 3.2a**. Poly(ethylene glycol) (M_n= 1500 g mol^{-1}) and methacrylic based diol (MA) were copolymerized using dimethyl carbonate via polycondensation. Different copolymers were synthesized, having 5, 10 and 20 wt.% of methacrylic diol respect to the overall diol. These polymers are named as PEO_{34}-PC 5 wt.% MA, PEO_{34}-PC 10 wt.% MA and PEO_{34}-PC 20 wt.% MA. The polymerization was organocatalysed by DMAP, in a two steps reaction as previously explained: 1st step: 130 °C, 7 h and 2nd step: 170 °C and high vacuum, overnight. The temperature of the second step was maintained in 170 °C, as metacrylic diol started to cross-link at 180 °C, even if few ppm of hydroquinone were added. The chemical structures of the polycarbonates were confirmed by ^{1}H NMR, which is shown in **Appendix Figure A10,** indicating the presence of methacrylic pendant units**.** The molar mass of the methacrylic functional poly(ethylene oxide carbonate) before cross-linking was measured by GPC based on narrow PS standards, showing a M_n value of 20,000 g mol^{-1}. The functional methacrylic poly(ethylene oxide carbonate) was further cross-linked by ultraviolet light in the presence of a photoinitiator, **Scheme 3.2b**. The polymer, targeted LiTFSI amount, and the photoinitiator were dissolved in ACN. Once the solvent was evaporated, the dry films were exposed under ultraviolet

light. After UV treatment a free standing solid membrane was obtained as shown in the picture, **Scheme 3.2b**.

Scheme 3.2. a) Synthetic route to cross-linkable methacrylic functional PEO_{34}-PC, and b) schematic representation of the post-polymerization, via ultraviolet light.

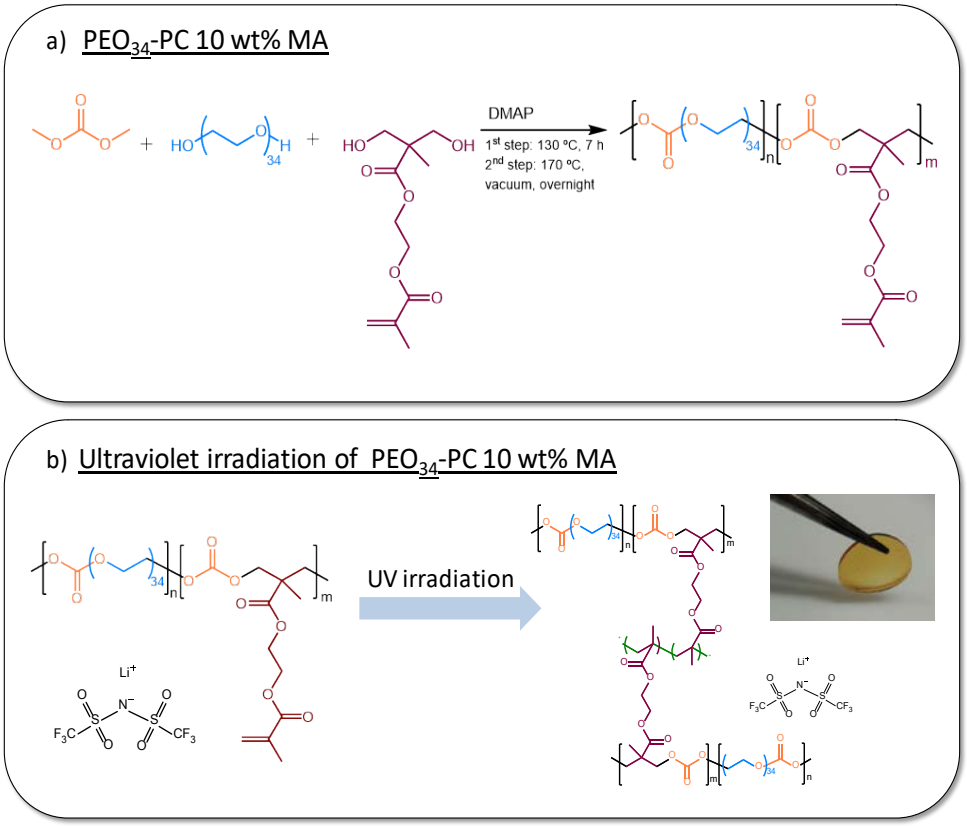

After ultraviolet treatment, the PEO_{34}-PC copolymer became insoluble in common organic solvents. Furthermore, FTIR-ATR was used to investigate the chemical nature of the cross-linking reaction. It has to be mentioned that this analysis was carried out before the addition of LiTFSI. FTIR-ATR analysis of PEO_{34}-PC 10 wt.% MA, **Figure 3.12a**, confirmed the disappearance of double bonds, in 1717 cm^{-1} and, besides, new bands were described; 1680 cm^{-1}, 720 cm^{-1}, and 700 cm^{-1}, corroborating the formation of

the cross-linked network due to the reactivity of the methacrylic units. Additionally, we performed DSC analysis to study the effect of the cross-linked network on the thermal properties of PEO_{34}-PC 10 wt.% MA, as it can be observed, **Figure 3.12b**. The glass transition of the non-cross-linked to the cross-linked network was compared, which was significantly increased; the glass transition of the non cross-linked polymer was found to be -55 °C, whereas the glass transition of cross-linked polymer electrolyte was -45 °C. Besides, the enthalpy of melting is decreased once the polymer is cross-linked (from 134 J g^{-1} to 110 J g^{-1}).

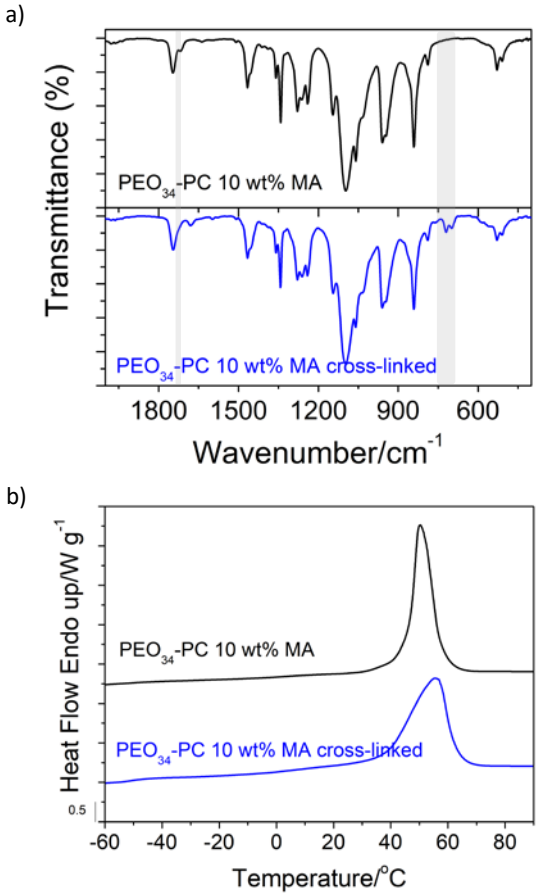

Figure 3.12. a) FTIR-ATR analysis, and b) DSC traces of the 2nd heating scan at 20 K min^{-1} of PEO_{34}-PC 10 wt.% MA before and after cross-linking.

The cross-linked architecture of PEO_{34}-PC 10 wt.% MA containing 30 wt.% of LiTFSI was confirmed by the study of the viscoelastic properties through AR-G2 rheometer, at 30 °C, 70 °C and 100 °C. **Figure 3.13** depicts the double-logarithmic plots of G' and G'' *vs.* angular frequency of PEO_{34}-PC 10 wt.% MA containing 30 wt.% of LiTFSI. As it can be observed from the figure, the storage modulus of the material is above the loss modulus at all temperatures, which means that the polymer is in the rubbery plateau region, confirming a three-dimensional network. Nevertheless, G' and G'' values depends on frequency and temperature, which could be argued with the remaining methacrylic groups after the post-polymerization. All in all, the rheological experiments confirmed the solid nature of the free standing SPE membrane even at high temperatures. Additionally, the thermal stability was studied by thermogravimetic analysis, **Figure 3.14**. The onset temperature (T_{onset}) for PEO_{34}-PC 10 wt.% MA containing 30 wt.% of LiTFSI was found to be 275 °C.

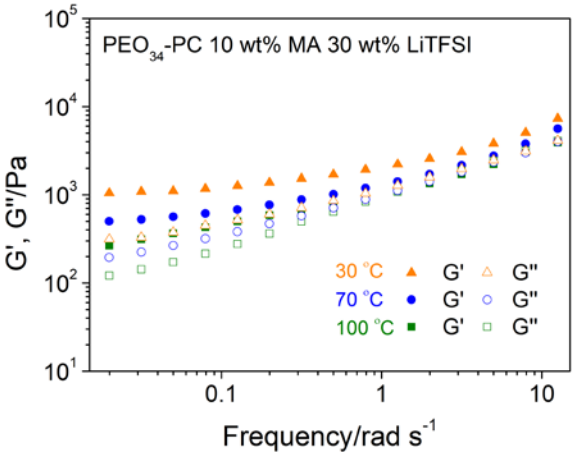

Figure 3.13. a) Storage and viscous modulus (G' and G'', respectively) of cross-linked PEO_{34}-PC 10 wt.% MA containing 30 wt.% LiTFSI at 30 °C, 70 °C and 100 °C.

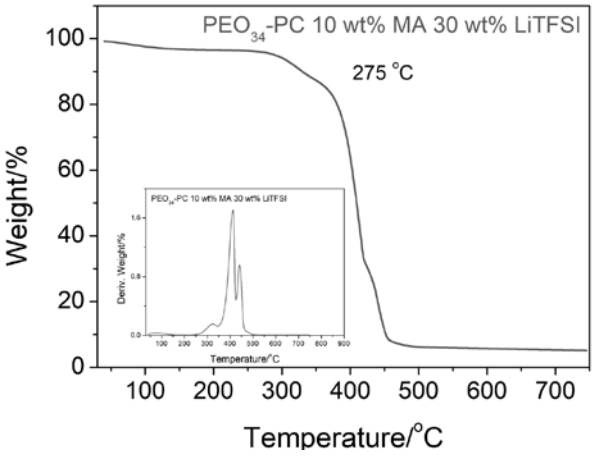

Figure 3.14. Thermogravimetric analysis of PEO_{34}-PC 10 wt.% MA containing 30 wt.% LiTFSI.

3.2.2.1 Electrochemical characterization of the cross-linked PEO_{34}-PC

First, the effect of methacrylic content in the copolymer was evaluated, which should affect the cross-linking density of SPEs, and therefore, the ionic conductivity. Thus, PEO_{34}-PC copolymers with 5, 10 and 20 wt.% of methacrylic monomer and 30 wt.% of LiTFSI were investigated. Even though 5 wt.% methacrylic monomer gives slightly higher ionic conductivity ($3.6 \cdot 10^{-5}$ S cm^{-1} at room temperature), 10 wt.% of methacrylic diol was observed to be the minimum amount to succeed in a free standing SPE. Besides, the ionic conductivity lightly decreases from $3.2 \cdot 10^{-5}$ S cm^{-1} with 10 wt.% MA to $9.4 \cdot 10^{-6}$ S cm^{-1} with the addition of 20 wt.% of MA at room temperature. Therefore, the polymer with 10 wt.% of methacrylic monomer was chosen for further studies.

Second, electrochemical properties were investigated varying the LiTFSI concentrations in the polymer with 10 wt.% methacrylic diol, with the aim of determining the optimum composition for testing in lithium-based battery. The salt concentration was varied from 15 wt.% to 80 wt.% (**Figure 3.15a**). The highest

conductivity value of $3.2 \cdot 10^{-5}$ S cm^{-1} at room temperature is obtained with 30 wt.% of LiTFSI, equivalent to an O:Li mole ratio of 1:16. We have to remark, that this value is not compromised by the cross-linked network, compared with $3.7 \cdot 10^{-5}$ S cm^{-1} for the non-cross-linked PEO_{34}-PC at ambient temperature, that we previously determined. Besides, the ionic conductivity showed at 70 °C is $1.3 \cdot 10^{-3}$ S cm^{-1}, which is higher than for the non-crosslinked PEO_{34}-PC ($3.5 \cdot 10^{-4}$ S cm^{-1}), could be attributed to the higher amount of carbonate groups present on the system than PEO_{34}-PC. The trend with cross-linked SPEs is comparable to the case of non-cross-linked ones; when the salt concentration is lower than 30 wt.% of LiTFSI, the crystallinity is pronounced, as shown in DSC analysis, **Figure 3.15b**, and these crystalline domains restrict the ion conduction. Therefore, the ion movement is increased while the crystallinity is suppressed, the case of 30 wt.% of LiTFSI. Besides, if the salt concentration is increased more than 30 wt.%, the ionic conductivity decreases due to the increase on the glass transition temperature. With the high amount of LiTFSI, 80 wt.%, the glass transition increases more than 10 °C respect to 30 wt.% of LiTFSI, which provokes that the ionic conductivity decreases one order of magnitude. This ionic conductivity behaviour has more similarity to PEO based SPEs, rather than polycarbonate SPEs. In the later case, a higher salt concentration, generally increases the ionic conductivity.[22]

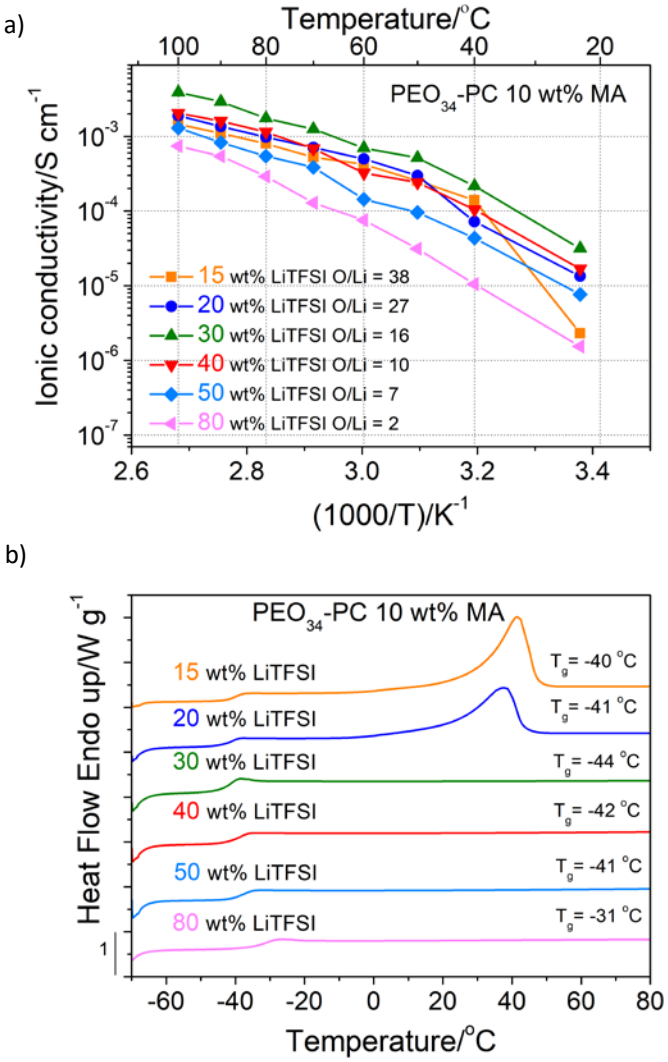

Figure 3.15. a) Ionic conductivities, and b) DSC measurements of cross-linked PEO_{34}-PC 10 wt.% MA with different LiTFSI concentration. DSC traces recorded during the second heating scan at 20 K min^{-1}.

Then, we measured the lithium transference number at 70 °C using Bruce and Vincent method in order to see if the carbonate group is involved in any electrochemical property. The LiTFSI concentration was varied between 15 wt.% to 50 wt.% to study

the effect of salt concentration on the transference number, the results are shown in Figure 3.16a. The lithium transference number varies with the LiTFSI composition, showing the highest value of 0.59 for the SPE containing 30 wt.% of LiTFSI (experimental results in Figure 3.16b). This value compares favourably with PEO-based SPE with 30 wt.% LiTFSI, which is close to 0.17. This clearly shows the previous observations of other authors on the favourable effect of carbonate groups on the lithium transference number;[14] the carbonyl group of carbonate helps to dissociate the LiTFSI, leading to a favourable lithium mobility. This optimum value of 30 wt.% LiTFSI can be discussed with the ideal balance of Li cation and the amount of carbonate groups on the system: i) a lower concentration of salt than 30 wt.% LiTFSI, can lead in free carbonate groups and also, in lower cations in the systems; and ii) a system with higher LiTFSI concentration, not all the Li cations can be coordinated by carbonate moieties and they will coordinate with EO units. Therefore, the lithium transference number will decrease.

Using this lithium transference values and the total ionic conductivity, we could calculate lithium cation conductivity at 70 °C, Figure 3.16a. As expected, SPE containing 30 wt.% of LiTFSI presents the highest lithium ionic conductivity among all the samples, $7.4 \cdot 10^{-4}$ S cm^{-1}, hence this composition was further investigated.

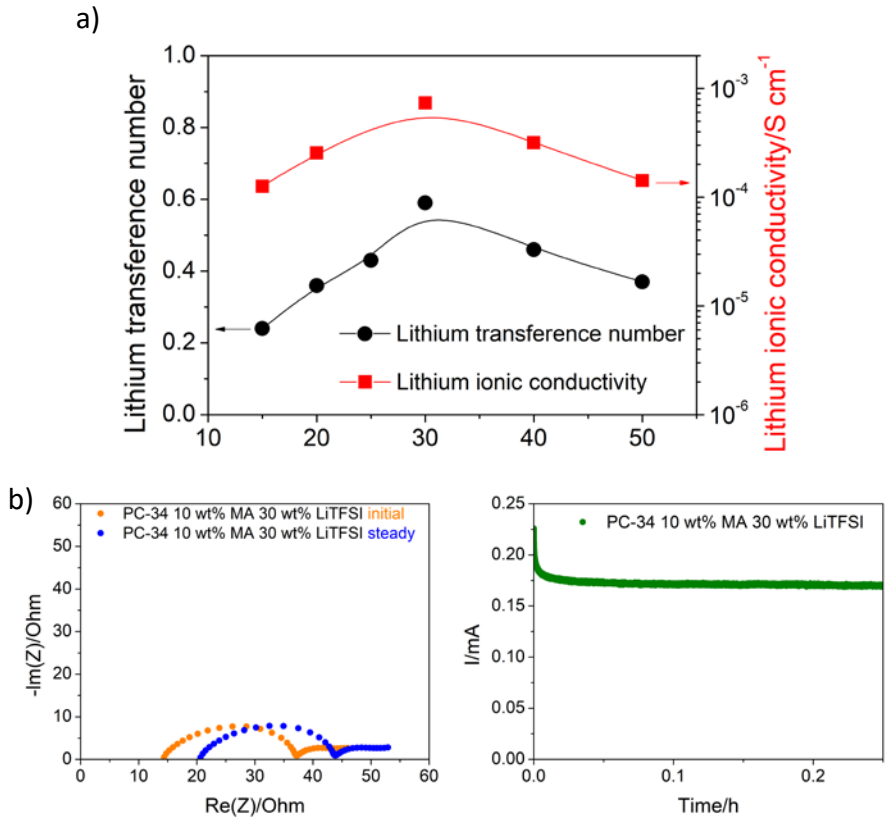

Figure 3.16. a) Lithium transference number in black (●) and lithium ionic conductivity in red (■) of different cross-linked PEO_{34}-PC 10 wt.% MA membranes at 70 °C. b) EIS and CA experiments of PEO_{34}-PC 10 wt.% MA with 30 wt.% LiTFSI.

^{7}Li solid-state NMR experiments were used to investigate the lithium cation environment and dynamics, and their dependence on the LiTFSI salt content. Pulsed field gradient diffusion measurements were used to measure the ^{7}Li self-diffusion coefficients, **Figure 3.17**. These data show a clear trend of decreasing lithium cation diffusion coefficients as the salt content is increased. Faster timescale, shorter-range dynamics were also probed via ^{7}Li T_1 relaxation measurements, which were fitted using the same method as outlined in our previous section.[23] The resulting graphics

and parameters are shown in **Figure 3.18** and **Table 3.4**, again as a function of the LiTFSI content. The quadrupolar coupling constant C_Q gives an insight into the symmetry of the Li^+ coordination environment (via the local electric field gradient), and the decreasing value as LiTFSI content increases reflects the Li^+ environment becoming slightly more symmetric on average. Alongside this trend, the correlation time τ_c increases while the activation energy for this motional process decreases with increasing LiTFSI concentration. The former implies a decrease in the local dynamics around the Li^+ while the latter implies that the local dynamics become more energetically favourable. This apparent contradiction would be best explained by a change in the local coordination environment as the LiTFSI content increases, which is also what the changing C_Q values imply. This is most likely the effect of the competing coordination of the Li^+ by the TFSI anions and the ether oxygens of the polymer. These results can lead to understand why lithium ionic conductivity is decreased with the increase of LiTFSI concentration. Different environments can affect on a higher/lower lithium ionic conductivity when LiTFSI concentration is varied.

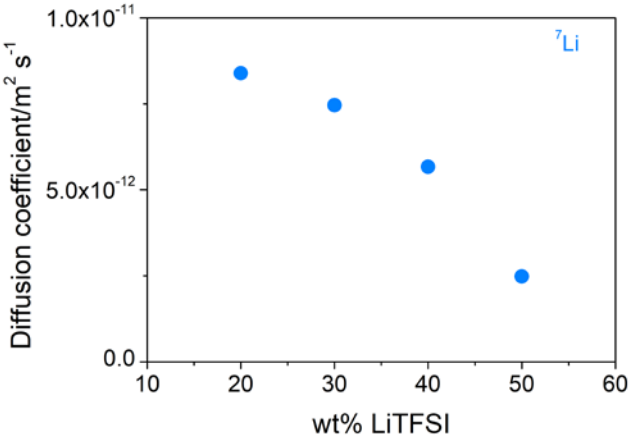

Figure 3.17. ^7Li diffusion coefficients as a function of wt.% LiTFSI measured using pulsed field gradient NMR at 70 °C.

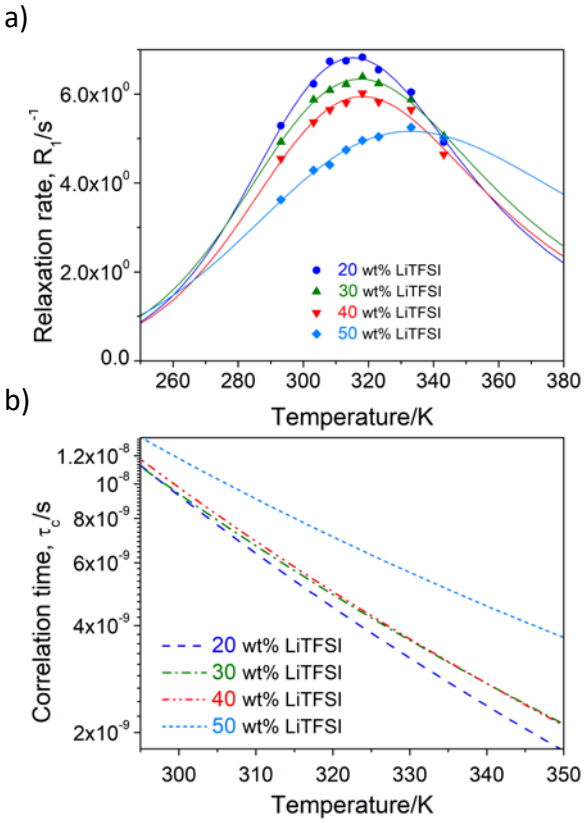

Figure 3.18. a) Fitting of the ^{7}Li relaxation rate data, and b) temperature dependent ^{7}Li motional correlation times.

Table 3.4. ^{7}Li quadrupolar coupling constants (C_Q), motional correlation times (τ_c) and activation energies (E_A) extracted from the fitting of the NMR T_1 relaxation times.

Samples	C_Q (kHz)	τ_c (ns) at 343.15 K	E_A (kJ mol^{-1})
20 wt.% LiTFSI	26.59±0.49	2.17±0.04	28.83±0.53
30 wt.% LiTFSI	25.64±0.47	2.53±0.05	26.02±0.48
40 wt.% LiTFSI	24.83±0.46	2.52±0.05	26.90±0.49
50 wt.% LiTFSI	23.14±0.43	4.25±0.08	20.24±0.37

The electrochemical stability of the SPE based on PEO_{34}-PC 10 wt.% MA containing 30 wt.% of LiTFSI was investigated at a scan rate of 0.5 mV s^{-1} at 70 °C, **Figure 3.19**. The anodic limit of the SPE was 4.9 V *vs.* Li/Li^+. During the cathodic scan, we observed a peak corresponding to the lithium plating process between 0 and -0.5 V *vs.* Li/Li^+ and the peak corresponding to the reverse process – stripping of lithium – between 0 and 0.6 V *vs.* Li/Li^+. The wide electrochemical stability, up to 4.9 V, opens opportunities to employ the membrane in different Lithium battery technologies.

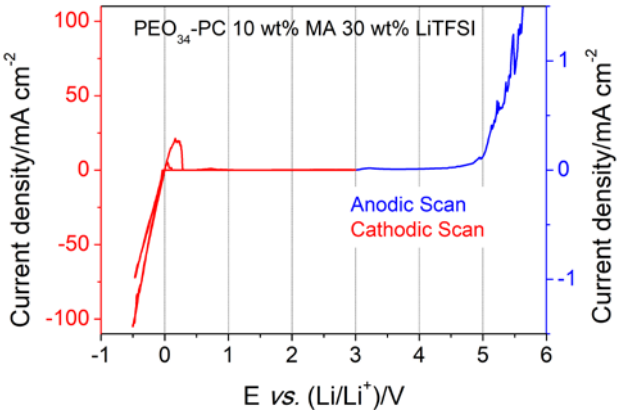

Figure 3.19. Electrochemical stability of cross-linked PEO_{34}-PC 10 wt.% MA containing 30 wt.% LiTFSI. Cyclic voltammetry was carried out at 0.5 mV s^{-1} at 70 °C.

3.2.2.2 Cross-linked PEO_{34}-PC-SPE in Lithium symmetric cells

To further confirm the viability of the SPE in Li-based cells, lithium symmetric cells were assembled and cycled at different current densities at 70 °C, **Figure 3.20**. At 0.1 mA cm^{-2}, the cell over-potential is around 50 mV which is comparable with state-of-the-art polymer electrolytes commonly used in the Li-based symmetric cells.[24] Increasing the applied current density from 0.1 mA cm^{-2} to 0.5 mA cm^{-2}, the overpotential of the symmetric cell also increased to 200 mV. The increased cell over-potential is due to the kinetics limitation of the Li charge transfer in the SPE and/or

the solid electrolyte interphase (SEI) layer of Li/electrolyte. Even if a plateau cannot be observed due to the TFSI anion, we can say that this SPE can sustain high current densities. The impedance spectroscopy showed no significant change on the resistance of the SEI layer (corresponds to the first semicircle at high frequencies) with the variation on current density at the Li stripping/plating process. Besides, the second semicircle that is observed in Nyquist plot at low frequencies can be related to the mass transfer process.

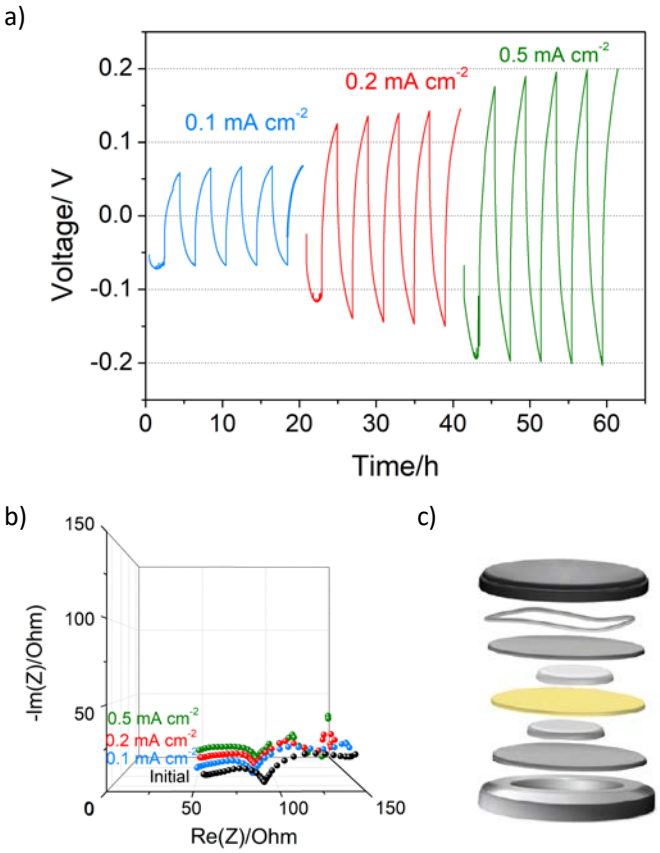

Figure 3.20. Lithium symmetric cell of cross-linked PEO_{34}-PC 10 wt.% MA containing 30 wt.% LiTFSI. a) The evolution of overpotential with different current densities, b) Nyquist plot after applying different current densities, and c) Scheme of symmetric cell assembly.

3.2.2.3 Full solid-state rechargeable battery Lithium-SPE-NMC-cell based on cross-linked PEO_{34}-PC

Due to the promising results in the previous section, the cross-linked PEO_{34}-PC was tested in Nickel-Maganese-Cobalt oxide (NMC) (111) based cathode, **Figure 3.21**. NMC is used as a high voltage cathode, and as PEO_{34}-PC shows stability up to 4.9 V, it may be suitable for this high voltage cathodes. For this preliminary results, the formulation of the SPE was slightly modified. The linear PEO_{34}-PC was employed, with the combination of 14 wt.% LiTFSI. In order to improve the mechanical properties, 5 wt.% of poly(ethylene glycol)diacryalte was used. The battery cycling (4.2 V-2.8 V) at C/20 was performed at 50 °C and 70 °C. As expected, a better capacities were obtained at higher temperature reaching almost 200 mAh g^{-1} and 160 mAh g^{-1} at 70 °C and 50 °C respectively at the begining, where a higher ionic conductivity is estimated. Even if, there is a capacity faiding, in the case of cell cycled at 70 °C the capacity retention is about 77 %, whereas in the cased of 50 °C, it is about 60 %, in both cases good efficiencies are determined. Although the battery can be optimize to improve the performance, these values for a all solid state battery are promising.

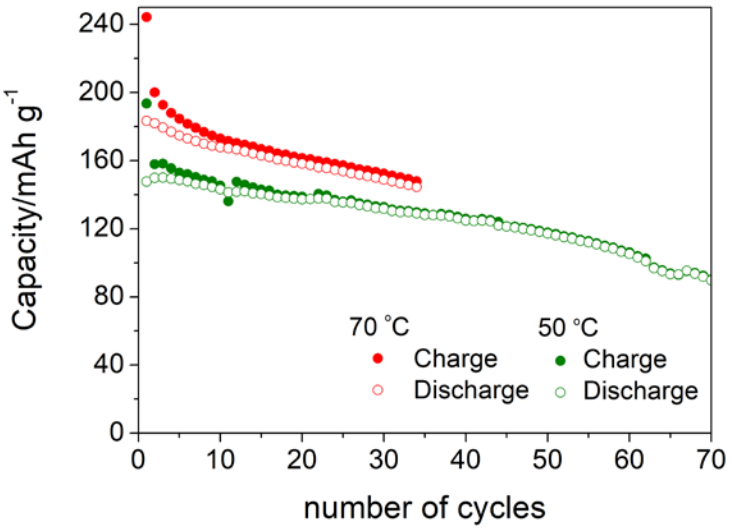

Figure 3.21. NMC-cell performance at 70 °C and 50 °C, using PEO_{34}-PC based SPE.

3.3 Conclusions

In this chapter, we investigated the combination between ethylene oxide and carbonate units on several polymers on its thermal and electrochemical properties. Using melt polycondensation technique, a series of $PEO_{2\text{-}45}$-PC were synthesized. The PEO-PC copolymers were formulated as solid polymer electrolytes by adding different amounts of bis(trifluoromethane)sulfonimide lithium salt to the synthesized polymer. The optimum SPEs, showing the lowest glass transition temperature, was based on the poly(ethylene oxide)/carbonate having a high amount of EO units (34) between carbonate links. This polymer is semicrystalline, but the crystallinity is avoided by the addition of the LiTFSI salt. The highest ionic conductivity value of $3.7 \cdot 10^{-5}$ S cm^{-1} at room temperature was observed in the case of 30 wt.% LiTFSI. This ionic conductivity behaviors of these SPEs are similar to PEO-SPEs, where the glass transition increases

with the salt content. However, FTIR spectra revealed the favourable coordination between the carbonate groups and the lithium cation.

Therefore, in order to further investigate the role of EO units and carbonate groups, free-standing solid polymer electrolyte was developed by incorporating 10 wt.% of methacrylic monomer into the poly(ethylene oxide$_{34}$ carbonate) main chain. These membranes showed promising electrochemical values, such as high lithium ionic conductivity, transference number and electrochemical stability window of $7.4 \cdot 10^{-4}$ S cm^{-1}, 0.59 and 4.9 V respectively, at 70 °C with 30 wt.% of LiTFSI. In non cross-linked and cross-linked SPEs, solid ^{7}Li NMR analysis showed a change on coordination environment while LiTFSI concentration is varied, which can be correlated with lithium diffusion and ionic conductivity trends. Furthermore, it was shown the ability of PEO-PC SPE to transport lithium in a lithium symmetric cell at 70 °C. Finally, a full solid-state lithium-SPE-NMC-cell was built showing promising preliminary results.

3.4 Experimental part

3.4.1 Materials

Dry dimethyl carbonate (99+ %) (DMC) and 4-dimethylaminopyridine (DMAP) (99%) were purchased from Across Organics. The diol diethylene glycol, hexaethylene glycol and poly(ethylene glycol) (M_n 1,500 g mol^{-1}) were supplied by Fisher Scientific and the diols triethylene glycol, tetraethylene glycol, poly(ethylene glycol) (M_n 600 g mol^{-1}), poly(ethylene glycol) (M_n 1,000 g mol^{-1}), and poly(ethylene glycol) (M_n 2,000 g mol^{-1}) by Merck. All diols were dried by azeotropic distillation in toluene for 8 h and DMAP was dried applying vacuum for 4 h at room temperature prior to use. Lithium bis(trifluoromethane)sulfonimide (LiTFSI) (99.9%) was supplied from Solvionic. Tetrahydrofuran (GPC grade) was obtained from Scharlab, acetonitrile (HPLC grade),

diethyl ether (Extra Pure, SLR, Stabilised with BHT), methanol (MeOH) (Certified AR for Analysis) and dichloromethane (DCM) (Cerfified AR for Analysis) from Fisher Scientific, toluene (HPLC grace) from Merck and deuterated chloroform (99.8%) from Deutero GmbH.

3.4.2 Synthesis of linear poly(ethylene oxide carbonate)s

Poly(ethylene oxide) diols were polymerized by melt polycondensation with dimethyl carbonate as reported in the previous chapter. In a typical experiment, a 2:1:0.01 mole ratio of DMC:diol:DMAP was used for the diols containing between 2-6 EO units: diethylene glycol, triethylene glycol, tetraethylene glycol, hexaethylene glycol; PEO_2-PC, PEO_3-PC, PEO_4-PC, PEO_6-PC. On the other hand, for diols containing higher amount of EO, PEG600, PEG1000, PEG1500, PEG2000, a mole ratio of 8:1:0.01 was required for a reasonable molar mass, as it was studied by our group; PEO_{13}-PC, PEO_{22}-PC, PEO_{34}-PC and PEO_{45}-PC.[25] For the first set of polymers, the 1st step last 4 h at 130 °C, whereas for the second ones, 7 hours of the 1st step was required. However, in both cases the, second step was the same: 180 °C and vacuum, overnight. Once the polymerization was completed, all polymers were dissolved in dichloromethane and purified by precipitation in methanol the ones with 2-6 EO units, and in cold diethyl ether the other serie. The complete disappearance of the monomers was determined by ^{1}H NMR, ^{13}C NMR and FTIR-ATR. The following example is given for PEO_6-PC: ^{1}H NMR ($CDCl_3$, 500 MHz): δ = 4.28 (t, OCOOC**H**$_2$, 4H), 3.72 (t, OCOOCH$_2$C**H**$_2$, 4H), 3.64 (s, OC**H**$_2$C**H**$_2$O, 16H). ^{13}C NMR ($CDCl_3$, 125 MHz): δ = 155.14 (O**C**OO), 70.63 (O**C**H$_2$), 68.88 (OCOOCH$_2$**C**H$_2$), 67.05 (OCO**C**H$_2$CH$_2$).

3.4.3 Preparation of poly(ethylene oxide carbonates) based polymer electrolytes

Solid polymer electrolytes containing different amount of PEO_x-PC polymer matrix and LiTFSI salt were prepared by solvent casting method from solution in acetonitrile (ACN) (0.4 g of polymer/salt in 0.5 mL dry ACN) directly casted onto the stainless steel (SS) spacers. First, ACN was removed under vacuum at room temperature during 24 h, and then, the evaporation was completed in an oven inside an argon filled glovebox, increasing the temperature up to 60 °C and applying vacuum for 24 h.

3.4.4 Synthesis of cross-linkable poly(ethylene $oxide_{34}$ carbonate)

The synthesis of UV-curable polycarbonate was performed using the same synthetic process as previously described. The following amounts of reactants were used in the synthesis: DMC (1.5 mL, 17.84 mmol, 8 eq), diols (1 eq): PEG1500 (2 g, 1.33 mmol, 0.6 eq) and bis-MPA methacrylic (MA) (0.22 g, 0.9 mmol, 0.4 eq.), and DMAP (2.7 mg, 0.0223 mmol), 0.01 eq). 2,2-bis(hydroxymethyl)-propionic acid (MA) was synthesized in three steps following previously described work.[26] 10 wt.% of UV curable monomer respect to the overall diol used was incorporated. It was necessary to add few ppm of hydroquinone in order to prevent the polymerization from the double bonds during the polycondensation steps. During the first 7 hours of the polycondensation, the reaction was maintained at 130 °C, and later, the temperature was increased up to 170 °C and high vacuum was applied overnight. Once the reaction was stopped, the polymer was dissolved in dichloromethane and powdered in cold diethyl ether, obtaining 80 % of yield. The disappearance of the monomers was confirmed by ^{1}H NMR. Moreover, the double bonds of the methacrylic diol could be determined by ^{1}H NMR. In the final polymer, 23 mol % of MA was achieved. The polymer was characterized by ^{1}H NMR ($CDCl_3$, 400 MHz): δ= 6.13, 5.57 (s, C=C$\underline{\mathbf{H}}_2$, 2H), 4.45-4.29 (d, (OCOOC$\underline{\mathbf{H}}_2$C, 4H), 4.28 (t, OCOOC$\underline{\mathbf{H}}_2$CH_2, 4H), 3.82 (t, OCOC$\underline{\mathbf{H}}_2$C$\underline{\mathbf{H}}_2$OCO, 4H), 3.71

(t, $OCOOCH_2C\underline{H}_2$, 4H), 3.64 (s, $OCOCH_2CH_2OC\underline{H}_2C\underline{H}_2$, 128H), 1.95 (s, $OCOOCH_2CC\underline{H}_3$, 3H), 1.25 (s, $H_2C{=}CC\underline{H}_3$, 3H). The yield of the polymerization was determined by gravimetry (yield = 70 %).

3.4.5 Preparation of free standing polymer electrolytes

For the preparation of ultraviolet cross-linked SPEs, the polymer, the salt (LiTFSI), and the UV initiator (2-hydroxy-2-methylpropiophenone (1 wt.% respect to the initial MA amount)), were dissolved in ACN. In each SPE a specific LiTFSI concentration was added: 0 wt.%, 15 wt.%, 20 wt.%, 25 wt.% 30 wt.%, 40 wt.%, 50 wt.% and 80 wt.%. Once the solutions were stirred during 10 minutes, they were cast onto a silicon mold. The solvent was removed at room temperature and later by applying high vacuum. Finally, the films were passed 3 times from a xenon arc lamp (Helios Italquartz, 45 mW cm^{-2}). Before performing any electrochemical characterization, the SPEs were first dried under vacuum at room temperature during 24 h, and after, the evaporation was completed in an oven inside an argon-filled glove box, increasing the temperature up to 60 °C and applying vacuum for 24 h.

3.4.6 Preparation of solid polymer electrolytes for full-cell

Free standing polymer electrolytes were prepared as follow: 1 g of polymer and 0.1665 g LiTFSI were dissolved in 0.2 mL methanol. 5 wt.% of poly(ethylene glycol) diacrylate (PEGDA) (M_n 575) and photoinitiator (1 wt.% *vs.* PEGDA), 2-hydroxy-2-methylpropiophenone were added to the solution. After stirring the solution during 10 minutes, first, the solvent was slowly evaporated at room temperature and the evaporation of the solvent was completed applying high vacuum at room temperature overnight. Finally, the membranes were passed 3 times from xenon arc lamp (Helios Italquartz, 45 mW cm^{-2}). Before performing any electrochemical characterization, the SPEs were first dried under vacuum at room temperature during

24 h, and after, it was completed increasing the temperature up to 60 °C and applying vacuum for 24 h.

3.4.7 Cathode preparation

The cathode preparation was carried out inside of an argon filled glove box. The cathode was composed by NMC (111) : C65 : polymer electrolyte (PEO_{34}-PC 14wt.% LiTFSI 5 wt.% PEGDA) (60:10:30 wt.%). 0.33 g of cathode were mixed in 26 drops of NMP. The cathode was left stirring overnight and the next day, it was casted on top of carbon coated aluminium foil using a Dr. Blade (250 mm). The NMP evaporation was ensured by first drying it in the oven during 24 h at room temperature and later, by increasing the temperature until 50 °C for another 24 hours under vacuum. The NMC loading were 0.164 mAh cm^{-2} and 0.266 mAh cm^{-2} at 70 °C and 50 °C respectively.

3.4.8 Characterization methods

^{1}H and ^{13}C Nuclear Magnetic Resonance (NMR) spectra were recorded on Bruker spectrometers at 500 MHz at room temperature, using deuterated chloroform. Attenuated Total Reflectance Fourier Transform Infrared Spectroscopy measurements (ATR-FTIR) were conducted on a Bruker ALPHA Spectrometer.

The absolute molar masses of poly(ethylene oxide carbonates) were analyzed by SEC/MALS/RI. The equipment was composed of a LC20 pump (Shimadzu) coupled to a DAWN Heleos multiangle (18 angles) light scattering laser photometer equipped with an He–Ne laser (λ = 658 nm) and an Optilab Rex differential refractometer (λ = 658 nm), (all from Wyatt Technology Corp., USA). Separation was carried out using three columns in series (Styragel HR2, HR4, and HR6; with pore sizes from 10^2 to 10^6 Å). Filtered toluene was used for the calibration of the 90° scattering intensity. The

detectors at angles other than 90° in the MALS instrument were normalized to the 90° detector using a standard (PS 28 770 g mol^{-1}; Polymer Labs), which is small enough to produce isotropic scattering, at a flow rate of THF through the detectors of 1 mL min^{-1}. In addition, the same standard and conditions were used to perform the alignment (interdetector delay volume) between concentration and light-scattering detectors and the band-broadening correction for the sample dilution between detectors. The analyses were performed at 35 °C and THF was used as a mobile phase at a flow rate of 1 mL min^{-1}. $\partial n/\partial C$ was measured for PEO_2-PC, PEO_3-PC, PEO_4-PC and PEO_6-PC being around 0.06 mg mL^{-1}. On the other hand, for the materials containing higher amount of ethylene oxide units, the $\partial n/\partial C$ of PEO was used (0.136). The absolute molar mass was calculated from the RI/MALS data using the Debye plot (with first-order Zimm formalism) by using the ASTRA software version 6.0.3 (Wyatt Technology, USA).

Besides, molar mass distributions of PEO_{34}-PC 10wt.% MA was measured by size exclusion chromatography (SEC). The sample was diluted in THF (GPC grade) to a concentration of approximately 5 mg mL^{-1} and filtered through a 0.45 mm nylon filter. The SEC set up consisted of a pump (LC-20A, Shimadzu), an autosampler (Waters 717), a differential refractometer (Waters 2410) and three columns in series (Styragel HR2, HR4, and HR6 with pore sizes ranging from 102 to 106 Å). Chromatograms were obtained in THF (GPC grade) at 35 °C using a flow rate of 1 mL min^{-1}. The equipment was calibrated using narrow polystyrene standards ranging from 595 to $3.95 \cdot 10^{-6}$ g mol^{-1} (5^{th} order universal calibration).

Differential Scanning Calorimetry (DSC) was performed on a DSC Q2000 differential calorimeter (TA Instruments). All the experiments were performed under ultrapure nitrogen flow. Samples of 5 mg were used. Measurements were performed by placing

the samples in sealed aluminum pans. The samples were first heated at a rate of 20 K min^{-1}, from 25 °C to 100 °C and they were left 3 min at 100 °C to avoid the influence of thermal history, in order to be able to compare the crystallization/melting temperature afterwards. Subsequently, the sample was cooled down to -70 °C at a rate of 2 K min^{-1} and subsequently heated to 100 °C at 20 K min^{-1} after waiting at -80 °C during 3 min. In order to determine the glass transition temperature, it was performed a fast cooling (50 K min^{-1}) at the data was recorded during the heating scan at 20 K min^{-1}.

The mechanical properties were analysed by rheological measurements using an AR-G2 rheometer (TA Instruments) with parallel geometric plates (diameter 12 mm). Angular frequency sweeps were performed in the range of $6^2 < \omega < 6^{-2}$ rad s^{-1} at different temperatures (70 °C, and 100 °C) in the linear viscoelastic regime. The time required for a frequency sweep was 5 min. Each measurement was repeated at least two times observing a good reproducibility. On the other hand, the thermogravimetry analysis was performed at N_2 atmosphere at 10 K min^{-1} in Q500 TA Instruments.

Ionic conductivity (σ) of the polymer electrolytes was determined by AC impedance spectroscopy over the frequency range from 100 mHz to 1 MHz with an amplitude of 10 mV in a VMP3 (Biologic, Claix, France) potentiostat. The conductivities were analyzed in a temperature range during the cooling scan from 100 °C to 25 °C. All cells were assembled in an argon filled glove box (M-Braun), avoiding any water and oxygen. The polymer electrolytes were sandwiched between two stainless steel (SS) electrodes. In all the cases the average surface area of the electrode is 2.01 cm^2. The polycarbonates were closed in CR2016 coin cells. Lithium transference number was calculated based on Bruce and Vincent method at 70 °C.[27] The electrolytes were sandwiched between two lithium disks in CR2032 coin cells. Before the analysis, the

cells were left to stabilize at 70 °C for 24 h. The lithium ionic conductivity was calculated by multiplying the total ionic conductivity with lithium transference number at 70 °C.[28] Electrochemical stability window was determined by applying cyclic voltammetry (CV) of the polymer electrolyte at 70 °C. The anodic limit was evaluated between open circuit potential (OCV) and 6 V *vs*. Li/Li^+ at a constant rate of 0.5 mV s^{-1}. On the other hand, the cathodic scan was determined between OCV and -0.5 V *vs*. Li/Li^+ using the same scan rate. Before performing the experiment, the electrolytes were left stabilizing for 24 h at 70 °C. The polymer electrolyte was sandwiched between a metal lithium disk and a working electrode. Metallic lithium served as a reference and counter electrode. Besides, stainless steel disk was used as working electrode during anodic stability study, whereas copper disks for cathodic measurements. The samples were sealed in CR2032 coin cells.

Symmetric cell test was performed at 70 °C after stabilization at that temperature during 48 h. The SPE was sandwiched between two lithium metallic dicks. Currents of 0.1, 0.2 and 0.5 mA cm^{-2} were applied with a polarization period of 1 hour

Full cell analysis was performed at 70 °C after stabilization at that temperature during 24 h. The SPE was sandwiched between a lithium metallic dicks and NMC 111 based cathode. The capacity among the cycles was evaluated at C-rate of C/20 between 4.2 V and 2.8 V. (Cathode loading: 70 °C, 0.164 mAh cm^{-2} and 50 °C, 0.266 mAh cm^{-2}).

The ^7Li NMR longitudinal relaxation times (T_1) were measured on a 300 MHz Bruker Avance III spectrometer with ^7Li Larmor frequencies of 116.64 MHz using a saturation recovery pulse sequence. These experiments were performed at various temperatures ranging from 293.15 to 343.15 K using a Bruker 5 mm Diff50 pulsed field gradient (PFG) NMR probe. The sample temperature was controlled to within ±1 K with 10 minutes temperature equilibration time.

Diffusion coefficients were measured at 70°C using the same NMR probe with the stimulated echo pulse sequence. The maximum gradient strength was 2400 G cm^{-1} and the repetition time was around 5 s. The gradient pulse length and diffusion time were chosen to be appropriate resulting the attenuation curves. Resulting signal decays were fitted to the Stejskal-Tanner equation.[21]

3.5 References

1. Fenton, D. E.; Parker, J. M.; Wright, P. V., Complexes of alkali metal ions with poly(ethylene oxide). *Polymer* **1973,** *14* (11), 589.

2. (a) Armand, M., Polymer solid electrolytes - an overview. *Solid State Ionics* **1983,** *9*, 745-754; (b) Oteo, U.; Martinez-Ibañez, M.; Aldalur, I.; Sanchez-Diez, E.; Carrasco, J.; Armand, M.; Zhang, H., Improvement of the Cationic Transport in Polymer Electrolytes with (Difluoromethanesulfonyl)(trifluoromethanesulfonyl)imide Salts. *ChemElectroChem* **2019,** *6* (4), 1019-1022.

3. Brandell, D.; Priimägi, P.; Kasemägi, H.; Aabloo, A., Branched polyethylene/poly(ethylene oxide) as a host matrix for Li-ion battery electrolytes: A molecular dynamics study. *Electrochimica Acta* **2011,** *57*, 228-236.

4. (a) Bouchet, R.; Maria, S.; Meziane, R.; Aboulaich, A.; Lienafa, L.; Bonnet, J.-P.; Phan, T. N. T.; Bertin, D.; Gigmes, D.; Devaux, D.; Denoyel, R.; Armand, M., Single-ion BAB triblock copolymers as highly efficient electrolytes for lithium-metal batteries. *Nat Mater* **2013,** *12* (5), 452-457; (b) Porcarelli, L.; Shaplov, A. S.; Bella, F.; Nair, J. R.; Mecerreyes, D.; Gerbaldi, C., Single-Ion Conducting Polymer Electrolytes for Lithium Metal Polymer Batteries that Operate at Ambient Temperature. *ACS Energy Letters* **2016,** *1* (4), 678-682.

5. Panday, A.; Mullin, S.; Gomez, E. D.; Wanakule, N.; Chen, V. L.; Hexemer, A.; Pople, J.; Balsara, N. P., Effect of molecular weight and salt concentration on

conductivity of block copolymer electrolytes. *Macromolecules* 2009, *42* (13), 4632-4637.

6. (a) Chung, S.; Wang, Y.; Persi, L.; Croce, F.; Greenbaum, S.; Scrosati, B.; Plichta, E., Enhancement of ion transport in polymer electrolytes by addition of nanoscale inorganic oxides. *Journal of power sources* 2001, *97*, 644-648; (b) Croce, F.; Persi, L.; Scrosati, B.; Serraino-Fiory, F.; Plichta, E.; Hendrickson, M., Role of the ceramic fillers in enhancing the transport properties of composite polymer electrolytes. *Electrochimica Acta* 2001, *46* (16), 2457-2461.

7. Thiam, A.; Antonelli, C.; Iojoiu, C.; Alloin, F.; Sanchez, J.-Y., Optimizing ionic conduction of poly(oxyethylene) electrolytes through controlling the cross-link density. *Electrochimica Acta* 2017, *240*, 307-315.

8. Meyer, W. H., Polymer electrolytes for lithium-ion batteries. *Advanced materials* 1998, *10* (6), 439-448.

9. (a) Mindemark, J.; Imholt, L.; Montero, J.; Brandell, D., Allyl ethers as combined plasticizing and crosslinkable side groups in polycarbonate-based polymer electrolytes for solid-state Li batteries. *Journal of Polymer Science Part A: Polymer Chemistry* 2016, *54* (14), 2128-2135; (b) Morioka, T.; Nakano, K.; Tominaga, Y., Ion-Conductive Properties of a Polymer Electrolyte Based on Ethylene Carbonate/Ethylene Oxide Random Copolymer. *Macromolecular Rapid Communications* 2017, *38* (8), 1600652-n/a.

10. He, W.; Cui, Z.; Liu, X.; Cui, Y.; Chai, J.; Zhou, X.; Liu, Z.; Cui, G., Carbonate-linked poly(ethylene oxide) polymer electrolytes towards high performance solid state lithium batteries. *Electrochimica Acta* 2017, *225*, 151-159.

11. Tominaga, Y.; Nakano, K.; Morioka, T., Random copolymers of ethylene carbonate and ethylene oxide for Li-Ion conductive solid electrolytes. *Electrochimica Acta* 2019, *312*, 342-348.

12. (a) Morioka, T.; Ota, K.; Tominaga, Y., Effect of oxyethylene side chains on ion-conductive properties of polycarbonate-based electrolytes. *Polymer* 2016, *84*, 21-26; (b) Tominaga, Y.; Shimomura, T.; Nakamura, M., Alternating copolymers

of carbon dioxide with glycidyl ethers for novel ion-conductive polymer electrolytes. *Polymer* 2010, *51* (19), 4295-4298.

13. Abraham, K. M.; Jiang, Z.; Carroll, B., Highly Conductive PEO-like Polymer Electrolytes. *Chemistry of Materials* 1997, *9* (9), 1978-1988.

14. Kimura, K.; Motomatsu, J.; Tominaga, Y., Correlation between Solvation Structure and Ion-Conductive Behavior of Concentrated Poly(ethylene carbonate)-Based Electrolytes. *The Journal of Physical Chemistry C* 2016, *120* (23), 12385-12391.

15. Bloembergen, N.; Purcell, E. M.; Pound, R. V., Relaxation effects in nuclear magnetic resonance absorption. *Physical review* 1948, *73* (7), 679.

16. Hayamizu, K.; Tsuzuki, S.; Seki, S.; Fujii, K.; Suenaga, M.; Umebayashi, Y., Studies on the translational and rotational motions of ionic liquids composed of N-methyl-N-propyl-pyrrolidinium (P13) cation and bis(trifluoromethanesulfonyl)amide and bis(fluorosulfonyl)amide anions and their binary systems including lithium salts. *The Journal of Chemical Physics* 2010, *133* (19), 194505.

17. Maitra, A.; Heuer, A., Cation Transport in Polymer Electrolytes: A Microscopic Approach. *Physical Review Letters* 2007, *98* (22), 227802.

18. Agrawal, R. C.; Pandey, G. P., Solid polymer electrolytes: materials designing and all-solid-state battery applications: an overview. *Journal of Physics D: Applied Physics* 2008, *41* (22), 223001.

19. Chen, X.; Chen, F.; Forsyth, M., Molecular dynamics study of the effect of tetraglyme plasticizer on dual-cation ionomer electrolytes. *Physical Chemistry Chemical Physics* 2017, *19* (25), 16426-16432.

20. Chen, F.; Forsyth, M., Elucidation of transport mechanism and enhanced alkali ion transference numbers in mixed alkali metal-organic ionic molten salts. *Physical Chemistry Chemical Physics* 2016, *18* (28), 19336-19344.

21. Stejskal, E. O.; Tanner, J. E., Spin diffusion measurements: spin echoes in the presence of a time-dependent field gradient. *The journal of chemical physics* 1965, *42* (1), 288-292.

22. Tominaga, Y.; Nanthana, V.; Tohyama, D., Ionic conduction in poly(ethylene carbonate)-based rubbery electrolytes including lithium salts. *Polym J* 2012, *44* (12), 1155-1158.

23. Meabe, L.; Huynh, T. V.; Lago, N.; Sardon, H.; Li, C.; O'Dell, L. A.; Armand, M.; Forsyth, M.; Mecerreyes, D., Poly(ethylene oxide carbonates) solid polymer electrolytes for lithium batteries. *Electrochimica Acta* 2018, *264*, 367-375.

24. Appetecchi, G. B.; Alessandrini, F.; Duan, R. G.; Arzu, A.; Passerini, S., Electrochemical testing of industrially produced PEO-based polymer electrolytes. *Journal of Power Sources* 2001, *101* (1), 42-46.

25. Meabe, L.; Sardon, H.; Mecerreyes, D., Hydrolytically degradable poly(ethylene glycol) based polycarbonates by organocatalyzed condensation. *European Polymer Journal* 2017, *95*, 737-745.

26. Ronco, L. I.; Basterretxea, A.; Mantione, D.; Aguirresarobe, R. H.; Minari, R. J.; Gugliotta, L. M.; Mecerreyes, D.; Sardon, H., Temperature responsive PEG-based polyurethanes "à la carte". *Polymer* 2017, *122*, 117-124.

27. Evans, J.; Vincent, C. A.; Bruce, P. G., Electrochemical measurement of transference numbers in polymer electrolytes. *Polymer* 1987, *28* (13), 2324-2328.

28. Kato, Y.; Yokoyama, S.; Yabe, T.; Ikuta, H.; Uchimoto, Y.; Wakihara, M., Ionic conductivity and transport number of lithium ion in polymer electrolytes containing PEG–borate ester. *Electrochimica Acta* 2004, *50* (2), 281-284.

CHAPTER 4.

Synthesis and characterization of Single-ion poly(ethylene oxide carbonate) polymer electrolyte

CHAPTER 4.

Synthesis and characterization of Single-ion poly(ethylene oxide carbonate) polymer electrolyte

4.1 Introduction

Poly(ethylene oxide) PEO including a dissolved lithium salt has been the gold standard solid polymer electrolyte (SPE) in the area of lithium batteries for more than 40 years. As discussed in the previous chapters, polycarbonates are being highly investigated as alternatives to PEO due to the higher lithium transfer number of its SPEs (t_{Li+}>0.5 *vs*. t_{Li+}>0.2 for PEO). A popular approach to further improve lithium transport number is anchoring the negatively charged ion to the polymeric chain, named as single-ion conducting polymer electrolyte (SIPE). Several monomers including weak anionic species have been investigated;[1] being the most studied SIPE, the lithium poly(styrenesulfonyl(trifluoromethylsulfonyl lithium salt).[2] This polymer and the methacrylic version has been included in a variety of block copolymer formulations

combining it with PEO segments.[3] Nowadays, the best SIPEs reported in the literature is based on the combination of PEO and pending sulfonamide units, which gives ionic conductivity values of 10^{-4} S cm^{-1} at 70 °C and lithium transference numbers close to unity.

As discussed in the previous chapters, several groups have reported the successful combination of ethylene oxide (EO) units and carbonate groups in the same copolymer.[4] EO units tend to decrease the glass transition, and consequently, increases the ionic conductivity, whereas the favorable weak coordination of carbonates and lithium cation promotes the lithium conductivity. Respect to this approach, in chapter 3, we proposed a new class of polymer host for lithium battery applications, consisting of ethylene oxide-carbonate segments, poly(ethylene oxide carbonates), PEO-PC. In chapter 3, a solid polymer electrolyte containing lithium bis(fluorosulfonyl)imide salt (LiTFSI) resulted in high ionic conductivity ($3.2 \cdot 10^{-5}$ S cm^{-1} at 25 °C and $1.3 \cdot 10^{-3}$ S cm^{-1} at 70 °C) and high lithium transference (0.6) at 70 °C.

Taking into account both strategies, in this chapter we show a new single-ion conducting polymer, which includes the three most successful chemical units in the area of polymer electrolytes: ethylene oxide, carbonate and lithium-sulfonamide groups. Single-ion poly(ethylene oxide carbonate) SIPCs are synthesized through the versatile polycondensation approach, showing a high ionic conductivity and lithium transference number close to unity. Once the composition of single-ion conducting polymer electrolyte was optimized, the electrochemical properties and symmetric cell performance of SIPC electrolyte were compared with the analogue conventional solid polymer electrolyte reported in chapter 3.

4.2 Results and discussion

4.2.1 Synthesis and characterization of Single-ion Conducting Poly (ethylene oxide carbonates) (SIPC)

In the present work innovative single-ion conducting polymer electrolytes are synthesized via step-growth polycondensation. This versatile polymerization technique gives the opportunity to combine different chemical structures, allowing the design of polymers with targeted properties to fit the end-use application requirements. This synergetic result has already been proven in chapter 3 by the combination of ethylene oxide (EO) units and carbonate groups.[5] Here, well studied EO units and carbonate groups are included to the single-ion polymer electrolyte. EO units are able to enhance the ionic conductivity, as they tend to show low glass transition, whereas, carbonates groups are claimed to improve the lithium transference number and electrochemical stability.[5] On the other hand, among the all anions proposed[1b] trifluoromethylsulfonylimide (TFSI) containing anionic species, like lithium ((3-((3-hydroxy-2-(hydroxymethyl)-2-methylpropanoyl)oxy)propyl)sulfonyl) ((trifluoromethyl)sulfonyl)amide, bis-MPTFSI, contains one of the most delocalized anion, which will expect to be able to promote the salt dissociation.[1b] This diol was synthesized based on a previous report.[6]

Scheme 4.1 describes the synthetic protocol employed in this polymerization. Polycarbonates are obtained by polycondensation in a mole ratio of DMC:diols:DMAP, 8:1:0.01.[7] This polymerization includes two step reactions, were high temperature (130 °C - 180 °C) and high vacuum (< 0.2 kPa) are necessary. The final chemical structure was determined by ^{1}H NMR in DMSO-d_6 (**Appendix Figure A11**).

Scheme 4.1. Synthesis of single-ion conducting polymers via polycondensation.

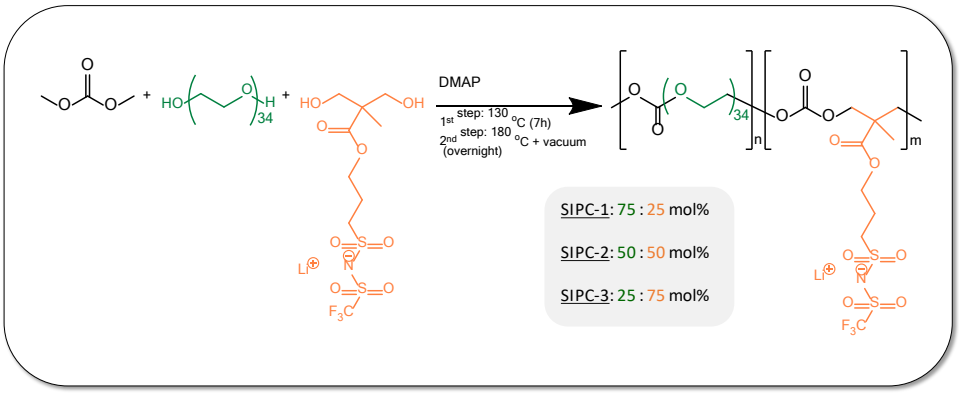

Three different copolymer compositions were targeted in order to design the optimal single-ion polymer electrolyte composition; PEO_{34}:bis-MPTFSI: 75:25 mol% (SIPC-1), 50:50 mol% (SIPC-2), and 25:75 mol% (SIPC-3). The properties of the polymer compositions are summarized in **Table 4.1**. Lithium content on the polymers was calculated by liquid ^{7}Li NMR, **Appendix Figure A12**. Thereby, the lithium concentration was estimated and a good correlation between each composition was observed. Lithium concentration is nearly three times higher in SIPC-2 than in SIPC-1. A similar increase in lithium concentration is observed when comparing SIPC-3 and SIPC-2. In addition, the molar masses of the polycarbonates were analysed in the GPC using DMF (10 mM of LiBr) as eluent, which ranged between 15-55 kDa. The dispersities obtained are in the typical range found for step-growth polymerization processes.

Table 4.1. Final polymers compositions and molar masses. [a] ^{7}Li NMR in DMSO-d_6.

Sample	SYNTHESIS		mmol Li/g polymer [a]	GPC (10 mM LiBr in DMF) (g mol^{-1})		
	PEO_{34}	Bis-MPTFSI		M_n	M_w	Đ
SIPC-1	75 mol%	25 mol%	0.21	55,000	77,000	2.0
SIPC-2	50 mol%	50 mol%	0.58	15,000	21,000	1.4
SIPC-3	25 mol%	75 mol%	1.9	15,000	19,000	1.3

4.2.2 Ionic conductivity and thermal properties of single-ion poly(ethylene oxide carbonates) SIPCs

Figure 4.1b shows the DSC traces of the SIPCs with various lithium concentration as a function of temperature. Both SIPC-1 and SIPC-2 exhibits an endothermic transition at 45 °C and 41 °C, respectively, corresponding to the melting of the crystalline EO phase. On the other hand, SIPC-3 does not exhibit any endothermic transition, indicating the amorphous nature of the polymer. The copolymers showed low glass transition values of -42 °C /SIPC-1, -38 °C/SIPC-2 and -36 °C/ SIPC-3. To better understand the impact of the lithium monomer incorporation on the crystallinity of EO phase, the degrees of crystallinity of the SIPCs were characterized, Equation 4.1. The percentage of the crystalline EO of 43 wt.%, 38 wt.% and 0 wt.% were calculated for SIPC-1, SIPC-2 and SIPC-3, respectively, suggesting that the incorporation of lithium monomer in the polymer chain hinders the crystallization of the EO segment. Similar observation was reported when lithium salt is added to PEO homopolymer.[8]

$$C_r = \frac{\Delta H_f}{w_{PEO} \times \Delta H_f^o} \times 100$$ **Equation 4.1.** The weight percentage of PEO crystallinity.

Where ΔH_f is the enthalpy of fusion calculated by DSC during the second heating scan at 10 °C min^{-1} (J g^{-1}). W_{PEO} is PEO percentage in the polymer and ΔH_f^o is the fusion enthalpy of fully crystalline PEO, 205 J g^{-1}.

The ionic conductivities of the SIPCs with various content of lithium concentrations were also measured via electrochemical impedance spectroscopy in a temperature range of 100 °C – 25 °C, and the results are presented in Figure 4.1a. At room temperature, the ionic conductivity of the SIPCs is as followed: SIPC-3 > SIPC2 > SIPC-1. It is well known that the ion conduction of lithium ion in PEO-based polymer electrolytes is governed by the segmental motion of the ethylene oxide chains in the

amorphous phase.[9] Therefore, below the melting temperature of the crystalline EO phase, the ion conduction of these SIPCs materials is mainly dictated by the degree of the crystallinity of the polymer. Increasing the lithium content from 25 mol% to 50 mol% (SIPC-1 to SIPC-2) only results in a slight decrease of the percentage of crystalline EO phase, going from 43 % to 38 %. This coincides with a slight increase of the ionic conductivity at 25 °C, going from $1.36 \cdot 10^{-7}$ S cm^{-1} to $2.28 \cdot 10^{-7}$ S cm^{-1}, when the lithium content is increased from 25 mol% to 50 mol%. At a lithium content of 75 mol% (SIPC-3), no crystalline EO phase is formed and a significant increase on the ionic conductivity is observed (e.g. $8.94 \cdot 10^{-7}$ S cm^{-1} at 25 °C).

Above the melting temperature of the crystalline EO phase (T> 50 °C), the lithium ion conduction is now governed by the O/Li molar ratio (incorporating carbonate oxygen), since all EO units are now readily available for conduction. It seems that SIPC-2 contains the best balance between oxygen and lithium molar ratio, O:Li = 35, whereas in the SIPC-1, the amount of lithium ion is the limiting factor to promote high ionic conductivity, O:Li molar = 110. On the other hand, the lower ionic conductivity of SIPC-3 (O:Li = 6) could be due to the fact that there are not sufficient carbonate/EO units available to coordinate with lithium ions and promote efficient dissociation from the anionic polymer backbone. A similar trend was observed when the same lithium based monomer was employed as polymer electrolyte.[6] The SIPC-2 exhibits an ionic conductivity of $1.2 \cdot 10^{-4}$ S.cm^{-1} at 70 °C. It is worth mentioning that such a high value of ionic conductivity in temperature range is unusual in a solid single-ion conducting polymer electrolyte,[1b] and it is likely due to the unique combination of ethylene oxide and carbonate units promoting ion pair dissociation. However, the contribution of EO units is also pronounced, if we compared with a only carbonate containing SIPE, 10^{-5} S cm^{-1} at 70 °C is determined, whereas in our case, the value is higher.[1a]

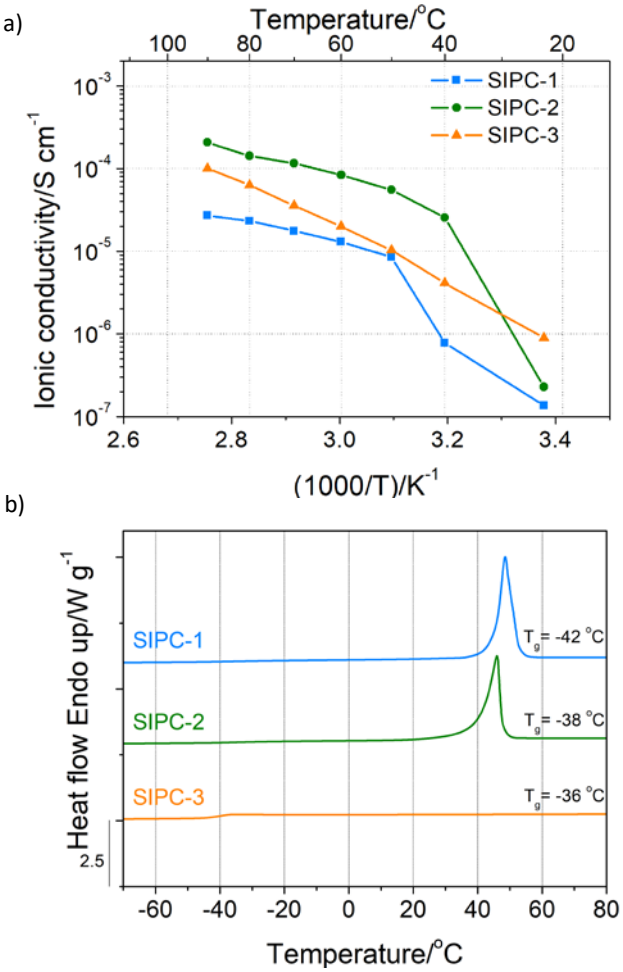

Figure 4.1. a) Ionic conductivity, and b) thermal properties of SIPC-1, SIPC-2 and SIPC-3, (DSC, 2nd heating scan at 10 K min^{-1}).

4.2.3 Semi-interpenetrated free standing films between SIPC and PEG diacrylate (PEGDA)

SIPCs-based polymer electrolytes have low glass transition (around -40 °C) and are linear polymers. Therefore, above the melting temperature of the crystalline phase, the mechanical properties of SIPCs are not sufficient for use as solid state electrolytes, since in this application the polymer electrolyte also acts as a separator. To improve

the mechanical properties of SIPCs, the polymers were cross-linked with a small amount of PEG diacrylate (M_n = 575) (PEGDA). For this study, the SIPC-2 was chosen due to its high ionic conductance above room temperature. Upon ultraviolet irradiation, free standing films of a single ion conducting poly(ethylene oxide carbonate) with an small amount of networked PEGDA was obtained. However, it is important to note for the following discussion that the SIPC backbone is not involved in the cross-linking polymerization process and only a semi-interpenetrated cross-linked network of PEGDA is formed. This network is likely to act as a molecular mesh-like component, which allows the retention of the mechanical integrity of the blend material at temperatures above the melting temperature of the EO crystalline phase. The conditions were optimized and two formulations were analysed: 5 wt.% and 10 wt.% of PEGDA.

The ionic conductivity and thermal analysis of the interpenetrated free standing polymer electrolytes were characterized, and compared with non-cross-linked SIPC-2 (Figure 4.2). The ionic conductivity is not significantly impacted when only 5 wt.% of cross-linker is used. The SIPC-2 containing 5 wt.% of PEGDA shows an ionic conductivity of $3.2 \cdot 10^{-5}$ S cm^{-1} at 70 °C, whereas without the interpenetrated polymer network, an ionic conductivity of $1.2 \cdot 10^{-4}$ S cm^{-1} is obtained. However, when 10 wt.% of PEGDA is incorporated, a drastic decrease of the ionic conductivity is observed ($9.6 \cdot 10^{-7}$ S cm^{-1}). Since the decrease in ionic conductivity is also observed at temperatures above the melting temperature of the EO crystalline phase, it is unlikely to be due to difference in the degree of crystallinity, but rather a result of restricted mobility of the SIPC-2 polymer and the interpenetrated PEGDA network. This is indirectly probed by the increase of glass transition of the overall system. For instance, when 5 wt.% PEGDA is added, an increase in the glass transition temperature of the

system is observed, going from-39 °C to-28 °C, thereby causing the decrease in ionic conductivity.

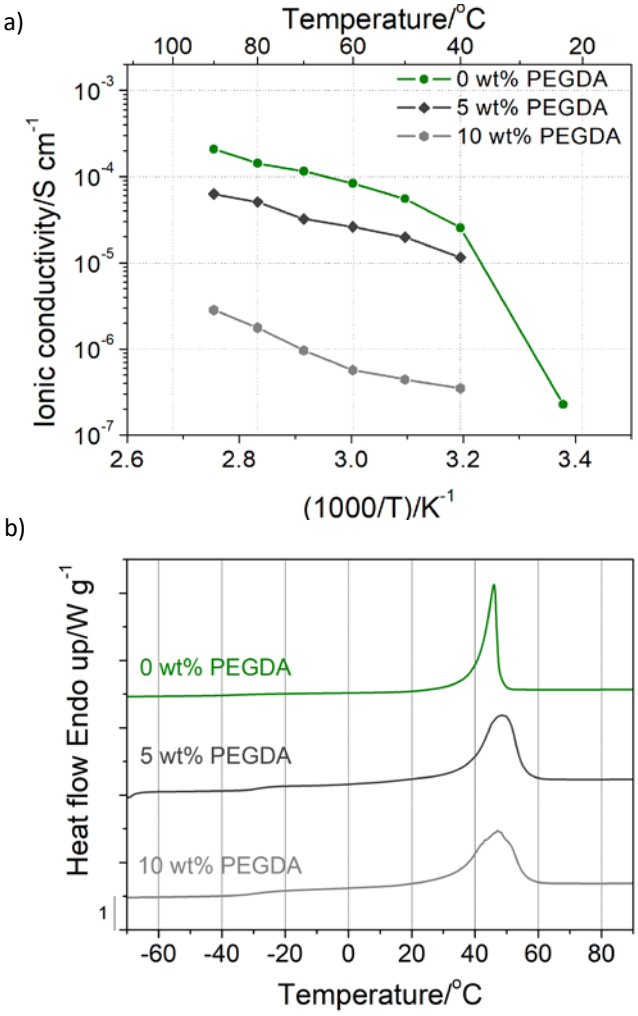

Figure 4.2. a) Ionic conductivity, and b) thermal properties of SIPC-2 with 0, 5 and 10 wt.% PEGDA, (DSC, 2nd heating scan at 10 K min^{-1}).

Additionally, the mechanical study of interpenetrated cross-linked architecture of SIPC-2 with 5 wt.% PEGDA was performed by AR-G2 rheomether, at 70 °C and 100 °C. Figure 4.3 depicts the viscoelastic properties in the double-logarithmic plots of G' and G'' *vs.* angular frequency. The material's response does not dependent on the temperature, and the storage modulus is above the loss modulus in both temperatures, meaning that the polymer electrolyte is in the rubbery region. The good mechanical stability of the interpenetrated cross-linked polymer electrolyte can be concluded. Additionally, the thermogravimetric analysis of SIPC-2 5 wt.% PEGDA performed at N_2 atmosphere, shows thermal stability up to 390 °C, Figure 4.4.

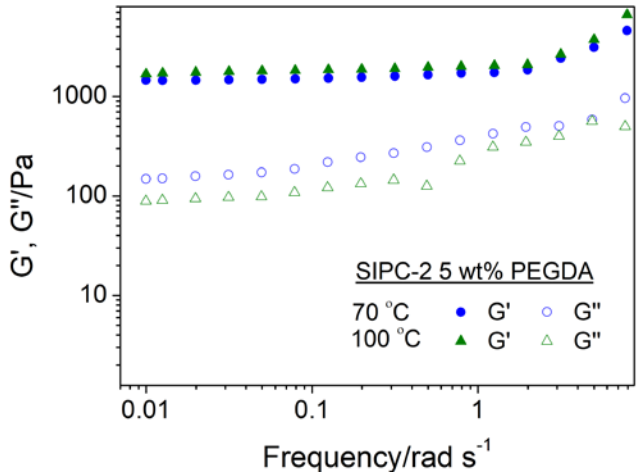

Figure 4.3. Mechanical properties of SIPC-2 with 5 wt.% PEGDA.

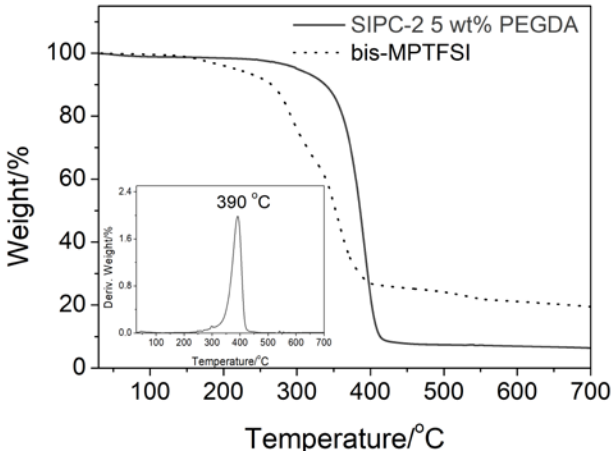

Figure 4.4. Thermal stability of SIPC-2 with 5 wt.% PEGDA and bis-MPTFSI.

4.2.4 Single ion conducting polymer electrolyte *vs.* conventional ion polymer electrolyte

Single ion conducting polymer electrolytes have attracted a lot of attention in the recent years due to their potential application for energy storage devices. However, to our best knowledge, there are few examples of comparisons between a single ion conducting polymer electrolyte and its analogous conventional SPE. Therefore, in this work, we have compared, SIPC-2, which shows the most promising electrochemical properties among the family, with analogous PEO_{34}-PC:LiTFSI SPE system.[5, 8] So, to formulate a similar conventional SPE, we added 0.58 mmol Li/g polymer LiTFSI to a PEO_{34}-PC with similar chemical composition in order to compare both systems, **Scheme 4.2**. PEO_{34}-PC was described in chapter 3. We need to remark that in both systems 5 wt.% PEGDA was added to improve the mechanical properties and allow for further characterization which required free standing films.

Scheme 4.2. Chemical structure of both single-ion and conventional polymer electrolyte poly(ethylene oxide carbonate).

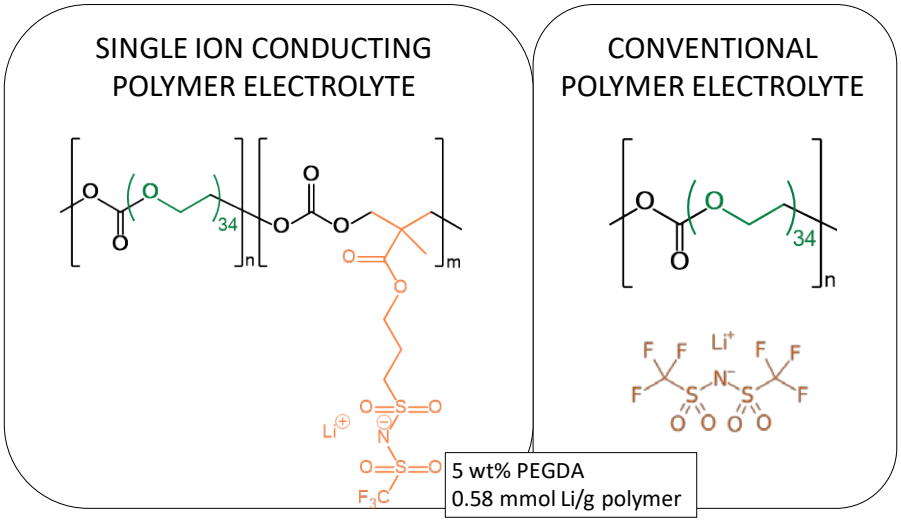

Firstly, the lithium-ion transference numbers of both system was evaluated using Bruce and Vincent method,[10] **Figure 4.5a**. A lithium transference number of 0.89 is obtained for the SIPC-2, confirming the single-ion conducting nature of this polymer. Besides, in the conventional SPE system, a value of 0.23 was measured. Secondly, the ionic conductivity of both systems was analysed at 70 °C, **Figure 4.5b**. As expected the total ionic conductivity at 70 °C of SIPC-2 is lower than in PEO_{34}-PC system. Besides, when comparing the lithium conductivity of each system (ionic conductivity multiplied by lithium transference number), in the case of SIPC-2 a value of $2.9 \cdot 10^{-5}$ S cm^{-1} is detected, while in the case of conventional SPE is $7.9 \cdot 10^{-5}$ S cm^{-1}. Although, still the lithium conductivity is higher for PEO_{34}-PC system than for SIPC-2, a better performance is expected for SIPC-2, as the concentration gradients of salt and cell polarization should be absented.

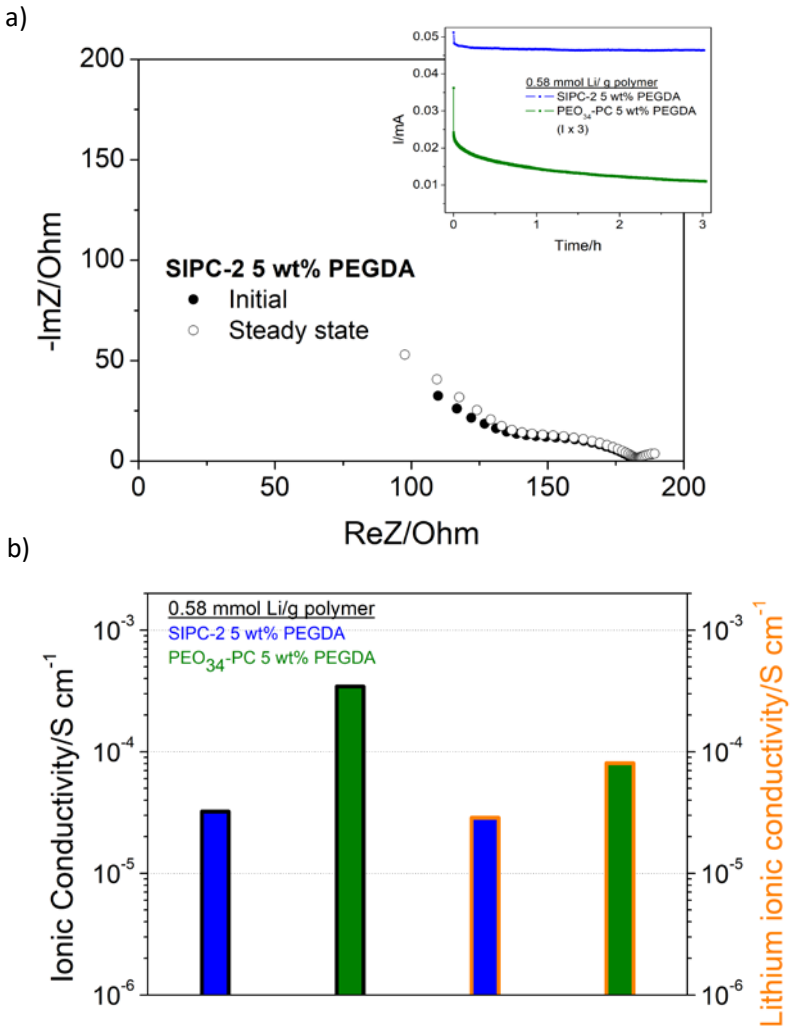

Figure 4.5. Comparison of SIPC-2 and PEO_{34}-PC. a) Lithium transference number analysis at 70 °C. EIS and CA, and b) total ionic conductivity and lithium ionic conductivity at 70 °C.

Next, ^{7}Li solid state NMR was employed to investigate lithium cation environments and lithium dynamics at different temperatures, **Figure 4.6**. Pulsed field gradient diffusion measurements were used to measure ^{7}Li and ^{19}F shelf-diffusion coefficients

at different temperatures, **Figure 4.6a**. Diffusion NMR analysis allows to quantify the contribution in term of mobility for each ionic specie by targeting specific nuclei. For the host polymer PEO_{34}-PC, a clear trend can be observed: TFSI anion diffuses faster than lithium cation, being more pronounced at higher temperatures. Thus, most of the conduction observed by EIS measurements, is likely due to the anion mobility (which is in good agreement with the lithium transference number). Conversely, for SIPEs, since the anion is covalently bonded to the polymer backbone, its diffusion is extremely limited. This means that in the case of SIPC-2, the ionic conduction is mainly due to the lithium ion mobility, as opposed to the conventional SPE system. When comparing the ^{7}Li diffusion of the SIPC-2 with the conventional SPE, the lithium diffusion of SIPC-2 is higher than PEO_{34}-PC-system, suggesting a faster lithium mobility.

^{7}Li relaxation, T_1 experiments are dominated by the molecular reorientation. The ^{7}Li relaxation rates, ($R_1 = T_1^{-1}$), for both systems are shown in **Figure 4.6b**. From the data a different relaxation behaviour can be observed for both system. The relaxation rate of conventional SPE could be fitted using the Bloembergen, Purcell and Pound (BPP) model for nuclear spin relaxation as in the Chapter 3.[5, 8] As it was analysed before, we expect that quadrupolar interaction will be the dominant mechanism for ^{7}Li longitudinal relaxation for this polymer.[5, 8] However, in the SIPC-2 system, at high temperature, the relaxation rate is not dependant on the temperature, and therefore, does not follow BPP model. This assumption lead to the understanding of having a distribution of sites. These sites, will show different local dynamics, which will cause multiple relaxation mechanisms on the system.

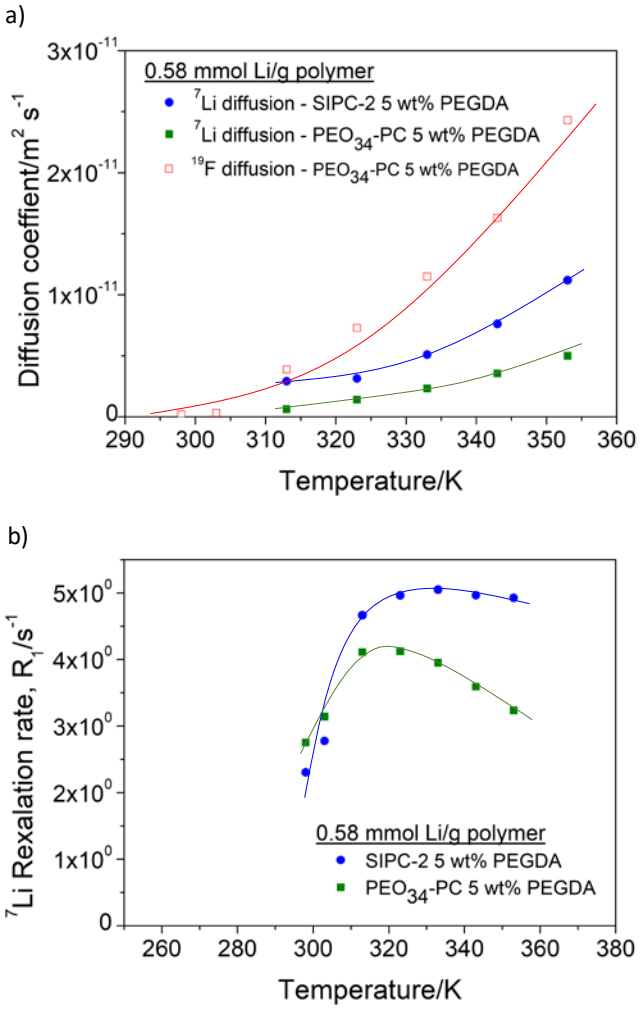

Figure 4.6. a) ^{7}Li NMR lithium coefficient, and b) ^{7}Li relaxation rate, R_1, of SIPC-2 5 wt.% PEGDA and PEO_{34}-PC 0.58 mmol LiTFSI/g polymer 5 wt.% PEGDA at different temperatures. The lines have been drawn in the figures to help to follow the trends.

In order to understand the lithium diffusion data, the conformation and coordination of ions is monitored by FTIR-ATR. $TFSI^-$ anion holds two SO_2 groups, which are prone to coordinate with the lithium cation, **Figure 4.7.** In-phase ($\nu_a{}^{ip}SO_2$) and out-of-phase

($\nu_a^{op}SO_2$) antisymmetric stretching vibrations of SO_2 are pronounced around 1350 and 1330 cm^{-1} respectively, **Figure 4.7a,b**.[11] Although it is well known that each vibration is a results of cis and trans conformations, it is reported that the trans conformation is more associated with the $\nu_a^{ip}SO_2$ vibration, and reciprocally for the cis conformation with the $\nu_a^{op}SO_2$ vibration.[11] Therefore, the conformation distribution can be analysed qualitatively at different temperatures. In each system a change on the conformation is clearly observed with temperature increase. At temperature bellow 80 °C, each system show different conformation distributions. In SIPC-2 system, an equal contribution of both cis and trans conformations can be observed, **Figure 4.7a**, which may be induced by the steric hinderance of the backbone. Besides, in PEO_{34}-PC system, although both conformations are detected, trans conformation appears to be the most predominant. However, in both system, at 100 and 90 °C, the cis conformation is mainly pronounced. Additionally, as Yoon *et al.* observed that cis conformation can enhance the lithium transport.[12] Interestingly, in our SIPC-2 system, at temperature below 80 °C, there is a more important contribution of cis conformation than in PEO_{34}-PC system. This could explain why higher lithium diffusion coefficients were obtained for SIPC-2 system than for PEO_{34}-PC system.

Moreover, Lasse and co-workers studied the different coordination types between lithium cation and TFSI anion.[11] However, analysing this wavenumber range of the spectrum (1400 -1300 cm^{-1}) is difficult to deduce the coordination in our systems. In both systems, $Li(trans)_2$, $Li(cis)_2$ and Li(cis-trans) are the combination possibilities. More insigne information can be obtained from the symmetric stretching vibration (wavenumber range of 1160 cm^{-1} – 1100 cm^{-1}). However, unfortunately, this vibration is overlapped with C–O–C band of EO units at 1104 cm^{-1} [8] and we cannot conclude any clear coordination.

a) SIPC-2 5 wt% PEGDA

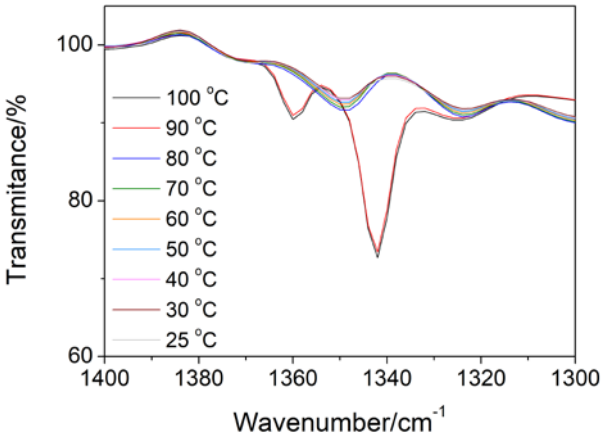

b) PEO_{34}-PC 0.58 mmol Li/ g poly. 5 wt% PEGDA

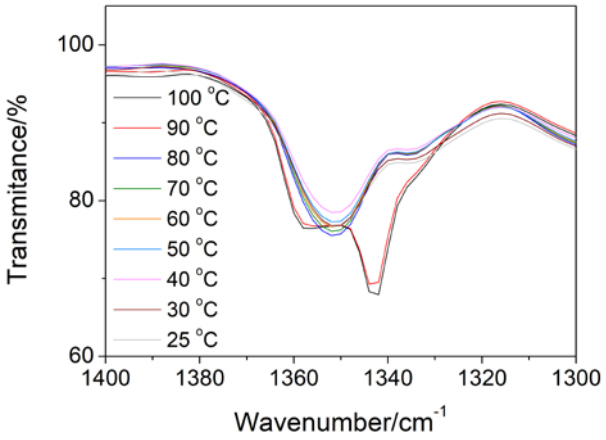

Figure 4.7. FTIR-ATR comparison of the systems at different temperature a) SIPC-2 5 wt.% PEGDA, and b) PEO_{34}-PC 0.58 mmol Li/g polymer 5 wt.% PEGDA.

The lithium transport properties of both systems were measured in a lithium symmetric cell at 70 °C, **Figure 4.8**. A current of 0.2 mA cm^{-2} was applied to both systems, with a polarization period of 1 hour. Such experiments allow to assess two major criteria of an electrolyte: i) its lithium transport properties, which needs to be sufficient to sustain the current density applied; and ii) its ability to form a highly conductive solid electrolyte interphase (SEI) under the defined cycling conditions

(also influenced its electrochemical stability towards lithium metal). A failure of an electrolyte to meet one of these two criteria will lead to poor cycling performance. It is worth mentioning that the SIPC-2 was not able to form a good SEI layer by itself and therefore lithium metal pre-treatment was needed to achieve good cycling performance. It is well known that the quality of the SEI formed is highly impacted by the type of lithium counter anion used, in which the bis(fluorosulfonyl) imide anion (FSI) has been shown to support the formation of high conductive SEI.[13] Therefore, lithium metal pre-treatment was performed by solvent casting LiFSI on the lithium surface from DME solution containing 2 M of LiFSI and evaporating the solvent under high vacuum prior cell assembly. (For more details on lithium pre-treatment procedure, see experimental section). From Figure 4.8, we can clearly observe that both systems are able to sustain the current density applied. However, the single ion system shows lower overpotential (80 mV *vs*. 180 mV) and a distinct plateau, indicating that the single-ion system exhibits better lithium transport properties, while the conventional SPE suffers from lithium transport limitation. The difference in lithium transport performance between the two systems is likely due to the presence of mobile TFSI anion in the conventional system that could promote the formation of a concentration gradient and limits the migration of the lithium ion through the electrolyte.

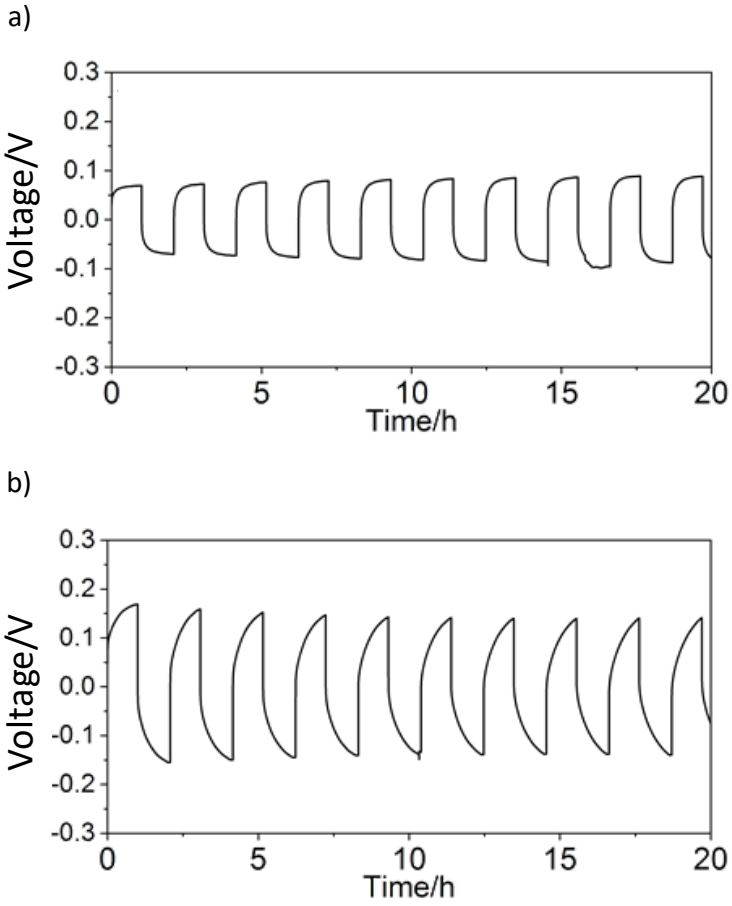

Figure 4.8. Symmetric cell at 70 °C applying 0.2 mA cm^{-2}: a) SIPC-2 5 wt.% PEGDA, and b) PEO_{34}-PC 0.58 mmol Li/g polymer 5 wt.% PEGDA.

Prior assessing any cycling performance of the single ion system in a full cell, the electrochemical stability towards oxidation has been assessed, using lithium-metal, SIPC-2 with 5 wt.% PEGDA and stainless steel cell at 70 °C, **Figure 4.9**. The SIPC-2 with 5 wt.% PEGDA shows the anodic limit at 4.9 V *vs.* Li/Li^+, which is commonly observed in carbonate containing polymer electrolytes.[5] Such high anodic limit should allow to use high voltage cathode such as lithium cobalt oxide (LCO) or lithium Nickel Manganese Cobalt (NMC).

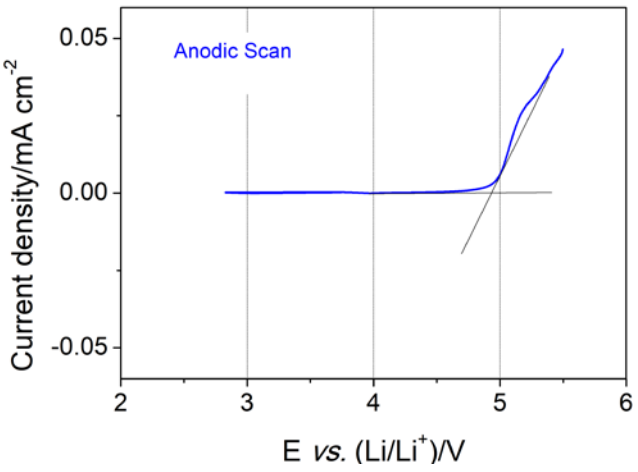

Figure 4.9. Electrochemical stability window of SIPC-2 with 5 wt.% PEGDA.

4.3 Conclusions

To conclude, the "ultimate" single-ion polymer electrolyte was synthesized combining the most successful chemical units in the area such as ethylene oxide, carbonate and sulfonamide. The single-ion conducting poly(ethylene oxide carbonate) copolymers showed high ionic conductivities and lithium transference number. The copolymer was compared with an analogue conventional polymer electrolyte containing equal molar lithium cation. Lithium interactions and mobility were compared by lithium PFG NMR, T_1 measurements and FTIR-ATR analysis. Analyzing both system a favorable lithium diffusion was obtained for SIPE, which could be attributed to SO_2 cis conformation. Finally, the performance of both polymer electrolytes on lithium symmetric cell was compared showing the single-ion polymer electrolyte lower overpotentials.

4.4 Experimental part

4.4.1 Materials

Dry dimethyl carbonate (99+ %) (DMC) and 4-dimethylaminopyridine (DMAP) (99%) were purchased from Acros Organics. The later was dried applying vacuum for 4 h at room temperature prior to use. Poly(ethylene glycol) (M_n 1,500 g mol^{-1}) was supplied by Fisher Scientific and it was dried by azeotropic distillation in toluene for 8 h. Lithium bis(trifluoromethane)sulfonimide (LiTFSI) (99.9%) was supplied from Solvionic and the photoinitiator, 2-hydroxy-2-methylpropiophenone (DAROCUR) and poly(ethylene glycol) diacrylate (M_n 575 g mol^{-1}) from Merck. Methanol (MeOH) (reagent grade), dimethylformamide (DMF) (reagent grade) and diethyl ether (Et_2O) (Extra Pure, SLR, Stabilized with BHT) were obtained from Scharlab and toluene (HPLC grade), Lithium bromide (reagent plus ≥99 %) and deuterated DMSO (99.8%) from Merck.

4.4.2 Ion exchange of bis-MPTFSI

Potassium ((3-((3-hydroxy-2-(hydroxymethyl)-2-methylpropanoyl)oxy)propyl) sulfonyl) ((trifluoromethyl)sulfonyl)amide (bis-MPTFSI) was synthesized based on the work described by L. Porcarelli et. al.[6] Before performing the polymerization, the ion exchange of bis-MPTFSI was carried out: potassium cation was changed to lithium cation. 1.01 equimolar amount of $LiClO_4$ was added to the solution of bis-MPTFSI in acetonitrile. After stirring overnight, the $KClO_4$ was removed by filtration, and ACN was removed from the filtrate by rotavap.

4.4.3 Synthesis of Single-ion Conducting Polycarbonates (SIPC)

The following example is given for the synthesis of SIPC-2 (PEO_{34}:bis-MPTFSI 50:50 mol%). Monomers, PEG1500 (PEO_{34}) (2 g, 1.33 mmol, 0.5 eq) and ester functionalized anionic diol (bis-MPTFSI) (0.523 g, 1.33 mmol, 0.5 eq.), together with the catalyst, DMAP, (3.25 mg, 0.0266 mmol, 0.01) were introduced into 10 mL schlenk flask inside

argon filled glove box. After, anhydrous dimethyl carbonate (DMC) (1.8 mL, 21.8 mmol, 8 eq.) was added to the schlenk flask. The schlenk flask was immersed in an oil bath and connected to the vacuum line. First, the reaction was maintained at 130 °C during 7 h, and finally, the temperature was increased to 180 °C and high vacuum was applied overnight. The purification of the SIPC was carried out by dissolving the polycarbonate in methanol and precipitating in cold diethyl ether. A yield of 85 % was calculated by gravimetric. Three polycarbonate compositions were tailored; 75:25 mol% (SIPC-1), 50:50 mol% (SIPC-2) and 25:75 mol% (SIPC-3). The polymer was characterized by ^{1}H NMR (DMSO-d_6, 400 MHz): δ= 4.55 (s, OCOOC**H**$_2$CC**H**$_2$OOCO, 4H), 4.18 (t, OCOOC**H**$_2$CH$_2$, 4H + OCOOCH$_2$CCOOC**H**$_2$), 3.61 (t, OCOOCH$_2$C**H**$_2$, 4H), 3.51 (s, OCOCH$_2$CH$_2$OC**H**$_2$C**H**$_2$O, 128H), 3.01 (m, OCOOCH$_2$CCOOCH$_2$CH$_2$C**H**$_2$), 1.99 (m, OCOOCH$_2$CCOOCH$_2$C**H**$_2$), 1.88 (s, OCOOCH$_2$CC**H**$_3$, 3H).

4.4.4 Preparation of SIPC and conventional polymer electrolyte

The SIPCs were dissolved in MeOH by strong stirring during 10 min (0.5 g mL^{-1}). The solutions were casted on silicon mold. Then, the solvent was allowed to evaporate at room temperature. The resulting polymers were further dried, under high vacuum and at 60 °C.

The preparation of free standing SIPC was achieved blending the polycarbonates with a cross-linkable polymer, PEG diacrylate (M_n 575) (PEGDA); both polymers (0.2 g) and photoinitiator (1 wt.% *vs.* PEG diacrylate), 2-hydroxy-2-methylpropiophenone, were dissolved in methanol (0.4 mL), stirred during 10 minutes. First, the solvent was slowly evaporated at room temperature and the evaporation of the solvent was completed applying high vacuum at room temperature overnight. Finally, the membranes were passed 3 times from xenon arc lamp (Helios Italquartz, 45 mW cm^{-2}).

Free standing conventional polymer electrolytes were prepared as follow: 0.9 g of polymer and LiTFSI (0.58 mmol Li/g polymer) were dissolved in 0.4 mL methanol. 0.1 g PEG diacrylate (M_n 575) and photoinitiator (1 wt.% *vs.* PEG diacrylate), 2-hydroxy-2-methylpropiophenone were added to the solution. After stirring the solution during 10 minutes, first, the solvent was slowly evaporated at room temperature and the evaporation of the solvent was completed applying high vacuum at room temperature overnight. Finally, the membranes were passed 3 times from xenon arc lamp (Helios Italquartz, 45 mW cm^{-2}).

Before performing any electrochemical characterization non-cross-linked and cross-linked electrolytes were first dried under vacuum at room temperature during 24 h, and after, the evaporation was completed, increasing the temperature up to 60 °C and applying vacuum for 24 h.

4.4.5 Preparation of symmetric cells

For symmetric cell analysis, the interpenetrated cross-linked polymer electrolytes were sandwiched between two metallic lithium disks and they were closed in a CR2032 coincells. In the case of the single ion conducting polymer electrolyte, the surface of metallic lithium had to be treated. Therefore, 5 µL of 2M LiFSI in DME was added in the interphases between lithium and polymer electrolyte. The DME was evaporated before closing the cell at 50 °C and under vacuum during 30 min.

4.4.6 Characterization methods

^{1}H, and ^{7}Li Nuclear Magnetic Resonance (NMR) spectra were recorded on Bruker spectrometers at 400 and 500 MHz at room temperature, in d_6-DMSO, respectively. Diffusion measurements were carried out on a 300 MHz Bruker Advance III spectrometer with a Diff50 pulsed field gradient probe and a stimulated echo pulse sequence. Relaxation measurements were carried out on the same hardware with a

saturation recovery pulse sequence. Attenuated Total Reflectance Fourier Transform Infrared Spectroscopy measurements (ATR-FTIR) were conducted on a Perkin-Elmer Spektrum ATR spectrometer.

The molar masses (M_n, M_w) and PDI of SIPCs were measured on a PL-GPC 50 gel permeation chromatograph (Agilent Technologies) equipped with an integrated IR detector, a TSK-GEL1SuperAW4000 column (Tosoh) and a SuperAW-L Guardcolumn (Tosoh). A 10 mM LiBr solution in DMF was used as an eluent with a flow rate of 0.5 mL min^{-1} at 50 °C. Calibration was performed with PEG standards.

Differential Scanning Calorimetry (DSC) was performed on a DSC Q2000 differential calorimeter (TA Instruments). All the experiments were performed under ultrapure nitrogen flow. Samples of 5 mg were used. Measurements were performed by placing the samples in sealed aluminium pans. The samples were first heated at a rate of 20 K min^{-1}, from 25 °C to 100 °C and they were left 3 min at 100 °C to avoid the influence of thermal history, in order to be able to compare the crystallization/melting temperature afterwards. Subsequently, the sample was cooled down to -70 °C at a rate of 10 K min^{-1} and subsequently heated to 100 °C at 10 K min^{-1} after waiting at -70 °C during 3 min. Finally, the sample was cooled down to -70 °C at a rate of 50 K min^{-1} and subsequently heated to 100 °C at 50 K min^{-1} after waiting at -70 °C during 3 min (T_g value was determined from this last scan).

The mechanical properties were analysed by rheological measurements using an AR-G2 rheometer (TA Instruments) with parallel geometric plates (diameter 12 mm). Angular frequency sweeps were performed in the range of $6^2 < \omega < 6^{-2}$ rad s^{-1} at different temperatures (70 °C, and 100 °C) in the linear viscoelastic regime. The time required for a frequency sweep was 5 min. Each measurement was repeated at least

two times observing a good reproducibility. On the other hand, the thermogravimetry analysis was performed at N_2 atmosphere at 10 K min^{-1} in Q500 TA Instruments.

Ionic conductivity, lithium transference number and electrochemical stability window were carried out in a VMP3 (Biologic, Claix, France) potentiostat and all cells were assembled in an argon-filled glove box (M-Braun). Ionic conductivity (σ) of the polymer electrolytes was determined by AC impedance spectroscopy over the frequency range from 100 mHz to 1 MHz with an amplitude of 10 mV. The conductivities were analysed in a temperature range down from 100 °C to 25 °C. The solid polymer electrolytes were closed in CR2032, sandwiched between two stainless steel (SS) electrodes. In all the cases the average surface area of the electrode is 2.01 cm^2. Lithium transference number was calculated based on Bruce and Vincent method at 70 °C.[10] The electrolytes were sandwiched between two lithium disks in CR2032. Before the analysis the batteries were left to stabilize at 70 °C during 24 h. Electrochemical stability window was determined applying cyclic voltammetry (CV) of the polymer electrolyte at 70 °C. The SIPC was sandwiched between SS and lithium metallic disk. The anodic limit was evaluated between open circuit potential (OCV) and 5.5 V *vs.* Li/Li^+ at a constant rate of 0.5 m V s^{-1}. Before performing the experiment, the electrolytes were left stabilizing during 24 h at 70 °C.

Symmetric cell tests were performed at 70 °C after stabilization at that temperature during 24 h. The SPEs were sandwiched between two lithium metallic disks.

The ^7Li NMR longitudinal relaxation times (T_1) were measured on a 300 MHz Bruker Avance III spectrometer with ^7Li Larmor frequencies of 116.64 MHz using a saturation recovery pulse sequence. These experiments were performed at various temperatures ranging from 293.15 to 343.15 K using a Bruker 5 mm Diff50 pulsed

field gradient (PFG) NMR probe. The sample temperature was controlled to within ±1 K with 10 minutes temperature equilibration time.

Diffusion coefficients were measured at 70°C using the same NMR probe with the stimulated echo pulse sequence. The maximum gradient strength was 2400 G cm^{-1} and the repetition time was around 5 s. The gradient pulse length and diffusion time were chosen to be appropriate resulting the attenuation curves.

4.5 References

1. (a) Deng, K.; Wang, S.; Ren, S.; Han, D.; Xiao, M.; Meng, Y., A Novel Single-Ion-Conducting Polymer Electrolyte Derived from CO2-Based Multifunctional Polycarbonate. *ACS Applied Materials & Interfaces* **2016,** *8* (49), 33642-33648; (b) Zhang, H.; Li, C.; Piszcz, M.; Coya, E.; Rojo, T.; Rodriguez-Martinez, L. M.; Armand, M.; Zhou, Z., Single lithium-ion conducting solid polymer electrolytes: advances and perspectives. *Chemical Society Reviews* **2017,** *46* (3), 797-815.

2. (a) Jangu, C.; Savage, A. M.; Zhang, Z.; Schultz, A. R.; Madsen, L. A.; Beyer, F. L.; Long, T. E., Sulfonimide-Containing Triblock Copolymers for Improved Conductivity and Mechanical Performance. *Macromolecules* **2015,** *48* (13), 4520-4528; (b) Bouchet, R.; Maria, S.; Meziane, R.; Aboulaich, A.; Lienafa, L.; Bonnet, J.-P.; Phan, T. N. T.; Bertin, D.; Gigmes, D.; Devaux, D.; Denoyel, R.; Armand, M., Single-ion BAB triblock copolymers as highly efficient electrolytes for lithium-metal batteries. *Nature Materials* **2013,** *12*, 452.

3. (a) Ho, H. T.; Tintaru, A.; Rollet, M.; Gigmes, D.; Phan, T. N. T., A post-polymerization functionalization strategy for the synthesis of sulfonyl (trifluoromethanesulfonyl)imide functionalized (co)polymers. *Polymer Chemistry* **2017,** *8* (37), 5660-5665; (b) Porcarelli, L.; Vlasov, P. S.; Ponkratov, D. O.; Lozinskaya, E. I.; Antonov, D. Y.; Nair, J. R.; Gerbaldi, C.; Mecerreyes, D.; Shaplov, A. S., Design of ionic liquid like monomers towards easy-accessible single-ion conducting polymer electrolytes. *European Polymer Journal* **2018,** *107*, 218-228; (c) Porcarelli, L.; Shaplov, A. S.; Bella, F.; Nair, J. R.; Mecerreyes, D.; Gerbaldi, C.,

Single-Ion Conducting Polymer Electrolytes for Lithium Metal Polymer Batteries that Operate at Ambient Temperature. *ACS Energy Letters* 2016, *1* (4), 678-682.

4. (a) Tominaga, Y.; Nakano, K.; Morioka, T., Random copolymers of ethylene carbonate and ethylene oxide for Li-Ion conductive solid electrolytes. *Electrochimica Acta* 2019, *312*, 342-348; (b) He, W.; Cui, Z.; Liu, X.; Cui, Y.; Chai, J.; Zhou, X.; Liu, Z.; Cui, G., Carbonate-linked poly(ethylene oxide) polymer electrolytes towards high performance solid state lithium batteries. *Electrochimica Acta* 2017, *225*, 151-159.

5. Meabe, L.; Huynh, T. V.; Mantione, D.; Porcarelli, L.; Li, C.; O'Dell, L. A.; Sardon, H.; Armand, M.; Forsyth, M.; Mecerreyes, D., UV-cross-linked poly(ethylene oxide carbonate) as free standing solid polymer electrolyte for lithium batteries. *Electrochimica Acta* 2019, *302*, 414-421.

6. Porcarelli, L.; Manojkumar, K.; Sardon, H.; Llorente, O.; Shaplov, A. S.; Vijayakrishna, K.; Gerbaldi, C.; Mecerreyes, D., Single Ion Conducting Polymer Electrolytes Based On Versatile Polyurethanes. *Electrochimica Acta* 2017, *241* (Supplement C), 526-534.

7. Meabe, L.; Sardon, H.; Mecerreyes, D., Hydrolytically degradable poly(ethylene glycol) based polycarbonates by organocatalyzed condensation. *European Polymer Journal* 2017, *95*, 737-745.

8. Meabe, L.; Huynh, T. V.; Lago, N.; Sardon, H.; Li, C.; O'Dell, L. A.; Armand, M.; Forsyth, M.; Mecerreyes, D., Poly(ethylene oxide carbonates) solid polymer electrolytes for lithium batteries. *Electrochimica Acta* 2018, *264*, 367-375.

9. (a) Devaux, D.; Bouchet, R.; Glé, D.; Denoyel, R., Mechanism of ion transport in PEO/LiTFSI complexes: Effect of temperature, molecular weight and end groups. *Solid State Ionics* 2012, *227*, 119-127; (b) Berthier, C.; Gorecki, W.; Minier, M.; Armand, M.; Chabagno, J.; Rigaud, P., Microscopic investigation of ionic conductivity in alkali metal salts-poly (ethylene oxide) adducts. *Solid State Ionics* 1983, *11* (1), 91-95.

10. Evans, J.; Vincent, C. A.; Bruce, P. G., Electrochemical measurement of transference numbers in polymer electrolytes. *Polymer* 1987, *28* (13), 2324-2328.

11. Lassègues, J.-C.; Grondin, J.; Aupetit, C.; Johansson, P., Spectroscopic Identification of the Lithium Ion Transporting Species in LiTFSI-Doped Ionic Liquids. *The Journal of Physical Chemistry A* 2009, *113* (1), 305-314.

12. Yoon, H.; Best, A. S.; Forsyth, M.; MacFarlane, D. R.; Howlett, P. C., Physical properties of high Li-ion content N-propyl-N-methylpyrrolidinium bis (fluorosulfonyl) imide based ionic liquid electrolytes. *Physical Chemistry Chemical Physics* 2015, *17* (6), 4656-4663.

13. (a) Wang, M.; Huai, L.; Hu, G.; Yang, S.; Ren, F.; Wang, S.; Zhang, Z.; Chen, Z.; Peng, Z.; Shen, C.; Wang, D., Effect of LiFSI Concentrations To Form Thickness- and Modulus-Controlled SEI Layers on Lithium Metal Anodes. *The Journal of Physical Chemistry C* 2018, *122* (18), 9825-9834; (b) Qian, J.; Henderson, W. A.; Xu, W.; Bhattacharya, P.; Engelhard, M.; Borodin, O.; Zhang, J.-G., High rate and stable cycling of lithium metal anode. *Nature communications* 2015, *6*, 6362.

Appendix

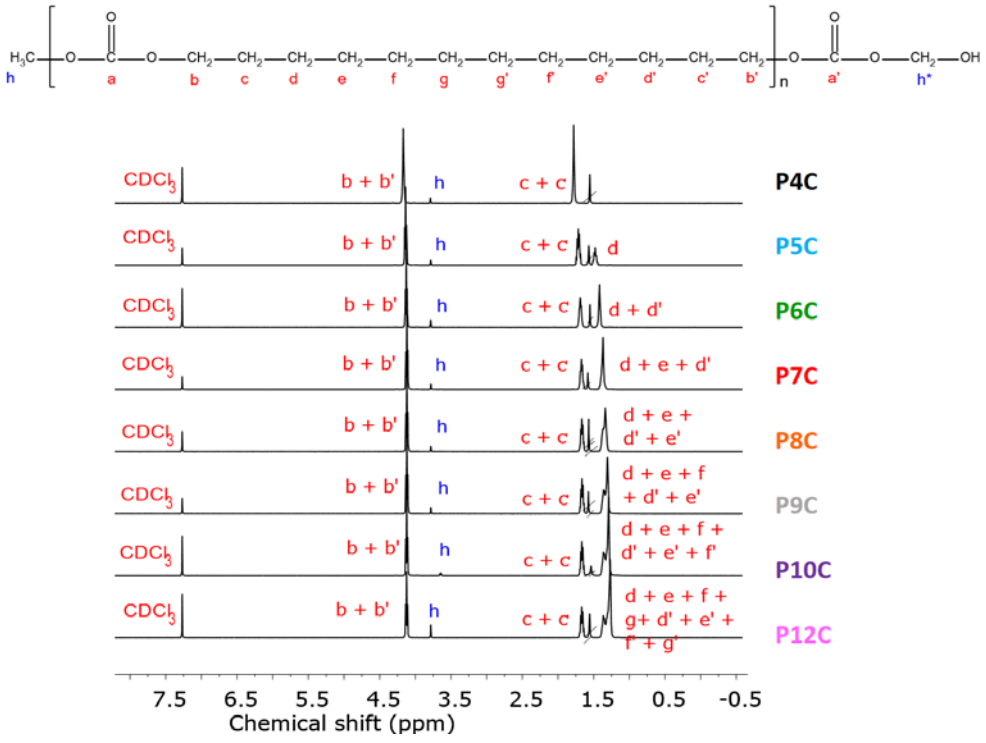

Figure A1. ^{1}H NMR spectra of aliphatic polycarbonates in $CDCl_3$.

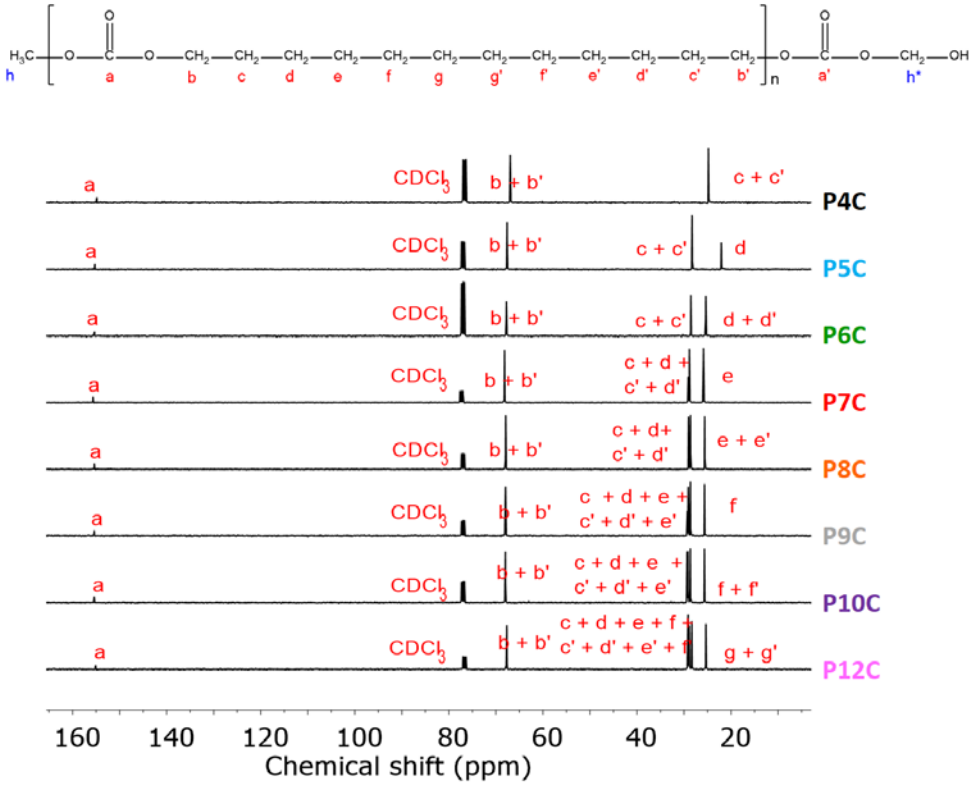

Figure A2. ^{13}C NMR spectra of aliphatic polycarbonates in $CDCl_3$.

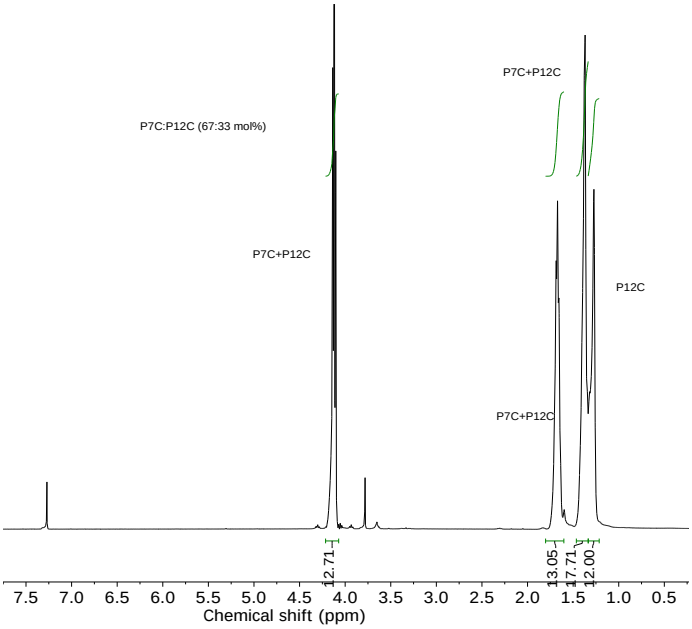

Figure A3. ^{1}H NMR spectra of P7C-P12C 70:30 mol% in $CDCl_3$.

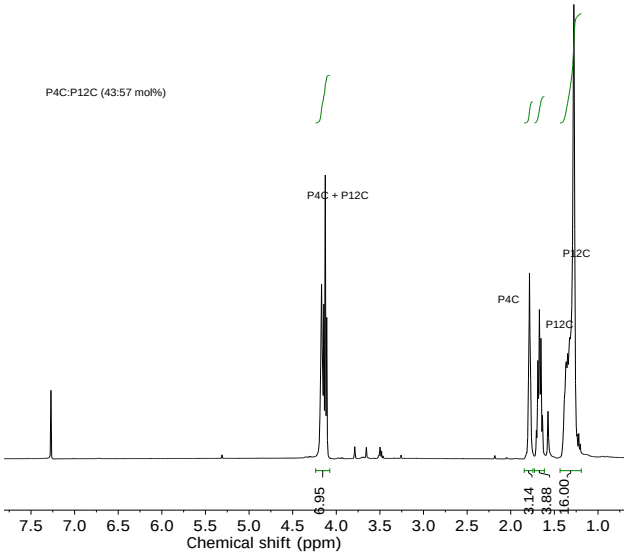

Figure A4. ^{1}H NMR spectra of P4C-P12C 50:50 mol% in $CDCl_3$.

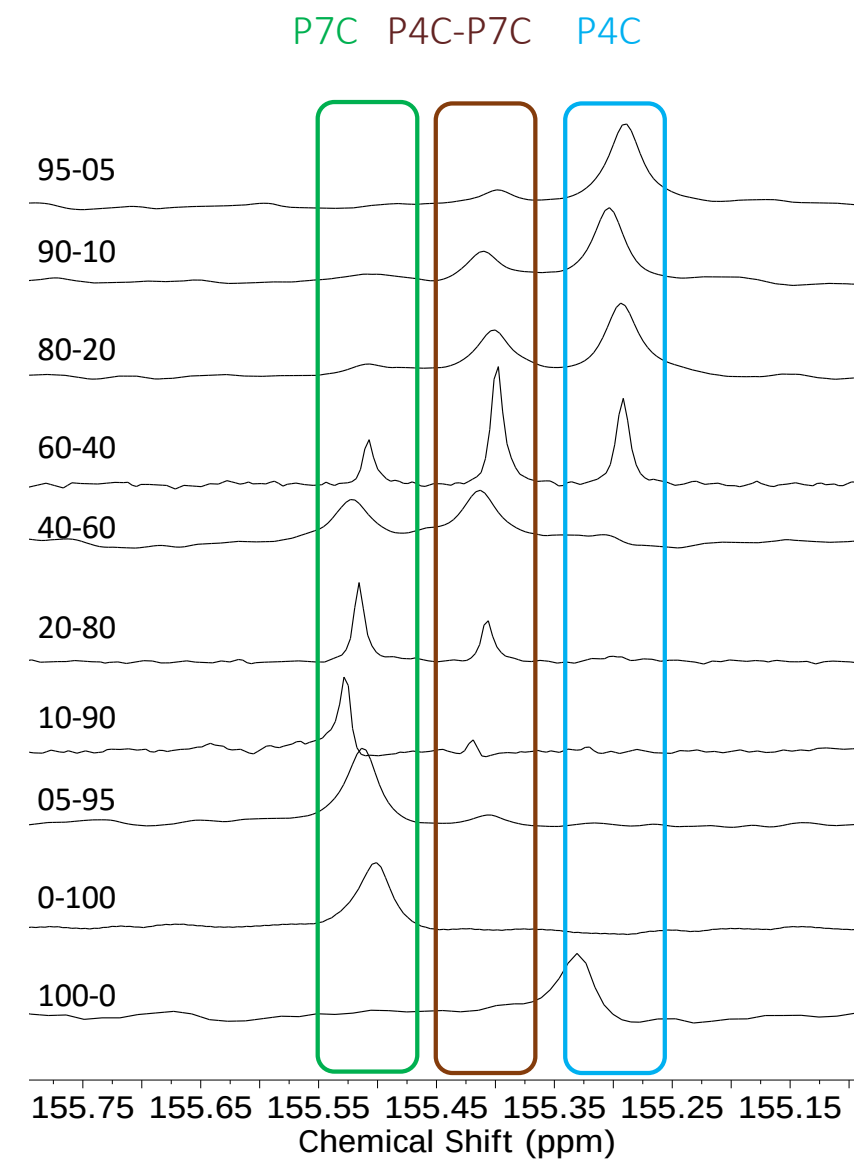

Figure A5. The signal of O<u>C</u>OO in ^{13}C NMR spectra of copolymers P4C-P7C with different mole ratios.

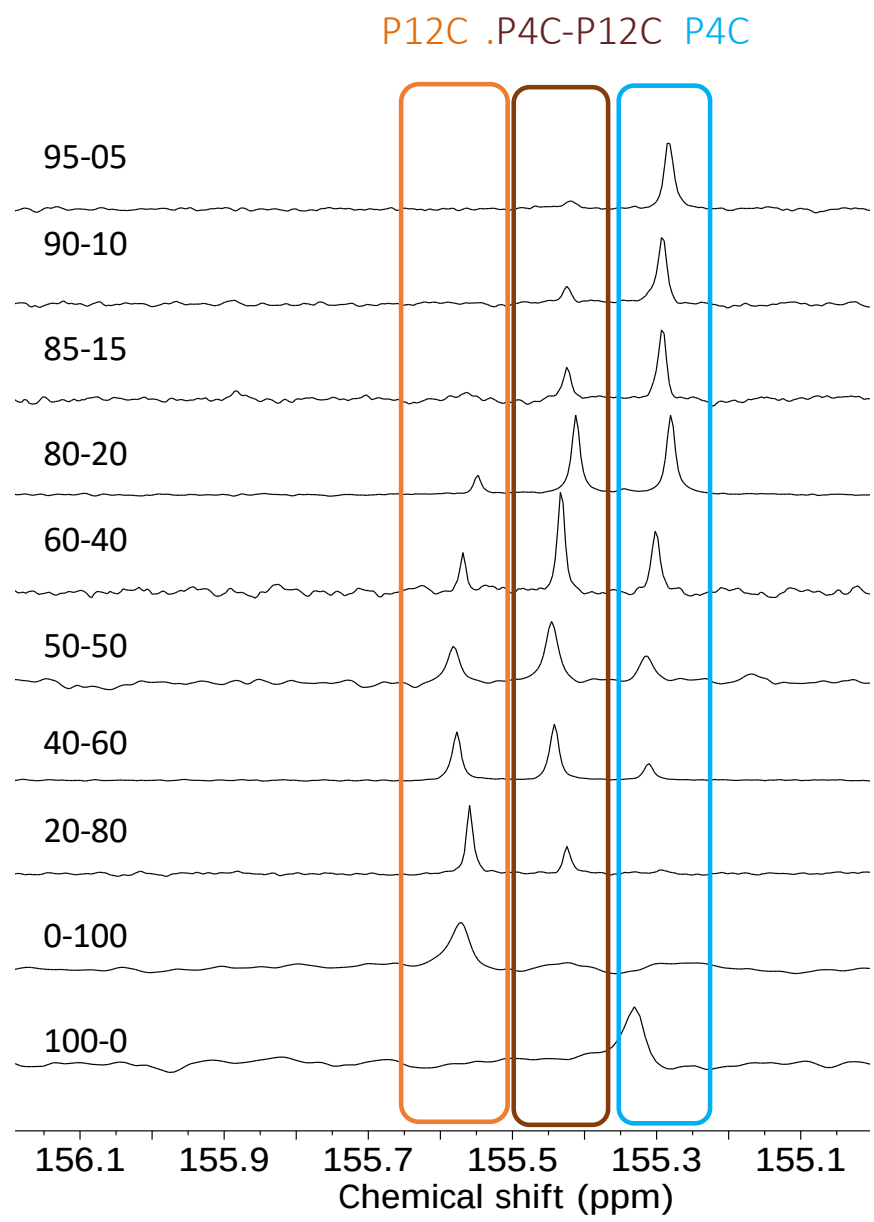

Figure A6. The signal of O<u>C</u>OO in ^{13}C NMR spectra of copolymers P4C-P12C with different mole ratios.

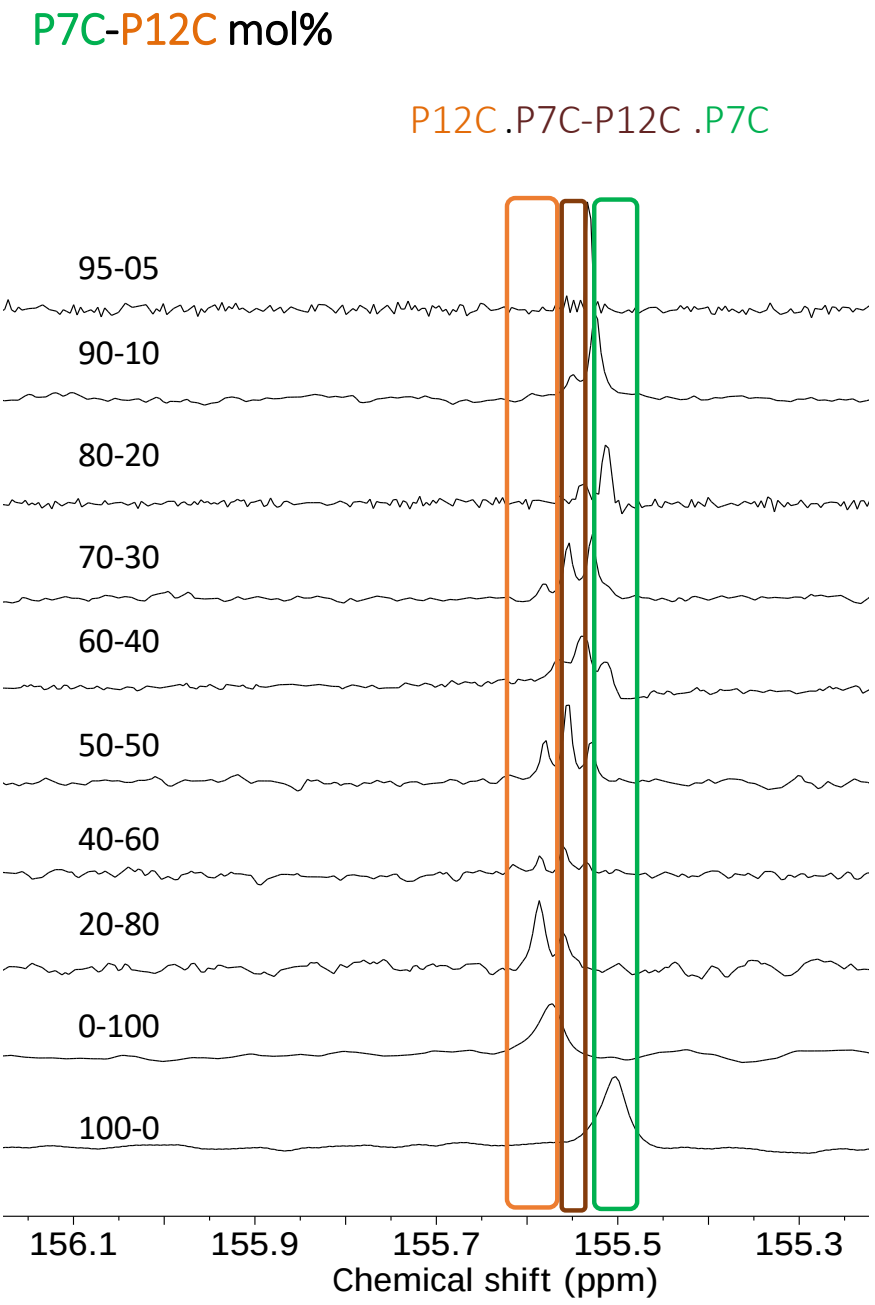

Figure A7. The signal of O<u>C</u>OO in ^{13}C NMR spectra of copolymers P7C-P12C with different mole ratios.

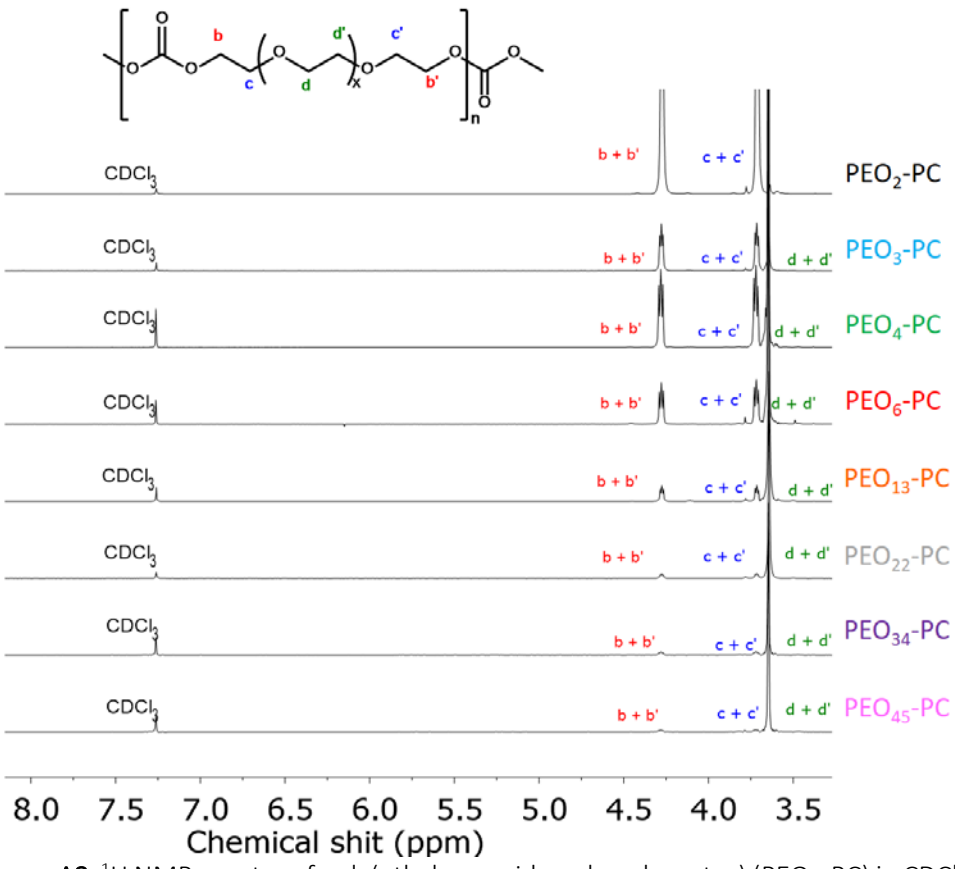

Figure A8. ^{1}H NMR spectra of poly(ethylene oxide polycarbonates) (PEO_X-PC) in $CDCl_3$.

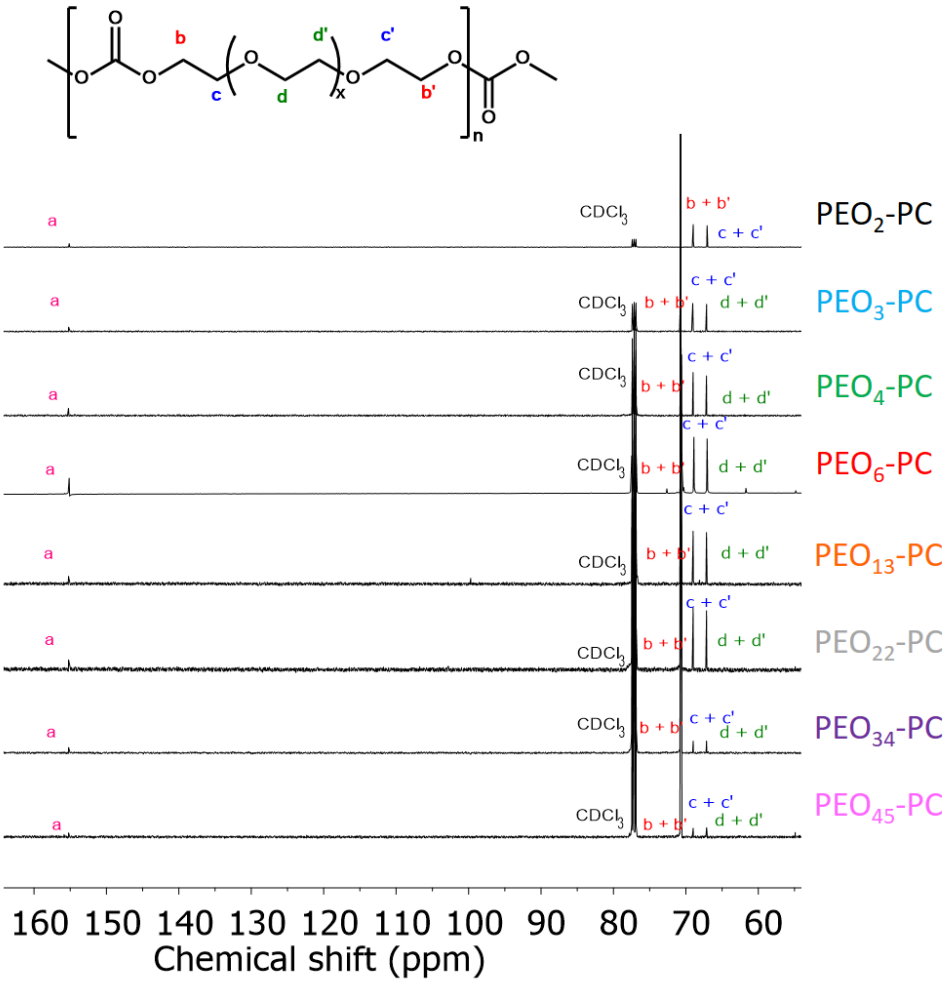

Figure A9. ^{13}C NMR spectra of poly(ethylene oxide polycarbonates) (PEO_X-PC) in $CDCl_3$.

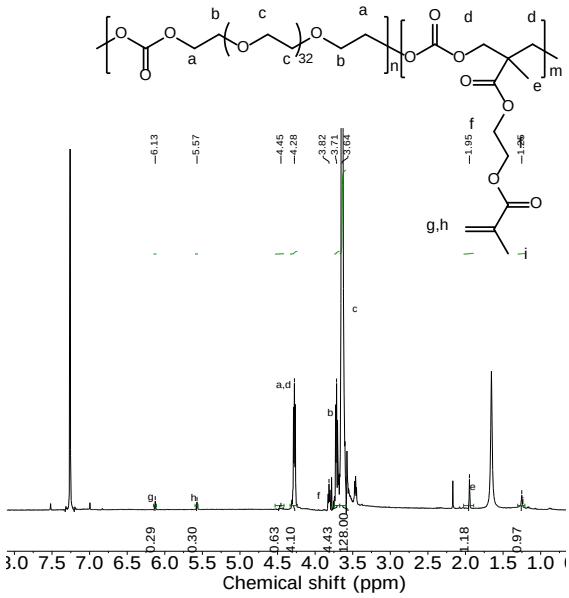

Figure A10. ^{1}H NMR spectra of PEO_{34}-PC 10 wt% MA in $CDCl_3$.

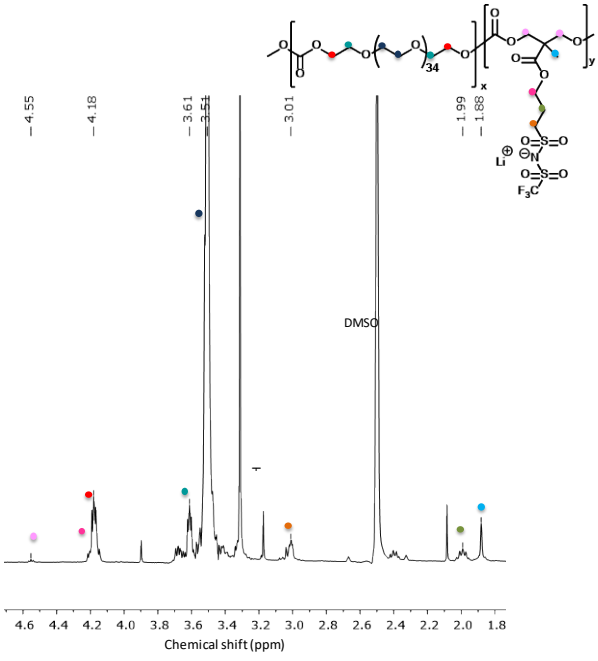

Figure A11. ^{1}H NMR spectra of SIPC-2 in DMSO-d_6.

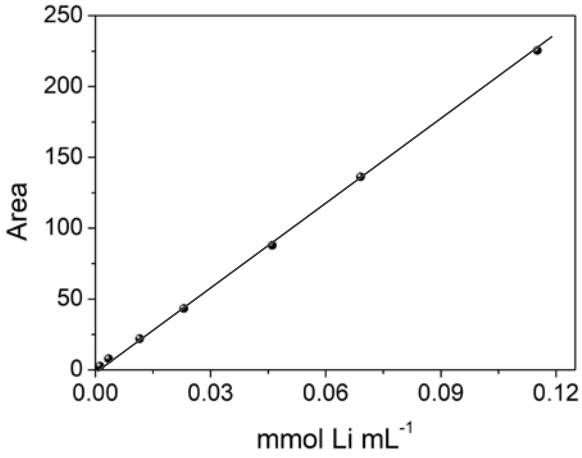

Figure A12. Calibration curve of different LiBr solutions in DMSO-d_6. The calibration curve was prepared by different LiBr solutions: 10, 6, 4, 2, 0.3, 0.1 mg mL^{-1}.

$$Y_{Area} = 1957.9 * X_{mmol\ Li} - 0.2962$$

$$R = 0.9997$$

CHAPTER 5.

Conclusions

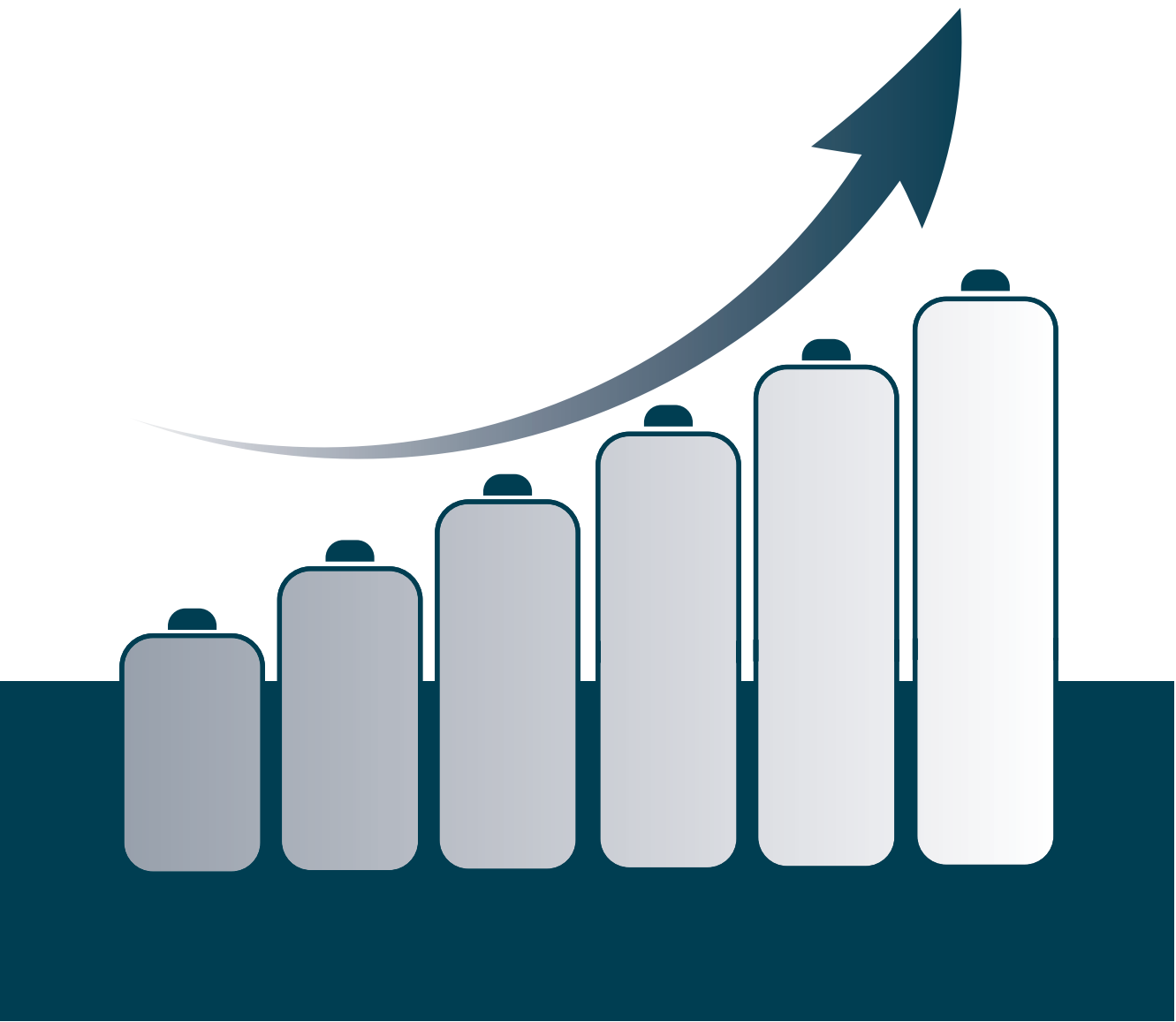

CHAPTER 5.

Conclusions

In this thesis, innovative polycarbonates were developed using the versatile and simple polycondensation technique. Three different families of polycarbonates have been successfully synthesized and evaluated as host materials for solid polymer electrolytes in lithium batteries as described in the different chapters.

In the preliminary work, the conditions for melt polycondensation technique were optimized by carrying out a screening of different reaction conditions such as stoichiometry of reactants and type of organocatalysts. Among the all analyzed organocatalysts, basic catalysts showed superior catalytic activity over the acid based ones. Among them, DMAP was selected, due to the high yield and high molar mass achieved.

In the second chapter, versatility of polycondensation on the synthesis of linear aliphatic polycarbonates was demonstrated. Homopolymers and copolymers containing different methylene units were successfully developed. According to the DSC analysis the effect of chemical structure on thermal properties were discussed, where an odd-even effect in the melting temperature of the homopolymers was observed. This study was complemented by the evaluation of aliphatic homopolymers as matrixes of solid polymer electrolytes by adding a lithium salt. A higher ionic conductivity was characterized for the polycarbonates containing higher number of methylene units, which could be attributed to the structure of the polymer; the addition of LiTFSI leads to unique properties due to crystallinity and long hydrophobic spacers. Using other host polymers (few methylene units), the behavior

was different; the addition of the salt leads to amorphous materials, therefore, the high LiTFSI concentration increases the glass transition temperature, which results in a lower ionic conductivity values. Still the overall values of ionic conductivity and mechanical properties of this type of aliphatic polycarbonates are relatively limited for being used as SPE.

In order to increase the ionic conductivity values, in chapter 3, the synthesis of poly(ethylene oxide carbonates) via polycondensation was described. The synthetic route and the availability of different diols containing ethylene oxide units allows to tune the length of EO segments between carbonate groups. The best SPEs, showing the lowest glass transition temperature, was based on the high amount of EO units (34) between carbonate links. Even though PEO-SPE type behaviour was observed in ionic conductivity, a favourable coordination between Li-cation and carbonate groups was also characterized. In order to further investigate the role of EO units and carbonate groups, free-standing solid polymer electrolytes were designed. The developed SPEs showed promising electrochemical values, such as high lithium ionic conductivity, transference number and electrochemical stability window, where the effect of both chemical structure could be deduced. EO units decreases the glass transition temperature, improving chain mobility, and consequently, the conductivity, and the favourable coordination of carbonate group and lithium cation promotes the lithium conduction. All these results were reflected in a NMC-cell, were promising results were obtained at 70 °C and 50 °C.

During the chapter 4, the synthesis of single-ion conducting polymer electrolytes was reported. In the polymer the most successful chemical units such as ethylene oxide, carbonate and sulfonamide were included. Single-ion conducting polymer electrolytes have attracted a lot of interest for application in high energy density

lithium metal batteries. This copolymer was synthesized by polycondensation between polyethylene glycol diol, dimethyl carbonate and a new functional diol including the lithium cation and sulfonamide anionic group. The beneficial effect of the combination between the three chemical groups produced the ultimate polymer electrolyte showing high ionic conductivity, good electrochemical window and high lithium transference values. Phase behavior and ionic conductivity were characterized, and lithium conductivity at 70 °C was carefully extrapolated. Lithium interactions and mobility were studied by lithium diffusion, NMR relaxation time measurements and FTIR-ATR analysis. This study was complemented by the direct comparison of single ion conducting polymer electrolyte with the analogous conventional SPE, where a favorable performance were observed in a lithium-lithium symmetric cell.

To sum up, in this thesis three polycarbonates families have been successfully developed via polycondensation. All the polycarbonates have been evaluated as host materials of solid polymer electrolytes adding LiTFSI. The consequences of the number of methylene and EO units, and the concentration of single-ion monomer on thermal and electrochemical properties have been studied. During this PhD thesis we developed innovative polymer electrolytes with excellent properties to be used as solid electrolytes in emerging battery technologies.

Laburpena

XXI. mendean erronka berriei aurre egin beharra dago. Gaur egungo bizi kalitateak eta etengabe eraldatzen ari den gizarteak, berrikuntza konstanteak eskatzen dituzte, zentzu horretan, energia, garapen ekonomiko eta sozialerako ezinbesteko osagaia da. Gaur egungo iraultza teknologikoa, ikatzean, petrolioan eta gasean ustiatutako energian oinarritzen da, energia iturri hauen kontsumoa mugatua, garestia, eta azken hamarkadetan gogor kritikatua izan delarik, karbono dioxido kantitate handiak isurtzen baitituzte.

Bestalde, energia berriztagarriak alternatiba egokia dira. Poliki bada ere, gizartearen energia kontsumoa, eguzki energian, eolikoan, hidraulikoan, geotermikoan eta bioenergiakoan oinarrituko da. Zoritxarrez, energia hauek aldizkako iturriak dira. Beraz, energia-biltegiratze sistema egonkorrak garatu beharra dago, Irudia 1. Aukera guztien artean, gailu elektronikoetarako, ibilgailu elektrikoetarako eta sare elektrikoen instalazioetarako biltegiratze elektrokimikoak aproposak dira. Gaur egun, Li-ion bateriak erabilienak dira, baina gizartearen aurrerakuntzekin, bateria berrien diseinua eta garapena beharrezkoak izango dira.

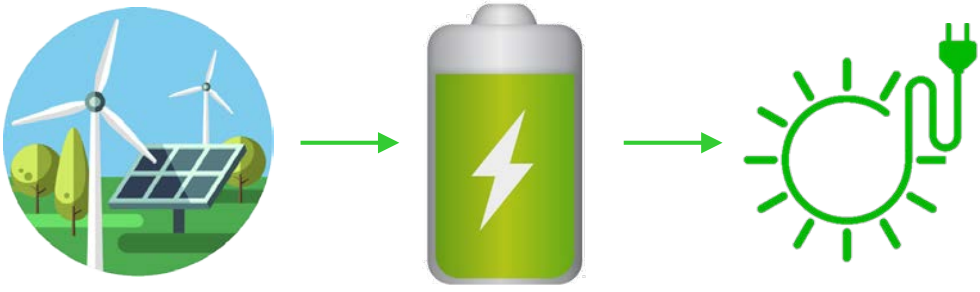

Irudia 1. Energia biltegiratzeko sistema elektrokimikoen garrantzia.

Bateria elektrokimiko bat 2 elektrodoz osatuta dago: elektrodo positiboa, katodoa, eta elektrodo negatiboa, anodoa. Bien artean elektrolitoa kokaturik dago. Bi elektrodoek potentzia kimiko desberdinak dituztenez, bateria bat deskargatzean, elektroiak anodotik (potentzia negatiboenetik), katodora (potentzia positibora) igarotzen dira. Bateria bat kargatzerako orduan, potentzia bat jarri behar da eta elektroiak anodora itzuliko dira. Elektrolitoak aldiz, konduktibitate ionikoa bermatu beharra dauka, elektroneutralitatea eraginez.

Orokorrean, bateria komertzialek, gatz bat disolbatzaile organiko batean disolbatutako elektrolito bat izan ohi dute. Hauek, hainbat propietate ezegoki dituzte: i) sukoitasuna; ii) ihesa; iii) hegazkortasuna; eta iv) toxikotasuna. Hala, gaur egungo ikerketa, material berrien garapenean oinarritzen da. Propietate horiek hobetzeaz gain, beste hainbat aspektu kontuan hartu beharrekoak dira:

- Konduktibitate ionikoa egokia
- Litio transferentzia zenbaki altua
- Egonkortasun elektrokimiko zabala
- Egonkortasun termikoa
- Egonkortasun mekanikoa
- Elektrodo eta elektrolitoaren arteko kontaktu egokia

Azken hamarkadetan hainbat elektrolito proposatu izan dira. Elektrolito solidoen artean, polimerikoak dira itxaropentsuenak. Poli(etilene oxidoa) izan da gehien ikertu den material polimerikoa; beirazko trantsizio tenperatura baxuko polimero semikristalinoa da. Gatz ugarirekin bateragarritasuna erakutsi duenez, gatz desberdinekin konduktibitate ionikoa aztertu izan ohi da. Zoritxarrez, polimeroaren semikristalinitatea dela eta, bateriek tenperatura altuetan funtzionatu ohi dute (70 °C-tik gora). Bestalde, poli(etileno oxidoa) duen talde polarrek, gatz desberdinen

disoziazioa eta disolbatzea eragiten dute. Aldiz, talde polarrek eragindako kooordinazio egonkorraren ondorioz, litio konduktibitatea jaisten da. Honela, neurtzen den konduktibitate osoaren zati handiena, anioiari dagokion mugikortasunari dagokio.

Litioaren konduktibitatea eta tenperatura baxu eta altuko baterien funtzionamendua bermatzeko asmoz, material desberdinak proposatu dira: polikarbonatoak, poliesterrak, polisiloxanoak eta polialkoholak esaterako. Horien artean, azken urteetan, polikarbonatoak oso propietate interesgarriak erakutsi dituzte: batetik, trantsizio tenperatura baxuko polimero amorfoa; bestetik, koordinazio egokia litio eta karbonato taldearen artean (poli(etileno oxido)arena baino ahulagoa).

Polikarbonatoaren estrukturaren eraginak elektrolito polimerikoan ikusteko asmoz tesi honetan hainbat familia polikarbonato sintetizatu dira. Historian zehar, polikarbonatoak 3 modu desberdinetan sintetizatu ohi dira: i) eraztun irekitzearen polimerizazio bidez; ii) CO_2 eta epoxi bidezko kopolimerizazioarekin; eta iii) polikondentsazio bidez, Eskema 2. Hirugarren hau hautatu da estrukturan aldaketa gehien emateko aukera ematen duen polimerizazioa delako. Horrela, tesian zehar hiru familia desberdin garatu dira, hiru kapitulu desberdinetan azaldu dena.

Eskema 2. Tesian zehar erabili den polimerizazioa: polikondentsazioa.

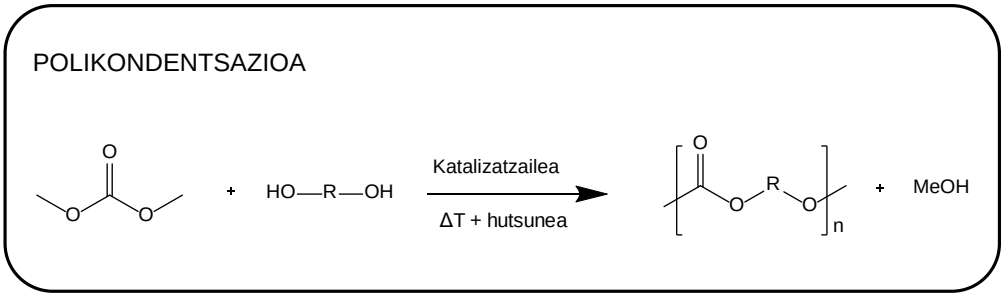

Lehenik eta behin, organokatalizatzaile egokia aztertu da. Analisatu direnen artean, katalizatzaile basikoek, katalizatzaile azidoek baino aktibitate katalitiko handiagoa erakutsi dute. Guztien artean DMAP-ek erakutsi ditu balio hoberenak.

Bigarren kapituluan jaso den moduan, polikarbonato alifatikoak sintetizatu dira, polikondentsasioaren eraginkortasuna erakutsiz. Komertzialak diren diol funtzionalitatea duten monomeroei esker, homopolimeroak eta kopolimeroak sintetizatu eta karakterizatu dira. Homopolimeroen erabilera, elektrolito polimeriko bezala, ebaluatuz osatu da kapitulua. Emaitzei erreparatuz, polikarbonatoen estrukturek, polimeroarekin masa molarrak eta gatz kantitateak hainbat propietateetan eragiten dutela ikusi da: kristalinitatearen eta beirazko trantsizio tenperaturan, eta ondorioz, konduktibitate ionikoan. Balio altuagoko eroankortasun ionikoa metileno talde altuko polimeroetan lortu da. Balio hauek, polimeroaren egitura dela eta, LiTFSI gehitzen denean, propietate bereziak sortzen dituzte: kristalinitatea eta karbonatoen arteko espazio hidrofobiko luzeak direla eta, konduktibitatearen balio altuak emanaz. Bestalde, beste material batzuetan, gatza gehitzeak material amorfoa eragiten duenean, gatz kontzentrazio altuek, beirazko trantsizio tenperatura igotzea ekartzen du, konduktibitatea jaitsiz. Esan beharra dago, material hauekin, inoiz argitaratu den konduktibitate ioniko balio altuenen artean dagoela.

Hirugarren kapituluan azaltzen den bezala, poli(etileno oxido karbonatoak) polikondentsazio bidez sintetizatu dira. Karbonato taldeen artean, etileno oxido kopurua aldatu da, eta honen eragina analizatu da. Karakterizazio kimikoa burutu ostean, propietate elektrokimikoak aztertu dira LiTFSI gatza gehituaz. Beirazko trantsizio tenperatura baxuena duen elektrolito polimerikoak konduktibitate ioniko altuena erakutsi du, etileno oxido unitate kopuru altua duen polikarbonatoak, 34

unitate. Nahiz eta karbonato kopurua txikia izan, hainbat teknikaren bitartez karbonato taldearen eragina analizatu ahal izan da. Horretarako, propietate mekanikoak hobetu behar izan dira, polimerizazioko kimika aldatuz. Behin propietate egokiak lortu direnean, propietate elektrokimikoak ebaluatu dira, bi talde kimikoen portaera nabarmenduz. Alde batetik, etileno oxidoari esker, beirazko trantsizio tenperatura jaitsi ahal izan da, hala, konduktibitate ionikoa hobetuz, eta bestalde, karbonato taldearen eragina litio transferentzia zenbakian eta egonkortasun elektrokimiko hobetuz nabarmendu da. Propietate guztiak, NMC-bateria batean islatu ziren, 70 °C eta 50 °C-tan emaitza onak lortuz.

Laugarren kapituluan adierazi bezala, ioi bakarreko konduktibitatea bermatzen duen polimeroen familia osatu da. Litio katioia da baterian erreakzio kimikoan parte hartzen duen ioia, beraz, anioiaren konduktibitatean eragozpenak besterik ez ditu ekartzen. Azken urteetan erabili den estrategia bat, anioia polimeroaren katera lotura kobalenteaz lotzea izan da. Oraingoan erabili den estrategia bera izan da. Gainera, polikondentsazioari esker hiru estruktura kimiko desberdin polimero kate berdinean batu ahal izan dira: ondo aztertuta dagoen etileno oxidoa, azken urteetan garrantzia hartu duen karbonato taldea, eta ioi bakarreko propietatea eman dion monomeroa. Talde kimiko guztiei esker, konduktibitate ioniko nahiko altuak lortu direnez, elektrolito polimeriko arrunt batekin konparatu ahal izan da. Bi sistemak konparatu ostean, ioi bakarreko polimero elektrolitoak propietate hobeak erakutsi ditu.

Laburbilduz, tesi honetan, polikondentsazio bidez polikarbonato 3 familia osatu dira. Polikarbonato guztiak elektrolito polimeriko bezala aztertu dira, LiTFSI gatza gehituaz. Propietate termikoetan eta elektrokimikoetan metileno eta etileno oxido kopuruaren, eta ioi bakarreko monomeroaren kontzentrazioaren eragina aztertu da.

Résumé

Le 21ème siècle doit faire face à de nouveaux défis sociétaux et environnementaux en lien avec l'amélioration de la qualité de vie qui nécessite une innovation permanente. Pour cela, la gestion de l'énergie est un élément clé. La révolution industrielle et ses développements technologiques ont beaucoup reposé sur les énergies fossiles issues du pétrole, du gaz et du charbon, avec les conséquences négatives que l'on connait aujourd'hui, liées en grande partie à l'émission de dioxyde de carbone. Dans ce contexte le développement des énergies renouvelables est nécessaire ; en effet progressivement les énergies basées sur le solaire, l'éolienne, l'hydraulique, la géothermie et les bio-ressources prennent le pas sur les énergies fossiles. Néanmoins, ces sources d'énergie sont bien souvent intermittentes, par conséquent, il est indispensable de développer des systèmes de stockage d'énergie fiables, **Figure 1**. Parmi toutes les options le stockage électrochimique semble être le plus prometteur pour les appareils électroniques, les véhicules électriques ainsi que les réseaux. Aujourd'hui, même si les batteries lithium-ion sont largement répandues, car relativement performantes, il reste indispensable de concevoir et de développer de nouvelles batteries répondant mieux encore aux nouvelles nécessités sociétales.

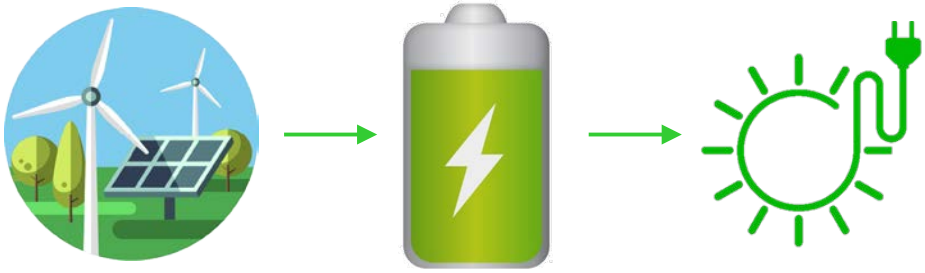

Figure 1. Importance des systèmes de stockage d'énergie électrochimiques.

Une batterie classique est constituée de deux électrodes: une électrode positive, la cathode, et une électrode négative, l'anode. Entre les deux se trouve l'électrolyte. Lorsqu'une batterie est en décharge, les électrons circulent, dans le circuit, de l'anode vers la cathode. Inversement, lorsque la batterie est en charge, une tension doit être appliquée et les électrons retournent à l'anode. Pour que cela fonctionne et garantir l'électro-neutralité l'électrolyte doit permettre la conductivité ionique des cations dans le sens opposé aux électrons.

Actuellement, et en général, dans les batteries commercialisées l'électrolyte est un liquide constitué d'un sel de lithium dissout dans un solvant organique. Celui-ci présente plusieurs risques: i) d'inflammabilité; ii) de fuite; iii) de volatilité; et iv) de toxicité. Ainsi, des recherches sont menées pour développer de nouveaux matériaux électrolytiques, qui en plus de répondre aux risques mentionnés précédemment, cherchent à optimiser les propriétés suivantes:

- Conductivité ionique élevée
- Nombre de transport du lithium élevé
- Stabilité électrochimique
- Stabilité thermique
- Stabilité mécanique
- Contact efficace entre l'électrolyte et les électrodes

Au cours des dernières décennies, plusieurs électrolytes solides ont été proposés et parmi eux les polymères sont les plus prometteurs (SPE pour *Solid Polymer Electrolyte*), en particulier le poly(oxyde d'éthylène) (PEO). En effet, le PEO est le polymère le plus largement étudié car il possède une faible température de transition vitreuse (T_g) et les groupes polaires d'oxyde d'éthylène (EO) sont capables de dissocier les sels de lithium. Cependant, en raison de la semi-cristallinité du polymère,

les batteries doivent fonctionner à des températures élevées (supérieures à 70 ° C, i.e. température de fusion). Aussi, en raison de la forte coordination des ions lithium par les groupes polaires, la conductivité spécifique des cations lithium diminue; ainsi, la majeure partie de la conductivité mesurée correspond à la mobilité des anions.

Afin de garantir une conductivité du lithium optimum et le fonctionnement des batteries à basses et hautes températures, différents polymères ont été proposés : polycarbonates, polyesters, polysiloxanes, polyalcools, etc. Parmi ceux-ci, les polycarbonates ont montré ces dernières années des propriétés très intéressantes. D'une part, le polymère présente une température de transition vitreuse basse avec un caractère amorphe; d'autre part, il présente une bonne coordination entre les ions lithium et les groupes carbonates, mais plus faible qu'avec le PEO.

Afin d'étudier l'impact de la structure chimique du polymère plusieurs familles de polycarbonates ont été synthétisées au cours de la thèse. Tout d'abord, les polycarbonates peuvent être synthétisés de trois manières différentes: i) par polymérisation par ouverture de cycle; ii) par copolymérisation de CO_2 et d'époxy; et iii) par polycondensation, Schéma 2. Cette troisième voie a été choisie car elle permet de contrôler facilement la structure du polycarbonate. Ainsi, pendant la thèse, nous avons étudié trois familles différentes, décrites dans trois chapitres.

Schéma 2. Technique de polymérisation utilisée au cours de la thèse : polycondensation.

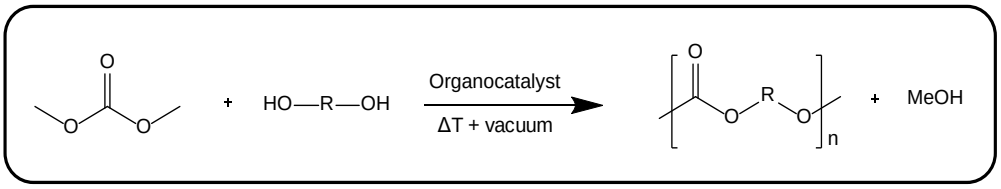

Dans le deuxième chapitre est présenté la synthèse de polycarbonates aliphatiques montrant l'efficacité de la polycondensation. Il est à noter que parmi tous les catalyseurs organiques analysés, les catalyseurs basiques ont montré une activité catalytique supérieure par rapport à celle des catalyseurs acides. En effet la 4-diméthylaminopyridine (DMAP) a montré les meilleurs résultats. En utilisant des monomères diols commerciaux, des polycarbonates (homopolymères et copolymères) ont été synthétisés puis caractérisés. L'étude a été complétée en utilisant ces polymères en tant que matrice électrolyte solide en ajoutant un sel de lithium (LiTFSI). Une conductivité ionique plus élevée a été observée pour les polycarbonates contenant un nombre d'unités méthylènes plus élevé, ce qui peut être attribué à la structure du polymère. L'ajout de LiTFSI a conduit à des propriétés uniques en raison de la cristallinité et de la présence de segments hydrophobes le long de la chaine. En utilisant des polymères avec peu d'unités méthylènes l'ajout du sel a conduit à des matériaux amorphes et l'augmentation de la concentration de LiTFSI entraine une augmentation de la T_g et donc une baisse de la conductivité ionique. Globalement, les valeurs de conductivité ainsi que les propriétés mécaniques de ces matrices polycarbonates aliphatiques restent relativement limitées pour une utilisation comme SPE.

Afin d'augmenter la conductivité des poly(oxyde d'éthylène carbonates) ont été synthétisés par polycondensation, cette étude est présentée dans le chapitre 3. La voie de synthèse ainsi que la disponibilité des différents diols contenant des unités oxyde d'éthylène ont permis de contrôler la longueur des segments OE entre les groupes carbonates. Les meilleures SPE, présentant les T_g les plus basses, sont obtenus avec un nombre élevé d'unités EO (34) entre les fonctions carbonates. Une coordination entre les ions lithium et les groupes carbonates a été observée, malgré un comportement de la conductivité ionique de type électrolyte-PEO. Afin d'étudier

plus avant le rôle des unités EO et des groupes carbonates, des électrolytes polymères solides auto-supportés ont été préparés. Ces SPE ont montré des caractéristiques électrochimiques prometteuses, telles qu'une conductivité ionique et un nombre de transfert du lithium élevés ainsi qu'une large fenêtre de stabilité électrochimique. Ceci a permis de mettre en évidence le rôle de la structure chimique des polymères. Il a été observé que l'insertion d'unités EO diminue la température de transition vitreuse, améliorant ainsi la mobilité des chaînes et par conséquent la conductivité. Aussi, la coordination entre les groupes carbonates et les ions lithium favorise la conduction cationique. Toutes ces caractéristiques ont permis d'aboutir à des résultats prometteurs en cellules à 70 °C et 50 °C (électrodes NMC).

Dans le chapitre 4 est présenté une étude centrée sur la synthèse d'électrolytes polymères de type ''*single-ion*'' composé d'unités chimiques EO, carbonates et sulfonamides. Ces dernières années, les électrolytes polymères de type ''*single-ion*'' (SIPE) ont suscité un vif intérêt pour une application dans les batteries haute densité d'énergie lithium métal. Dans ce travail, le copolymère a été synthétisé par polycondensation avec du polyéthylène glycol diol, du diméthyl carbonate et un nouveau diol fonctionnel comprenant le groupe anionique sulfonamide et le cation lithium. L'association de ces trois fonctions chimiques a permis de produire des électrolytes polymères présentant des conductivités ioniques élevées, une large fenêtre de stabilité électrochimique et des valeurs de nombre de transfert du lithium élevées. En parallèle, les interactions et la mobilité des ions lithium dans la matrice polymère ont été étudiées par RMN à gradient de champs pulsé et analyse FTIR-ATR. La comparaison entre un système ''*single ion*'' et SPE conventionnelle analogue (avec LiTFSI) a permis de mettre en évidence une diffusion plus favorable des ions lithium dans le système ''*single ion*''.

En résumé, au cours de cette thèse, trois familles de polycarbonates ont été synthétisé avec succès par polycondensation. Tous les polycarbonates ont été évalués en tant qu'électrolytes polymères solides après ajout de sel de lithium (LiTFSI). L'impact du nombre d'unités méthylène et OE, ainsi que de la concentration d'unités ''*single ion*'' sur les propriétés thermiques et électrochimiques ont été évalués. Aussi, nous avons développé des électrolytes polymères innovants présentant des propriétés adaptées pour une utilisation dans les technologies de batteries tout solide émergentes.

List of acronyms

EESS	Electrochemical energy storage systems
SPE	Solid polymer electrolyte
PEO	Poly(ethylene oxide)
EO	Ethylene oxide
SIPE	Single-ion conducting polymer electrolyte
TFSI	Trifuoromethylsulfonylimide
σ	Ionic conductivity
EIS	Electrochemical impedance spectroscopy
VTF	Vogel-Tamman-Fulcher
pfg-NMR	Pulsed Field Gradient NMR
NMR	Nuclear magnetic resonance
PEC	Poly(ethylene carbonate)
PTMC	Poly(trimethylene carbonate)
LiTFSI	Lithium trifuoromethylsulfonylimide
LiFSI	Lithium bis(fluorosulfonyl)imide
DMC	Dimethyl carbonate
DPC	Diphenyl carbonate
DMAP	4-Dimethylaminopyridine
TBD	1,5,7-Triazabicyclo[4.4.0]dec-5-ene
DBU	1,8-diazabiciclo[5.4.0]undeca-7-eno
MSA	Methanesulfonic acid
p-TFSA	p-toluenesulfonic acid

P**X**C	Aliphatic polycarbonates **X** = methylene units between the carbonate groups
PEO_x-PC	Poly(ethylene oxide carbonates) **X** = number of ethylene oxide units between the carbonate groups
FTIR-ATR	Fourier Transform Infrared-Attenuated total reflection
GPC	Gel permeation chromatography
TGA	Thermogravimetric analysis
DSC	Differential scanning chromatography
MeOH	Methanol
$CDCl_3$	Deuterated chloroform
DMSO-d_6	Deuterated dimethyl sulfoxide
DMC	Dimethyl carbonate
DCM	Dichloromethane
DMF	N,N-dimethylformamide
ACN	Acetonitrile
THF	Tetrahydrofuran
T_{Li+}	Lithium transference number
M_w	Weight average molecular weight
M_n	Number average molecular weight
Đ	Dispersity
T_g	Glass transition temperature
T_m	Melting temperature
T_c	Crystallization temperature
ΔH_m	Enthalpy of the melting
MA	2,2-bis(hydroxymethyl)-propionic acid

Bis-MPTSI	lithium ((3-((3-hydroxy-2-(hydroxymethyl)-2-methylpropanoyl)oxy)propyl)sulfonyl)((trifluoromethyl)sulfonyl)amide
PEGDA	Poly(ethylene glycol) diacrylate
NMC	Nickel Manganese Cobalt
$KClO_4$	Potassium perchlorate
$LiClO_4$	Lithium perchlorate
LiBr	Lithium bromide
SS	Stainless steal
CV	Cyclic voltammetry
OCV	Open-circuit voltage
V	Voltage

List of publications

1. Leire Meabe, Nicolas Goujon, Chunmei Li, Michel Armand, Maria Forsyth, David Mecerreyes, Single-ion conducting poly(ethylene oxide carbonate) as the "ultimate" solid polymer electrolyte. S*ubmitted*.

2. Idoia Arandia, Leire Meabe, Haritz Sardon, David Mecerreyes, Alejandro J. Müller. Synthesis and isodimorphic behavior of three different copolycarbonate random copolymer series. *Submitted.*

3. Leire Meabe, Tan Vu Huynh, Daniele Mantione, ,Chunmei Li, Luke A.O'Dell, Haritz Sardon, Michel Armand, Maria Forsyth, David Mecerreyes. UV-cross-linked poly(ethylene oxide carbonate) as free standing solid polymer electrolyte for lithium batteries. Electrochimica Acta (2019), 302, 414-421.

4. Farid Ouhib, Leire Meabe, Abdelfattah Mahmoud, Nicolas Eshraghi, Bruno Grignard, Jean-Michel Thomassin, Abdelhafid Aqil, Frederic Boschini, Christine Jérôme, David Mecerreyes and Christophe Detrembleur. CO_2-sourced polycarbonates as solid electrolytes for room temperature operating lithium batteries. Journal of Materials Chemistry A: 2019, 7(16), 9844–9853.

5. Jorge L. Olmedo-Martínez, Leire Meabe, Andere Basterretxea, David Mecerreyes, Alejandro J. Müller. Effect of Chemical Structure and Salt Concentration on the Crystallization and Ionic Conductivity of Aliphatic Polyethers. Polymers 2019, *11*(3), 452/1-452/13.

6. Amaury Bossion, Katherine V. Heifferon, Leire Meabe, Nicolas Zivic, Daniel Taton, James L. Hedrick, Timothy E. Long, Haritz Sardon. Opportunities for organocatalysis in polymer synthesis via step-growth methods. Progress in Polymer Science (2019), 90, 164–210.

7. Leire Meabe, Tan Vu Huynh, Nerea Lagoa, Haritz Sardon, Chunmei Li, Luke A. O'Dell, Michel Armand, Maria Forsyth, David Mecerreyes. Poly(ethylene oxide carbonates) solid polymer electrolytes for lithium batteries. Electrochimica Acta (2018), 264, 367-375.

8. Leire Meabe, Haritz Sardon, David Mecerreyes. Hydrolytically degradable poly(ethylene glycol) based polycarbonates by organocatalyzed condensation. European Polymer Journal (2017), 95, 737–745.

9. Leire Meabe, Nerea Lago, Laurent Rubatat, Chunmei Li, Alejandro J. Müller, Haritz Sardon, Michel Armand, David Mecerreyes. Polycondensation as versatile synthetic route to aliphatic polycarbonates for solid polymer electrolytes. Electrochimica Acta (2017), 237, 259–266.

10. Julieta Zataray, Amaia Agirre, Paula Carretero, Leire Meabe, José C. de la Cal, Jose R. Leiza. Characterization of poly (*N*-vinyl formamide) by size exclusion chromatography–multiangle light scattering and asymmetric-flow field-flow fractionation–multiangle light scattering. Journal of Applied polymer Science (2015), 132(34), n/a.

Conference presentations

1. 13th annual international electromaterials science symposium, Geelong, Australia 11th – 13th February, 2019.

   Flash presentation and poster presentation: Poly(ethylene oxide) carbonate: single ion conducting solid polymer electrolyte vs. dual ion conductor solid polymer electrolyte. Leire Meabe, Nicolas Goujon, Luke O'Dell, Chunmei Li, Maria Forsyth, David Mecerreyes.

2. ISPE-XVI: International Symposium of polymer electrolytes, Yokohama, Japan, 24th – 29th June, 2018.

   Flash presentation and poster presentation: Free standing solid polymer electrolyte films based on poly(ethylene oxide carbonates). Leire Meabe, Daniele Mantione, Luca Porcarelli, Chunmei Li, Haritz Sardon, Michel Armand, David Mecerreyes.

3. Journées GFP Sud-Ouest, Guethary, France, 5th – 6th April, 2018

   Oral presentation: Free standing polymer electrolytes based on poly(ethylene oxide-carbonates). Leire Meabe, Nerea Lago, Laurent Rubatat, Chunmei Li, Haritz Sardon, Michel Armand, David Mecerreyes. (Award: Best oral presentation).

4. eMRS-Spring meeting, Strasbourg, France, 22nd – 26th May, 2017.

   Oral presentation: Solid polymer electrolytes based on innovative polycarbonates. Leire Meabe, Nerea Lago, Laurent Rubatat, Chunmei Li, Lide M.

Rodríguez-Martinez, Haritz Sardon, Michel Armand, David Mecerreyes. (Award: Best oral presentation).

5. ISPE-XV: International Symposium of polymer electrolytes, Uppsala, Sweden, 14^{th} – 19^{th} August, 2016.
   Poster presentation: Synthesis by polycondensation of new aliphatic polycarbonates for polymer electrolytes. Leire Meabe, Nerea Lago, Laurent Rubatat, Chunmei Li, Haritz Sardon, Michel Armand, David Mecerreyes.

Courses and activities attended

COURSES

- Seminario de Caracterización de Materiales Mediante Técnicas de Análisis Térmico – 05/07/2017 – 05/07/2017
- Introduction to Structure and Properties of Polymers – 19/04/2016 – 28/07/2016
- Emulsion Polymerization Processes – 07/09/2015 – 11/09/2015

ACTIVITIES

- Cross-border Doctorials – 10/10/2016 – 14/10/2016
- Actividad práctica “Química para ti” – 10/02/2016
- Doktoregaiei Harrera egiteko I. jardunaldia – 4/12/2015

Collaborations

This thesis has been carried out in close collaboration with various universities and research centers.

The evaluation of different organocatalyst for polycondensation was performed at Yamagata University (Yonezawa, Japan) during 3 months internship, under the supervision of Dr. Kazuki Fukushima.

All the electrochemical characterization of chapter 2, chapter 3 and part of chapter 4, has been carried out in CIC energiGUNE (Vitoria-Gasteiz, Spain), where I regularly moved to perform the electrochemical characterization. This part was supervised by Dr. Chunmei Li.

Part of the electrochemical characterization and NMR study of chapter 4 was developed at Deakin University (Melbourne, Australia) during 3 months internship at Institute for Frontier Materials under the supervision of Dr. Nicolas Goujon and Prof. Maria Forsyth.

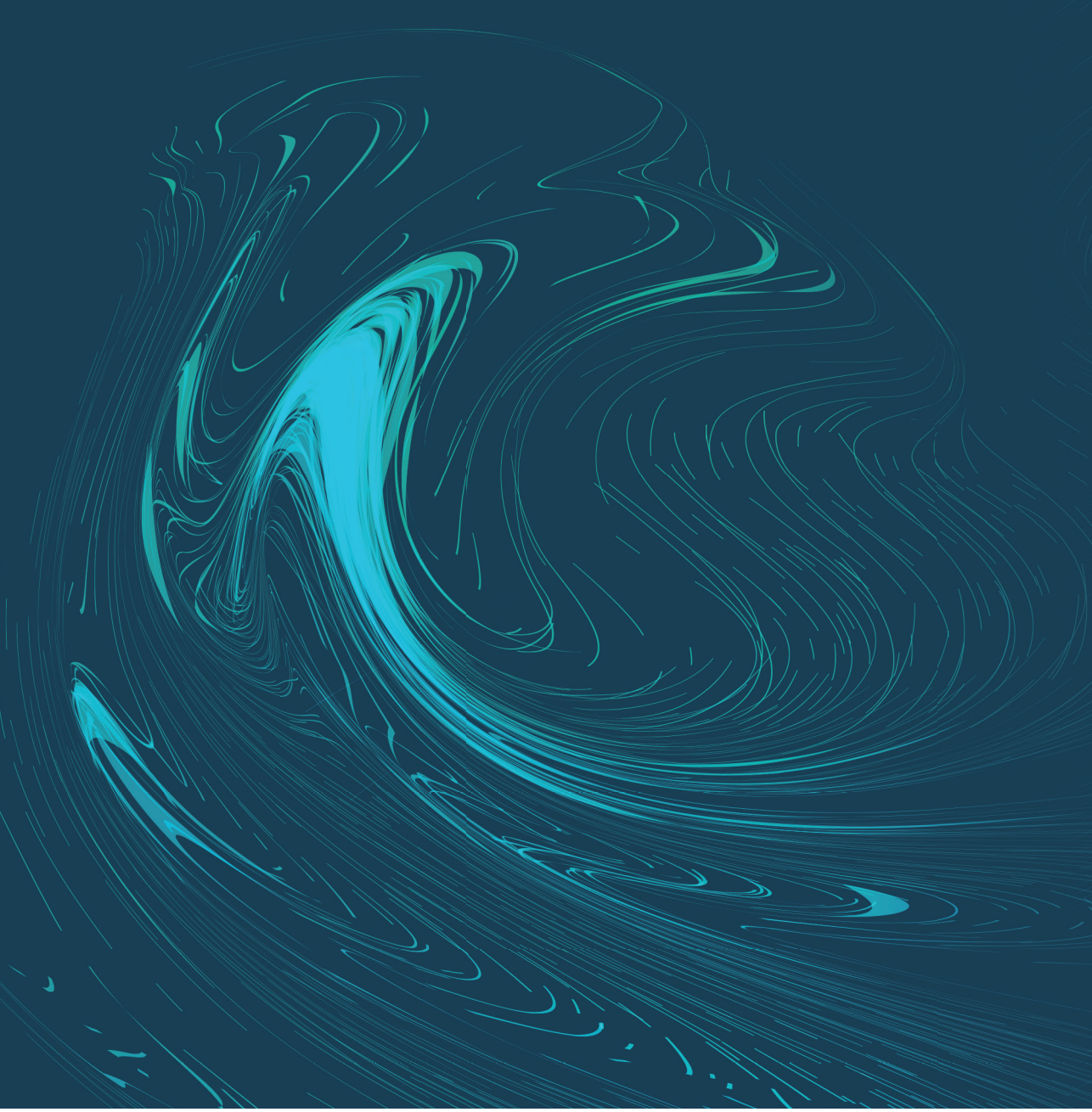

POLYMAT
Basque Center for
Macromolecular Design and Engineering

IPREM
Institut des sciences analytiques
et de physico-chimie
pour l'environnement et les matériaux

CIC
energiGUNE
energy cooperative
research centre

DEAKIN
UNIVERSITY